ADANA STU

LABORATORY INVESTIGATION OF THE EFFECTS OF AGGREGATE'S TYPE, SIZE AND POLISHING LEVEL TO SKID RESISTANCE OF SURFACE COATINGS

İSLAM GÖKALP

MSc THESIS

REPUBLIC OF TURKEY
ADANA SCIENCE AND TECHNOLOGY UNIVERSITY
GRADUATE SCHOOL OF NATURAL AND APPLIED SCIENCES
DEPARTMENT OF CIVIL ENGINEERING

LABORATORY INVESTIGATION OF THE EFFECTS
OF AGGREGATE'S TYPE, SIZE AND POLISHING
LEVEL TO SKID RESISTANCE OF SURFACE COATINGS

İSLAM GÖKALP

MSc THESIS

SUPERVISOR
ASSIST. PROF. DR. VOLKAN EMRE UZ

Adana 2016

Approval of the Graduate School of Natural and Applied Sciences

Director

Assoc. Prof. Dr. Osman SİVRİKAYA

I certify that this thesis satisfies all the requirements as a thesis for the degree of Master of Science.

Chairman of the Department

Prof. Dr. Faruk Fırat ÇALIM

This is to certify that I have read this thesis and that in my opinion it is fully adequate, in scope and quality, as a thesis for the degree of Master of Science.

Supervisor

Assist. Prof. Dr. Volkan Emre UZ

Adana Science and Technology University

Examining Committee Members

Prof. Dr. Erol TUTUMLUER

University of Illinois at Urbana-Champaign
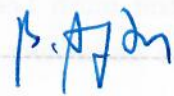
Prof. Dr. Mehmet SALTAN

Süleyman Demirel University

Prof. Dr. Serdal TERZİ

Süleyman Demirel University

Assist. Prof. Dr. Baran AYDIN

Adana Science and Technology University

LABORATORY INVESTIGATION OF THE EFFECTS OF AGGREGATE'S TYPE, SIZE AND POLISHING LEVEL TO SKID RESISTANCE OF SURFACE COATINGS

GÖKALP, İslam

Master of Science, Department of Civil Engineering

October 2016, 118 pages

ABSTRACT

The objective of this thesis is to investigate skid resistance performance of surface coatings which were produced at laboratory with different aggregate types, particle sizes and polishing levels. Six natural aggregates within three different origins such as limestone, basalt and boulder and four by-products including Electric Arc Furnace and Ferrochrome slags were used to prepare chip seal and slurry seal samples. Physical, mechanical and chemical properties of each aggregate were determined in accordance with European Committee for Standardization test methods and the results compared with the limitations given in Highway Technical Specifications of Turkey. Chip seal samples were prepared with seven different particle size ranging from 2.00 to 19.00 mm, whereas slurry seal samples were manufactured in three different gradations. Macro-textures of surface coating samples were determined with sand patch and outflow meter tests according to ASTM E 965, and ASTM E 2380 standard methods, respectively to determine the known effects of surface texture over skid resistance of the surface coatings.

Polishing of aggregates was performed via Micro-Deval apparatus according to ASTM D 6928 standard method which is used to evaluate abrasion resistant of pavement aggregates. To obtain polished aggregates in different levels, five different revolutions were applied in Micro-Deval test changing from 5250 to 52500 in Micro-Deval test. After the tests, polished aggregates were sieved and separated into four particle sizes in the range of 4.00 to 12.50 mm to prepare chip seal samples. For monitoring the aggregate surface at certain polishing levels, scanning electron microscope was utilized.

Finally, to identify the skid resistance of each surface coating sample, British Pendulum Tester, which is a widely known test device was utilized according to ASTM E 303 standard method. With regard to all analyses, the effect of macro and micro textures on skid resistance of chip seal samples produced with polished and unpolished aggregate was

evaluated. As a results of all analyses, micro-texture was found out a significant decisive feature in skid resistance performance evaluations.

Comparing to the skid resistance of surface coatings, samples produced with slags show better performance than the natural aggregates in each polishing level. Recovering slags do not only ensure benefits in environmental and economic aspects, but also utilizing slags in surface coating applications provides high skid resistant and long lasting pavement surface. It can be concluded with this study that, high skid resistant pavements can be constructed with slags, which consequently reduce slip-type traffic accidents and loss of life and property.

Keywords: *Surface coating, aggregate, EAF slag, Ferrochrome slag, polishing, pavement texture, skid resistance*

YÜZEYSEL KAPLAMALARDA AGREGA TÜR, BOYUT VE CİLALANMA SEVİYESİNİN KAPLAMA KAYMA DİRENCİNE OLAN ETKİSİNİN LABORATUVAR ORTAMINDA ARAŞTIRILMASI

GÖKALP, İslam

Yüksek Lisans, İnşaat Mühendisliği Bölümü

Ekim 2016, 118 sayfa

ÖZET

Bu tez çalışmasının amacı, laboratuvar ortamında farklı agrega tür, tane boyut ve cilalanma seviyelerinde üretilen yüzeysel kaplamaların kayma direnci performansının araştırılmasıdır. Sathi ve harç tipi yüzeysel kaplamalarının üretiminde kireç taşı, bazalt ve dere malzemesi kökenlerinde altı farklı doğal agrega ve elektrik ark fırını ile ferrokrom cüruflarını içeren dört farklı atık kullanılmıştır. Her bir agreganın fiziksel, mekanik ve kimyasal özelikleri EN standartlarına göre belirlenmiş ve elde edilen sonuçlar, Türkiye karayolları teknik şartnamesindeki şartname limitleri ile kıyaslanmıştır. Sathi kaplama örnekleri, 2.00-19.00 mm aralığında değişen yedi farklı tane boyutundan hazırlanırken, harç tipi kaplama örnekleri üç farklı gradasyonda üretilmiştir. Yüzey dokusunun kaplama kayma direncine etkisi bilindiğinden, yüzeysel kaplama örneklerinin makro dokuları, kum yama ve akış ölçer testleri ile sırasıyla ASTM E 965 ve ASTM E 2380 standart metotlarına göre belirlenmiştir.

Agregaların cilalandırılması, aşınmaya karşı direncin incelenmesinde kullanılan Micro-Deval cihazı aracılığı ile ASTM D 6928 standardına göre yapılmıştır Farklı seviyelerde cilalanmış agrega temin etmek için 5250'den 52500 değişen beş farklı devirlerde Micro-Deval testi uygulanmıştır. Testlerden sonra, cilalanan agregalar elenmiş, sathi kaplama örneklerinin hazırlanması için 4.00-12.50 mm aralığında değişen dört farklı tane boyutunda ayrıştırılmıştır. Agrega yüzeylerinin belirli cilalanma seviyelerinde görüntülenmesi için, taramalı elektron mikroskobu kullanılmıştır.

Son olarak, her bir numunenin kayma direncini belirlemek için çokça bilinen test cihazı, İngiliz sarkacı, ASTM E 303 standart test metoduna göre kullanılmıştır. Tüm analizler dikkate alınarak, makro ve mikro cinsinden yüzey dokusunun cilalanmamış ve cilalanmış durumdaki agregalar ile üretilmiş yüzeysel kaplamaların kayma direncine olan etkisi incelenmiştir. Kayma direnci ile ilişkilendirilen yüzey dokularının analizleri neticesinde, mikro dokunun kayma direnci performansında önemli ölçüde belirleyici olduğu görülmüştür.

Yüzeysel kaplamaların kayma direnci karşılaştırıldığında, her cilalanma seviyesinde cüruflar ile üretilmiş olan numunelerin, doğal agrega ile üretilmiş olan numunelerden daha iyi performans gösterdiği gözlenmiştir. Cürufların geri kazanımı ile sadece çevresel ve ekonomik açıdan yarar sağlanmış olunmayacak, aynı zamanda cürufların yüzeysel kaplamalarda kullanımı ile yüksek kayma direnci yüksek cüruflar ile uzun ömürlü kaplama yüzeylerin elde edilmesi sağlanacaktır. Bu çalışma ile yüksek kayma direncine sahip kaplamların inşa edilebileceği, böylelikle kayma tipi kazaların ve can ve mal kayıplarının azaltılabileceği sonucuna varılabilir.

Anahtar Kelimeler: *Yüzeysel kaplamalar, agrega, EAF cürufu, Ferrokrom cürufu, cilalanma, kaplama dokusu, kayma direnci,*

ACKNOWLEDGEMENTS

TABLE OF CONTENTS

LIST OF FIGURES

LIST OF TABLES

NOMENCLATURE

ASTM	American Society for Testing and Materials
CEN	European Committee for Standardization
ASIRT	Association for Safe International Road Travel
TSPA	Turkish Steel Producer Association
GDH	General Directorate of Highway
HTS	Highway Technical Specification
MTDs	Macro Texture Depths
BPN	British Pendulum Numbers
BPT	British Pendulum Tester
RNs	Revolution Numbers
PR	Penetration Numbers
SP	Sand Patch
OFM	Outflow Meter
OFT	Outflow Time
EAF	Electric Arc Furnace
SR	Skid Resistance
SS	Slurry Seal
SFC	Sideway Force Coefficients
LFC	Longitudinal Friction Coefficients
SMM	Slow-Moving Measurement
DFT	Dynamic Friction Tester
MSV	Magnesium Sulphate Value
SMA	Stone Mastic Asphalt
MD	Micro-Deval
XRD	X-Ray Diffractions
XRF	X-Ray Fluorescent
SEM	Scanning Electron Microscope
AIMS	Aggregate Imaging Systems
PSV	Polish Stone Value
RTM	Road Test Machine
LA	Los Angles
$MgSO_4$	Magnesium Sulphate
ASR	Aggregate Spreading Rate

ALD	Average Least Dimension
W_{24}	Water Absorption at 24 Hours Duration
Rpm	Revolutions per Minute
ρ_a	Apparent Density
ρ_{rd}	Oven Dry Density
ρ_{ssd}	Saturated Surface Dry Density
δ	Slip Angle
^{o}C	Celsius Degree
h	hour
kW	Kilo Watt
kN	Kilo Newton
kg	Kilogram
g	Gram
l	Liter
mm	Millimeter
kg/m^3	Kilogram per Cubic Meter

CHAPTER 1. INTRODUCTION

In Turkey, the great majority of freight and passenger transportation is carried on highways, and the main problem of this transportation mode is traffic accidents. Highway accidents account to thousands of deaths and injuries, and an enormous financial loss. Although, the human error has the greatest accident cause rate, road defects have an important contribution in factors that cause traffic accidents. Slip type accidents are the most common type of road defect related accidents and low skid resistant surface is the main reason. Skid resistance is the friction force occurred against the rotation of tire along the pavement surface and it is a significant parameter in terms of traffic safety (Rezaei et al., 2011). The importance of skid resistance is obvious because reduction in skid resistance cause an increase on traffic accidents (Mayora and Piña, 2009). Reduction in skid resistance under traffic and environmental conditions that causing polishing, bleeding, and raveling is usual, and there are many factors such as type of pavement, physical and mechanical properties of aggregates, the properties and amount of bitumen affect to the pavement long term skid resistance performance (Asi, 2007; Do and Cerezo, 2015; Fwa et al., 2003; Kogbara et al., 2016)

Texture is a road-related characteristic which has a very wide influence on pavements functional quality and traffic safety (Davis, 2001; Freitas et al., 2008). Pavement surface texture is simply defined as the deviations of the pavement surface from a true planar surface. Pavement surface textures consist of four major categories based on their wavelengths. These are: micro-texture, macro-texture, mega-texture, and unevenness with wavelengths range from 0 to 50 m (Henry, 2000a; Kogbara et al., 2016; Martino and Weissmann, 2008; Saykin et al., 2012). The methods for measuring pavement macro-texture which are responsible for facilitating the removal of water on a wet pavement surface when tire rolls on it, and improving friction are specified into three main groups. These are volumetric test methods, profile meters, and visualizing methods. The scope of this thesis was limited by volumetric methods which are sand patch (ASTM, 2012d) and outflow meter tests. Sand patch method include spreading a known volume of sand or glass within certain gradation in a circle on the pavement, and outflow meter test which measures the time for a known volume of water to flow from a specialized cylinder on the pavement surface (Kim and Lee, 2005; Meyer, 1991). The volumetric test methods for surface texture measurement are determined considerable due to their simplicity, low cost and portability (Doty, 1975). Surface coating is a coating type used as both to form a surface course and to extend the

service life or to restore texture of existing pavements. It is possible to categorize surface coatings in two ways depending on applications type. These are chip seals and slurry seals. Chip seal consists of spraying binder and spreading chips, whereas slurry seal is produced as a mixture of a certain amount of aggregate and bitumen. In general, chips seals and slurry seals are widely accepted for being effective, economical, and easy of application when compared with other pavement preservation and rehabilitation alternatives (Adams and Richard Kim, 2014; Praticò et al., 2015).

Skid resistance of pavements measurement is a difficult and complicated task. This is due to several factors which affect measurements coming from the pavement properties (texture, temperature, materials), which include tire properties (tread design, rubber composition, sliding velocity, temperature) and from the environmental and climatic conditions (Artamendi et al., 2013; Fwa et al., 2003; Kogbara et al., 2016; Mayora and Piña, 2009; Ong and Fwa, 2007). Accordingly, a number of devices and methods, which may provide different values for the same pavement surfaces have been developed in years to measure the most accurate value. Devices can be classified into three major group based on their operating principle. These are Longitudinal Friction Coefficient (LFC), Sideway Force Coefficient and Sliders (SFC), Stationary or Slow-Moving (SSM) measurement principles (Andriejauskasa et al., 2014; Do and Roe, 2008; Sandberg and Descornet, 1980). The last operating principle that covers devices mostly used for stationary testing is most preferable in laboratory applications. The devices in this class use rubber sliders that are attached either to the foot of a pendulum arm such as British Pendulum Tester (BPT) which is well known research tool in literature (Kogbara et al., 2016). BPT was developed by the British Road Research Laboratory and has been used due to its simplicity, low cost and portability. It is a dynamic pendulum impact-type tester used to measure the energy loss when a rubber slider edge is propelled over a test surface. In this research, a test method which is specified by ASTM E 303 (ASTM, 2012a) was performed in order to determine the skid resistance of pavement samples.

In this thesis, it was aimed to examine the effects of surface texture characteristic in terms of macro and micro texture of manufactured surface coating samples on surface skid resistance performance. To achieve this aim, ten types of aggregates including natural and by-products (limestone, basalt, boulder, and slags) have been provided from provinces located in the southern region of Turkey for a wide range of observation. To determine physico-mechanical properties some tests such as abrasion, fragmentation, thermal

2

weathering, polishing resistance test, dry unit weight and water absorption were conducted on each aggregate. Aggregates used for chip seal production considered for being in single-size and the gradations selected ranges 19.0 to 2.0 in mm for unpolished samples and 12.5 to 4.0 in mm for polished samples. Polishing of aggregates has been done with Micro-Deval apparatus conjunction with ASTM D 6928 (ASTM, 2012a). ASTM standard test method in the part B grading size , which ranges 12.5 to 4.75 mm have been conducted on each aggregates types in order to obtain polished aggregates in grain sizes of in different polishing levels with five different revolution numbers (RNs) applied in the MD test. RNs were applied as following 0, 5250, 10500, 21000, 31500, 52500 revolutions, which were specified in case of standard RNs as half, standard, double, triple and quintuple, respectively. After the polishing, the aggregates were sieved and separated into four grain sizes, 12.50-10.00, 10.00-8.00, 8.00,6.30 and 6.30-4.75 to produce chip seal samples. Bitumen with 70/100 penetration rate (PR) was utilized as binder. To ensure more adhesion between aggregates and binder, the bitumen modified with % 0.4 adjuvant as known DOP. All types of slurry seals which have been specified in ASTM D3910-11 (ASTM, 2012b) with certain gradations were manufactured with each type of aggregates using CRS-2 emulsion. Both chip seal and slurry seal samples, one hundred in total, were prepared on steel plates with 180 mm inner diameter and 3 mm depth. After production the samples, macro-texture depths for each samples have been determined with sand patch according to ASTM E 965-12 (ASTM, 2012d) and outflow meter according to ASTM E 2380-12 (ASTM, 2012e). Finally, to measure the skid resistance of samples BPT test method was implemented according to ASTM E 303 (ASTM, 2012a). With regard to the analyses, the effect of textures in terms of macro and micro texture on skid resistance of surface coating samples was determined.

The sustainability of human activity has become a key issue in the last two decades. The search for sustainability has driven the reuse of industrial by-products, thereby reducing the consumption of natural resources (Arribas et al., 2015). One of the efforts for sustainability in highway construction is reducing virgin material and increasing the use of waste materials as alternative pavement materials without reducing quality of pavement structure (Aschuri and Yamin, 2011). It is well-known that industry, construction and similar facilities produce large quantities of industrial byproducts. Slags are the important by-products of metallurgical industry, which have been treated, recycled and used worldwide (Reuter et al., 2004). Slag is an industrial byproduct outcome of not only the steel making process, but also manufacturing processes of ferrochromium. They have a complex chemical structure,

comprising mostly of oxides and silicates that are formed through the oxidation of various additives within the steel (Aziz et al., 2014; Yildirim and Prezzi, 2011). Well known that, slags have superior properties comparing to natural aggregates in terms of mechanical strength, stiffness, and wear resistance (Oluwasola et al., 2014)

Turkey is one of the biggest steel manufactures in the world with the full capacity of 50 million tons per year (TSPA, 2016). As considering the 10-15 % of the total production of steel is composed as slag, it can be concluded that nearly 6.5 million tons slag have been produced as the facilities works with their the full capacity (Gökalp et al., 2016; Uz et al., 2014). Utilization of steel slag instead of natural aggregates is vitally important for Turkey, To supply the demand amount of aggregate, more than a thousand of quarries are operating throughout Turkey. This condition leads to irreparable damage to the environment on behalf of destruction the nature. If it is possible, replacing all or some portion of natural aggregates with steel slag may lead to considerable economical and environmental benefits. However, the use of slags is mostly remained in theory in Turkey. This is causing to stand almost all slags to waste disposal areas. Thereof, there are needs to additional researches to determine the feasibility of utilizing this industrial by-products, technically as aggregate in pavement layers (Gökalp et al., 2016). In accordance with these concerns, feasibility of using slags, which are Electric Arc Furnace Steel Slags (EAFs) and Ferrochromium slags in surface coatings were evaluated within the scope of this study.

CHAPTER 2. LITERATURE REVIEW

2.1   Traffic Accidents

Today, the transportation industry offers a lot of options to people such as railway, seaway and airway, but in Turkey, the "highway or road transportation" generally is the main choice. Due to this fact, traffic accidents are of frequent occurrence in Turkey in line with other developing countries. Traffic accidents are one of the important problems and major concerns of all highway agencies throughout the world. As a result of traffic accidents,, deaths, injuries, disabilities and consequently, significant economic losses occur. According to the report published by Association for Safe International Road Travel (ASIRT), nearly 1.3 million people die in road crashes each year, on average 3,287 deaths a day, and 20-50 million people are injured or disabled. Additionally, road traffic crashes rank as the 9th leading cause of death and account for 2.2% of all deaths globally (ASIRT, 2016). In addition, some cost quantification studies show that cost of global traffic accident estimated at US$ 518 billion, with the costs in low-income countries (estimated at US$ 65 billion) exceeding the total annual amount received in development assistance (Aeron-Thomas et al., 2000). Thus, the traffic safety is subjected to vast and complex dimensions in which to be interacted together and consequently demands various knowledge and experiences (Pakgohar et al., 2011).

It has long been considered that traffic accidents are the results of the combined effects of behavioral, technological, and environmental factors (Edwards, 1999). The previous studies have point out that three contributing factors in traffic accidents. These are; human factors, road environment factors and vehicle factors which are involved in around 95%, 28% an 8% of crashes, respectively (Austroads, 2002; Híjar et al., 2000). According to the study performed on the traffic data in Tehran, Iran; human factor contributed in 97.5% of all accidents.

In contrast, the environmental factor had the second role and contributed in 70.5% of all road crashes. In addition, the vehicle factor contributed in 31.5% of all accidents (Pakgohar et al., 2011). In the light of present researches, it is possible to reveal that the safety of the road transportation network is dependent on many different factors. Table 2.1 shows the factors influence the traffic safety (Elias, 2014).

Table 2.1 Factors influence the traffic safety (Elias, 2014).

Factors	Parameters
Road User	Drivers fatigue, Alcohol usage, Drivers age, Mobile phone usage
Road Construction	• Geometric Properties: Alignments, Curves and type of crossing
	• Surface Properties: Rutting, Roughness, Skid resistance
Vehicles	Speed, Mobility, Vehicle safety

Road surface characteristics and traffic safety improvement works have a great importance on traffic safety (Sengoz et al., 2012). It is possible to reduce the severity of injuries and deaths from traffic accidents with improving the highway safety (Chang and Wang, 2006). The studies dealt with the effect of skid resistance performance on traffic accident presented that improving road skid resistance provide decreasing traffic accident, significantly. For examples, improving road skid resistance from 35% to 48%, provide 60% in traffic accident (Xiao et al., 2000).

Civil engineers must consider factors such as road surface properties in the pavement design for safer roads. Development of safer cars is a way how mechanical engineers may contribute to safer roads. Lastly, the behavior of the road user, which is the most important parameter in the safety of the road network and falls more under the influence of socially and legislatively driven actions., and cannot be possible to control by engineers (Elias, 2014; Híjar et al., 2000).

2.2 Pavement Surface Textures

The performance and service life prediction of any pavement type is very important for pavement engineers within pavement management system. Texture is a road-related characteristic which has a very wide influence on pavements functional quality and traffic safety. Surface texture depends on aggregate mineralogy, aggregate size and gradation, surface voids, pavement finishing techniques profile, and surface wear (Adams and Richard

Kim, 2014; Ahammed, 2009; Davis, 2001; Freitas et al., 2008). The irregularities of a pavement surface from the smooth horizontal plane are known as pavement surface texture. Texture influences several aspects of tire-pavement interaction depending on its sizes as defined by texture amplitude and wavelength. These are including resistance to skidding, tire-pavement noise, splash and spray, rolling resistance, and tire wear (Ahammed, 2009; Henry, 2000b).

Pavement surface texture is categorized into four main classes (Figure 2.1) based on texture amplitude and wavelength, which is defined as "the minimum distance between periodical repeated parts of the curves" as micro texture, macro texture, mega texture and unevenness. Micro texture refers to surface irregularities having a wavelength of less than 0.5 mm and a vertical amplitude of less than 0.2 mm, macro texture wavelength ranges from 0.5 mm to 50 mm and vertical amplitude ranges from 0.1 mm to 20 mm, mega texture has wavelengths in the order of 50 mm to 500 mm and vertical amplitudes of 0.1 mm to 50 mm. Lastly, surface irregularities having wavelengths (greater than 500 mm) exceeding the mega texture size are called roughness or unevenness (Bitelli et al., 2012; PIARC, 1987; Wambold and Henry, 1994) These various texture ranges that exist for a given pavement is given in the Figure 2.1 (Hall et al., 2009).
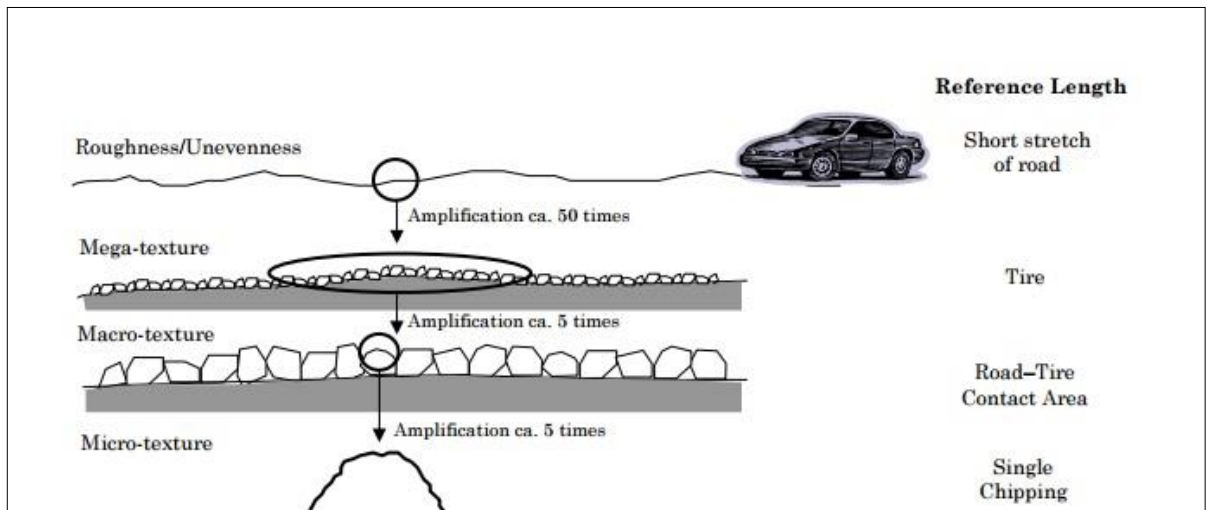
Figure 2.1 Various texture ranges that exist on pavement surface (Hall et al., 2009).

Among the most significant properties of road pavement, affected by surface texture, it is important to consider: friction, drainage, noise, wearing, comfort etc. Moreover, the

interaction phenomena depend on the exercise conditions such as speed, dimension, mass and suspension of vehicle, road characteristics, and environmental conditions etc. and depending on wavelength of roughness or unevenness. A proposal for identification of relationship between fields of texture types and interaction phenomena was presented by the World Road Association at Table 2.2 (Ech et al., 2009; Loprencipe and Cantisani, 2013; PIARC, 1987).

Table 2.2 Relationship between fields of texture types (Ech et al., 2007)

Texture Type	Length (mm)	Irregularities connected with	Irregularities have an influence on
Micro	< 0.5	• Surface of each aggregate depending on particle shape and angularity, texture of bituminous and cement mortar, surface texture of paving and setts and rock slabs, edges of grooves in concrete slabs	• Skid resistance on wet pavement at all speed • Skid resistance on dry moist pavement at all speed • High frequency tyre/pavement rumbling noise both at inside and outside the vehicle
Macro	0.5 - 50	• Mix design: aggregate particle size, shape, spacing and arrangement • Surface treatment: chipping bush hammering, aggregate exposure, grading (width, depth, frequency, and orientation of grooves) • Deficiencies: loss of clipping, cracks, wide joints • Surface or internal drainage of material	• Skid resistance at medium to high speed on wet pavement • Splash an spray • High and low frequency of tyre/pavement rumbling noise both at inside and outside the vehicle • Rolling resistance • Optical properties of pavements
Mega	50 -500	• Types of materials (natural stone setts or concrete paving block) • Regularity of laying and compaction method • Deficiencies: corrugation, rutting, loss of surface material, potholes, spalled joints n cracks, step faulting, frost damage • Local treatments: planning and repairs	• Vehicle control and stability • Comfort: high frequency mechanical vibrations in the steering and transmission gear • Water storage and loss of tyre/pavement contact: reduced grip • Low frequency rumbling noise (outside the vehicle) • Vibration of building along road
Roughness (Short)	> 500	• Quality of laying of the material (spreading and compaction) • Pavement deterioration by traffic (subsidence, depression with or without crazing) • Frost damage	• Loss of tyre-pavement contact, reduced steer ability, and grip (even on dry pavement) • Comfort: high frequency vibrations (resonance of unsprung masses) • Fuel consumption • Low frequency rumbling noise (outside the vehicle) • Vibration of building along road
Roughness (Long)		• Adjustment of laying equipment and guidance systems • Leveling • Deformation of sub-grade soil	• Vehicle stability • Comfort: high frequency vibrations (resonance of unsprung masses) • Fuel consumption • Infrasonic vibrations

Texture is the geometry of the road surface, and as aforementioned that categorized into four groups (micro, macro, mega-texture and evenness). Micro-texture roughly corresponding to the surface texture of individual aggregate particles, macro-texture corresponding to the sizes of the aggregate particles and the gaps between them, and mega-texture representing large-scale deformations and defects on the road surface. Additionally, pavement surface irregularities are continuous from pavement macro-texture to pavement micro-texture (Bitelli et al., 2012; Henry, 2000b; Kogbara et al., 2016; Kokkalis et al., 2002).The relations between pavement texture and different effects is given in Figure 2.2 (Hall et al., 2009).
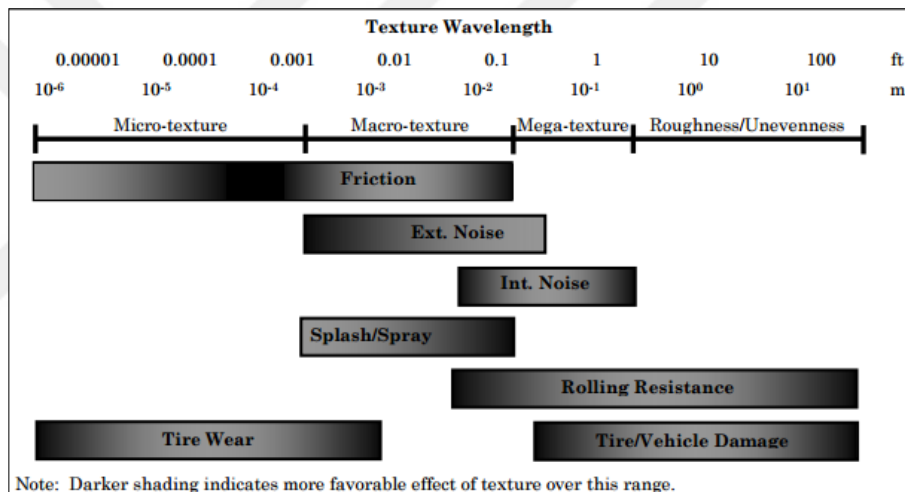
Figure 2.2 Texture wavelength influence on pavement–tire interactions (Hall et al., 2009).

As can be seen above figure that micro and macro texture are necessary for resistance to skidding such as the surface friction, developed at the tire-pavement contact for a given tire, mostly depends on the pavement surface micro and macro texture. On the other hand, rolling resistance, ride quality and vehicle wear characteristics are largely dependent on mega texture and roughness, a little bit depend on macro texture. However, in-vehicle noise and tire-pavement noise mainly depends on macro and mega textures.

2.3   Macro Texture Measurement Methods

Macro-texture can be measured by using many test methods including volumetric based methods such as outflow meters and sand patch, laser based methods such as laser profiler, laser texture scanner, and circular texture meter (CT Meter) and visualization

techniques such as, X-ray tomography, image processing methods and photogrammetry. Since these test methods provide different results, it is important to perform comparative studies and to develop relationships between them (Freitas et al., 2008).

Historically, the macro-texture has been measured using volumetric techniques, and the most common and widely accepted test procedure is sand patch method "Standard Test Method for Measuring Pavement Macro-texture Depth Using a Volumetric Technique" which designated by ASTM E 965 (ASTM, 2012d; Gransberg and James, 2005a; Gransberg and James, 2005b; Pidwerbesky et al., 2006). Although volumetric test methods are extensively used and inexpensive, they are time consuming and they require lane closure in the field (Goodman, 2009). While performing the test on the field, the operator may have great difficulty achieving a reasonable level of reproducibility according to the environment, weather, and traffic conditions and the method is not capable of being used in wet and windy conditions (Gransberg, 2007; Kelvin, 2005). A major limitation of this method is indicated in its inability to discriminate between active and idle voids. On the other hand, the appeal of this method to surface texture measurements is also indicated and linked to the simplicity, low cost and portability (Kelvin, 2005). The other volumetric test method to determine the surface macro-texture is outflow meter "Standard Test Method for Measuring Pavement Texture Drainage Using an Outflow Meter" which designated by ASTM E 2380. It measured the drainage capacity in terms of time needed for a known volume of water to escape between the base of the instrument and pavement surface. It was found to be extremely sensitive to local variations in the pavement texture, its repeatability was poor and the test is strongly up to the operator (Aktaş et al., 2011; ASTM, 2012e; Hegmon and Mozoguchi, 1970).

Earlier studies focused on volumetric test methods (the sand patch and outflow meter) to be put into practice on pavement surface for texture measurement have been discussed by Doty (Doty, 1975). In the study, test locations were selected as open-graded and dense-graded asphalt concrete, chip-sealed and fog-sealed asphalt concrete, and PCC pavements. The results of the testing indicated that the repeatability of the sand patch test was poor to fair and that the outflow meter test results were independent of water temperature. Some researchers used asphalt pavement cores for skid resistance evaluation in the laboratory under carefully controlled conditions. Sand patch and outflow meter test methods used for measuring surface textures of the cores and several variables which might influence the accuracy of the two methods were investigated. Comparison of the

results showed that the outflow meter gives more reliable results than the sand patch method. Also, they reported poor repeatability in sand patch results, especially between operators (Hegmon and Mozoguchi, 1970). It was indicated that differences in surface texture measuring can go over 300% between two operators on the same runway and with a single operator can vary over 100% along the runway (Sugg, 1979). A comparative analysis of macro-texture measurement tests including outflow meter and sand patch for was carried out (Aktaş et al., 2011). It was found out that the sand circle should be used on pavements with macro-texture greater than 0.79 mm and the outflow meter should be used on pavements with textures less than 1.26 mm. The point to consider as mentioned out by authors is that measuring macro-texture depth by these two methods can be accurately performed in the ranges from 0.79 mm to 1.26 mm on both asphalt and concrete pavements.

Alternatively, the technological devices such as laser based systems and image processing based systems are considered as rapid, however more expensive and may not be portable just like sand patch or outflow meter (Goodman, 2009). As agencies and individuals who are related to this issue recognized that there is a necessity to develop an alternative to the sand patch method of measuring surface texture, a vehicle mounted laser profiler is recommended where operator safety and traffic delays are a concern. A study was carried out to compare the results of surface macro-texture measurement methods including sand patch, laser profiler, laser texture scanner, circular texture meter, and X-ray computed tomography scanning using 26 laboratory specimens including SMA, HMA, CS. In the study, a best-fit line was drawn and coefficient of correlation (R^2) was computed for the two tests which are sand patch-laser scanner (R^2=0.9844), and sand patch-laser profiler (R^2=0.9068) (Fisco and Sezen, 2013). Another study focused on the evaluation of seal coat using macro texture measurements on field. It was confirmed that, there is a good correlation between the outflow meter and circular track meter. This points out that the outflow meter (OFM) could be used as portable and inexpensive device to measure seal coat quality. However, in the research there is threshold defined for using OFM. The threshold was defined with a mean profile depth (MPD) of 0.46 mm or less or an equivalent time of 14.5 seconds or greater (Martino and Weissmann, 2008). The surface texture properties of different flexible pavement including SMA and HMA roads within the boundaries of Izmir, Turkey were evaluated with sand patch and 3-D laser based test methods for the same objective. It was concluded that there is a good correlation between the results obtained by sand patch and 3-D laser based test methods (Sengoz et al., 2012). Replacing the sand patch test method

with image processing based methods was also evaluated, and an excellent correlation between them was occurred (Goodman, 2009). Correlations (R^2) ranges have been found from 40% to 80% between image output and physical measurements using sand patch test method in another research conducted in the same purpose (Gransberg et al., 2005b). As a result of a study related with pavement surface macro-texture using sand patch test and close range photogrammetric approaches indicated that the macro texture depths found out by photogrammetric approaches close to the results obtained by traditional sand patch method where coefficient of correlation ranged between 98% - 99.9% (Sarsam and Ali, 2015). The study dealt with asphalt pavement mean texture depth using multi-line laser and binocular vision was done, and the presented results gained by the advanced method shows good consistency (R^2= 81.58 - 86.38) with the sand patch method (Cui et al., 2015). The textures measured using the CT Meter and sand circle method have been compared in a study, and the coefficient of determination (R^2) has been found to be between 0.94 and 0.92 (Henry, 2000a). Considering the previous studies, it will be seen that there are many studies based on different test methods which implemented for same purpose. The studies presented in this thesis show us that researchers used volumetric test method to verify and to improve the models which they developed. It means that these methods which usually described as traditional test method are still useful, applicable and almost the first tool to test a model to be proposed.

2.4   Skid Resistance and Measurement Methods

Road pavements surface may deteriorate with time as a result of traffic usages environmental conditions, and poor maintenance and rehabilitation management (Sarsam and Al Shareef, 2015). One of the main factors influencing traffic safety is the friction between the vehicles' tyres and the road surface (Wallman and Åström, 2001). Skidding is the most common type of among the factors and caused by inadequate friction between the vehicles' tyres and the road surface. Skid resistance (SR) is identified as a property of the pavement surface that identify pavement surface roughness and impact on friction forces as the pavement exposed to wheel load and the most important surface characteristic of the pavement in terms of reasonable safety (Kogbara et al., 2016; Kumar, 2014) Investigations into the relationship between pavement skid resistance and accident occurrence have been carried out over many years (Lindenmann, 2006). The results confirmed the importance of adequate pavement friction for traffic safety as well as for achieving significant crash reductions. SR is dependent on various factors such as tyre load, pressure, tread depth,

and shape, road surface characteristics, water or ice presence on pavement, and driving speed. Based on these, factors influencing skid resistance were categorized as following: vehicle factors, road surface characteristics factors, road surface geometry factors, environmental factors, and driving factors (Andriejauskasa et al., 2014).

Surface properties such as rutting, roughness, and skid resistance are some of contributing factors to road traffic accidents. The most important factor is skid resistance, which refers to the frictional forces between pavement and tyre. If the tyres lose contact with the pavement then the vehicle starts to slide. Slip type accidents are the most common type of road defect related to accidents and low skid resistant surface is the main reason. The importance of skid resistance is obvious because reduction in skid resistance cause an increase in traffic accidents. Reduction in SR under traffic and environmental conditions that cause polishing, bleeding, and raveling is usual, and there are many factors such as type of pavement, physical and mechanical properties of aggregates, the properties and amount of bitumen, traffic level, highway class, pavement age, and environmental conditions affect to the pavement skid resistance performance (Asi, 2007; Do and Cerezo, 2015; Fwa et al., 2003; Kogbara et al., 2016; Saplioglu et al., 2013). SR performance of a pavement has been affected mainly by surface texture (macro and micro texture) during its service life. There are many reasons leading to undesired pavement surface texture. These include: aggregate polishing, stripping, and embedment causing flushing, bitumen bleeding, rutting based on water accumulation, surface contamination, and temperature, which decrease the micro and macro-texture (Ahammed, 2009; Bazlamit and Reza, 2005; Kim and Lee, 2005; Kumar, 2014). Also, it has shown from the studies (Fwa and Ong, 2008; Mayora and Piña, 2009; Meyer, 1991; Ong and Fwa, 2007) a strong relationship between wet-weather accidents and loss of pavement skid resistance.

SR of pavements measurement is mentioned as a reasonably complicated task by the researchers. Reason being, there are several factors which affect measurements coming from the pavement properties (texture, temperature, materials), from the tyre properties (tread design, rubber composition, sliding velocity temperature) and from the environmental and climatic conditions (Artamendi et al., 2013; Fwa et al., 2003; Kogbara et al., 2016; Mayora and Piña, 2009; Ong and Fwa, 2007). Accordingly, a number of devices and methods may provide different values for the same pavement surface have been developed in years to measure the most accurate value. Devices can be classified into three major group based on their operating principle. These are Sideway Force Coefficient (SFC),

Sliders, Stationary or Slow-Moving measurement (SSM) principles, and Longitudinal Friction Coefficient (LFC), (Andriejauskasa et al., 2014; Do and Roe, 2008; Sandberg and Descornet, 1980). There are a number of different skid resistance measurement methods and devices with different measurement speed, used tyre, wheel load, water film thickness.

SFC changes based on the tyre slip angle. Skid resistance measurement devices commonly are operating using fixed slip angle. Devices with fixed slip are thought to be better for monitoring purposes, because of supplying a continuous measurements. In contrast to this, variable slip ratio devices may measure short length of road. Thus, devices with fixed slip are more suitable for research purposes. (Andriejauskasa et al., 2014; Do and Roe, 2008; Sandberg and Descornet, 1980). Some of measurement devices that are being used in practice are shown in following table

Table 2.3 Some devices work based on SFC principle (Andriejauskasa et al., 2014).

No	Devices	Measurement Principle	Main Parameters	Tyre and wheel load
1	SKM	SFC	Slip angle: 20°; Water film thickness: 0,5 mm; Measurement speed: 50 km/h; Measurement interval: 100 m or other.	Tyre: Smooth profile ; Wheel load: 1960 N.
2	SCRIM	SFC	Slip angle: 20°; Water film thickness: 0.5 mm; Measures macro texture; Measurement speed: 50 km/h; Measurement interval: >10 m.	Tyre: Avon SCRIM smooth profile 76/508 (350kPa); Wheel load: 1960 N

SSM principle includes light, simple, portable and mostly used for laboratory or stationary testing devices. Static devices involve rubber sliders to make contact with the road surface via a mechanism that starts relative motion between the slider and the road. As given the table that two devices are used: (1) pendulum arm which swings and with a rubber slider contacts the surface until friction forces slow down the slider; and (2) DFT or rotating head with sliders, which is lowered on to the road so that friction between the sliders and the road causes the head to slow down (Andriejauskasa et al., 2014; Do and Roe, 2008; Sandberg and Descornet, 1980).

British Pendulum Tester (BPT) is well known and most commonly used for skid resistance measurement research tool in literature all around the world (Kogbara et al., 2016). BPT was developed by the British Road Research Laboratory had been used due to their

simplicity, low cost and portability. The BPT is a common method using for laboratory as well as field measurement of the low-speed friction of a road surface material. It is a dynamic pendulum impact-type tester used to measure the energy loss when a rubber slider edge is propelled over a test surface. The test method is specified by ASTM E 303 (ASTM, 2012a). It is widely suggested that the measured low-speed friction is largely governed by the surface micro-texture of the road material, and it is one of the simplest and cheapest instruments used in the measurement of friction characteristics of pavement surfaces. Many researchers and practitioners have considered the skid resistance measurements made by the BPT to be an indirect form of measurement of available micro-texture of the road material. Because, it is extremely versatile in its applications to many test situations and has received acceptance worldwide (Fwa et al., 2004).

The last measurement principle is namely LFC. It is based on a process of stopping a vehicle in moving via braking system at a straight line and transmitting the breaking forces to vehicle wheels. Following this process, angular speed of wheel decreases, kinetic vehicle rolling energy converts to thermal energy and the vehicle slows down. For instance where the braking force is too big, the vehicle wheel blocks itself and starts to slide on the road surface. Hence, tyre and road contact surface generates friction forces which slow down the vehicle. In here, LFC measurement devices create this wheel blocking process via creating controlled sliding process. The aim of utilizing slip ratio is to evaluate and compare wheel and vehicle speeds.

Slip ratio varies from 0 to 1, but the optimal slip ratio value varies from 0.15 to 0.20. Since, the highest LFC and shortest vehicle stopping distance is ensured in this ranges. As could be seen following table (Table 2.4) that almost all of devices work LFC measurement principle using fixed slip ratio. On the other hand, there are some devices such as Skiddometer BV-8 and SRM which have variable slip ratio. The main objective of this situation is to increase friction force until the wheel starts to block. Because of supplying a continuous measurement, devices with fixed slip ratio are considered to be better for monitoring purposes and are more suitable for research purposes. It could be possible to measure long length of road part via fixed slip ratio devices, thus it is preferred by the researchers.

Moreover, some of measurement devices that are being used in practice with LFC measurement principle are presented in Table 2.4.

Table 2.4 Some devices work based on LFC principle (Andriejauskasa et al., 2014).

No	Devices	Measurement Principle	Main Parameters	Tyre and wheel load
1	ADHERA	LFC	Slip ratio: 1 Water film thickness: 1,0 mm; Speed: 40 - 120 km/h;	Tyre: PIARC smooth profile165R15 (18 Wheel load: 2500 N.
2	BV-11	LFC	Slip ratio: 17 %; Water film thickness: 0,5-1,0 mm; Measurement speed: 70 km/h;.	Tyre: Trelleborg type T49 (140kPa); Wheel load: 1000 N.
3	GripTester	LFC	Slip ratio: 15%; Water film thickness: 0,5 mm; Measurement speed: 5-100 km/h;	Tyre: 254 mm diameter smooth profile ASTM 140kPa); Wheel load: 250 N
4	RoadSTAR	LFC	Slip ratio: 18%; Water film thickness: 0.5 mm; Measurement speed: 30, 60 km/h;	Tyre: PIARC with tread; Wheel load: 3500 N.
5	ROAR NL	LFC	Slip ratio 86%; Water film thickness: 0.5 mm; Measurement speed: 50, 70 km/h;	Tyre: ASTM 1551 (207kPa); Wheel load: 1200 N.
6	RWS NL Skid Resistance Trailer	LFC	Slip ratio: 86%; Water film thickness: 0.5 mm; Measurement speed: 50, 70 km/h;	Tyre: PIARC smooth profile 165R15 (200kPa); Wheel load: 1962 N.
7	Skiddometer BV-8	LFC	Slip ratio: from 1 to 14%; Water film thickness: 0.5 mm; Measurement speed: 40-80 km/h;	Tyre: AIPCR with Longitudinal tread 165R15; Wheel load: 3500
8	SRM	LFC	Slip ratio: from 1 to 15%; Water film thickness: 0.5 mm; Measurement speed: 40-80 km/h;	Tyre: AIPCR with longitudinal tread 165R15; Wheel load: 3500 N.
9	TRT	LFC	Slip ratio: 25%; Water film thickness: 0.5 mm; Measurement speed: 40-140 km/h;	Tyre: Smooth profile ASTM Wheel load: 1000 N.
10	SRT-3	LFC	Slip ratio: 1 Water film thickness: 0.5 mm; Measurement speed: 60 km/h.	Tyre with tread (200kPa).
11	IMAG	LFC	Slip ratio: 1 Water film thickness: 1.0 mm; Measurement speed: 65 km/h;	Tyre: PIARC smooth profile; Wheel load: 1500 N.
12	T2GO	LFC	Slip ratio: 20%; Marking for pedestrian/bicycle paths,	Two 75 mm width tyres.
13	VTI Portable Friction Tester	LFC	Marking for pedestrian/bicycle paths	-

Transverse friction measurement principle is performed when the vehicle is travelling in a horizontal curve and the vehicle wheels are turned. Angle between vehicle and turned wheel direction is called slip angle (δ). Slip angle induces friction between tyre and road, which in turn generates a centripetal force opposing the centrifugal force exerted on the vehicle in the bend, allowing the vehicle to follow round the curve. When braking force increases the wheel starts to slip over the road surface. (Andriejauskasa et al., 2014; Do and Roe, 2008; Sandberg and Descornet, 1980).

16

2.5 Pavement Surfacing

Pavement surfacing is widely used for preventative treatment of existing pavements or overlaying low volume roads. Besides, surface coatings are tools in maintaining and recovering skid resistance, which is a major safety component in pavement engineering (Cafiso and Taormina, 2007; Saykin et al., 2012). The performance of surface coatings depends on several factors including construction practices, properties and amounts of the materials, traffic, and weather conditions (Krugler et al., 2012).

2.5.1 Chip seals

A chip seal is an economical type of pavement surfacing which involves of layers of aggregate and bituminous binder and used to maintain, protect and prolong the life of the existing road. Chip seals have been successfully used on both low-volume and high-volume roads, though they are more commonly used on lower-trafficked roads. Chip seals are widely used in countries such as New Zealand, Australia, South Africa, Turkey, the United Kingdom and Canada (Gransberg and James, 2005b; Gürer et al., 2012; Terzi et al., 2013) as they are a cost-effective surfacing type which can be used both as a wearing course and a method of maintenance treatment. Chip seals make up large sections of the pavement network in countries such as New Zealand, Australia and South Africa. For instance, in New Zealand 95% of the road network, and in Turkey, 78 % of the rural road network, as well as 75% of the state highway network, is formed by chip-sealed pavement consists of chip seals (Gransberg and James, 2005a; Gürer et al., 2012).

There are numerous factors that affect the chip seal performance and should be taken into consideration throughout design and construction period. These are material properties such as aggregate type, gradation, type and amount of binder, surface, bitumen temperature, environmental conditions (rainy, windy, sunny etc.) time between aggregate spreading and rolling (Ball, 2005; Gransberg et al., 2005a; Gransberg, 2007; Gransberg and James, 2005b; Gundersen, 2008; Gürer et al., 2012; Karasahin et al., 2014; Kucharek et al., 2011; WSDOT, 2016; Zoghi et al., 2010). Chip seal performance is also affected by construction-related variables. These are uniform application rate of the binder on the surface, time delay between the binder and aggregate application, variety of material, equipment used during construction, weather before, during, and after constriction, volume of traffic (Gürer et al., 2012).

A chip seal is used to provide a suitable surface for vehicles and to protect the pavement structure from the impact of traffic loading. Moreover, it is utilized to keep water from

penetrating the pavement surfaces, to seal and resist reflection of small surface cracks, and raveled surfaces of the aged pavements, to reduce future cracking, distress and potholes, to provide an anti-glare surface during wet weather, to provide or improve skid-resistance and safety with high friction surface specifically in wet pavements (Anonymus, 2016a; Cenek and Jamieson, 2005; Karasahin et al., 2014; Karasahin et al., 2011; TNZ, 2005; WSDOT, 2016).

Chip seals generally have low initial cost, as they are usually applied on pavements that have adequate structural capacity and therefore the chip seal is not expected to provide added structural capacity, making them a suitable surfacing for low-volume roads. Accordingly, different types of chip seals exist which are used to enhance the performance of the pavement surface. The differences in the chip seal types depend on the construction method used and the number of binder and aggregate layers that make up the seal. The types of commonly used chip seals include single-coat seals, double-coat seals, void fill seals, texturizing seals, sandwich seals and racked-in seals (Gransberg et al., 2005a; Kodippily et al., 2011).

2.5.2 Slurry seals

A slurry seal is one of the most advanced surface treatment application for asphalt pavement preservation. It is a mixture of asphalt emulsion, well-graded fine aggregate, water, mineral filler, and chemical additives (Lee, 1977). When the mentioned ingredients are mixed, a creamy, homogenous and fluid mixture is created. Slurry seal is arranged with selected materials, scientific mix designs, technical specification, computerized equipment.

Slurry seals are able to applied to improve and correct distress of existing pavement surfaces not only on highways or city streets, but also airport runways, parking lots, and bridge decks which may have both flexible and rigid pavement surfaces (Hall et al., 2001; Hicks et al., 1997; Lee, 1977; Sheng-fei, 2011; Song et al., 2006; Thenoux et al., 1996). A slurry seal application is performed adequately on low volume roads, secondary roads and residential arteries. It is not designed to sustain heavy traffic and should not be applied in lifts thicker than about 1.5 times the maximum aggregate size (Kucharek et al., 2010). The primary goal of any slurry application is to preserve and extend the life of the existing pavement. The primary uses of slurry seals are crack sealing, surface sealing to improve and protect the old or new pavement surface from oxidation, water, moisture, and traffic wear, maintenance crazing, scaling, spalling, random cracking in rigid pavement surfaces, improvement of skid resistance, temporary skid resistance, and improvement of the visibility

of the surface (Kucharek et al., 2010; Kucharek et al., 2011; Lee, 1977; TNZ, 2005). Accordingly, it can be expressed that a good performing slurry surfacing is one that delivers the objective of its use for a long time and delivering a safe, comfortable and aesthetically pleasing road surface for the travelling public (Kucharek et al., 2010).

The primary advantages of using slurry seal coats are (1) Low cost, (2) a thin restorative surface layer due to its fluidity (3) ease of application, (4) minimal equipment and man power requirements, (5) low utilization of material and energy, (6) speed construction period, (7) extending the useful life of the pavement, (8) improving safety by providing a high skid resistance surface. On the other hand, there are disadvantages. The primary disadvantages are (1) short service life, (2) lack of design procedures and criteria, (3) numerous construction constraints, etc. (Anonymus, 2016a; Jianwen, 2006; Kai-bing, 2013; Lee and Orhan, 1984; Lee, 1977; TNZ, 2005).

2.6   Utilization of Slags in Pavement Construction

It is well known that aggregate is a very versatile construction material that used in almost all aspect of the infrastructure. Aggregate could be natural and artificial, mine waste, demolition materials, recycled materials or any other material. Aggregate mostly obtained from natural rocks makes up approximately 90% of the total volume or 95% of the mass of in pavement construction (Uz et al., 2014), dependently transportation industry always needs great amount of aggregates in required quality.

The sustainability of human activity has become an important aspect of developing and developed countries throughout the world in the last decade of the 20th century and the first decade of the 21st century (Fronek, 2012). Sustainability is the ability to use byproducts and/or waste materials from industry and recycled materials in such a way that the application of the material provides a beneficial use in the manufacturing or construction sector. One of efforts for sustainability in highway construction is reducing virgin material in road pavement construction and increasing the use of waste materials as alternative pavement materials without reducing quality of pavement structure (Arribas et al., 2015; Aschuri and Yamin, 2011; Fronek, 2012).

With a large portion of construction works in the transportation industry being comprised of aggregates causes increasing demand on the limited supply of natural aggregates. As the population of the world continues to grow, the need to construct, expand and repair the infrastructure increases, naturally. Thus, the demands on natural resources continue to grow. Unfortunately, natural aggregates are becoming increasingly scarce, and necessity of

desired quality aggregate is growing for construction. This situation have diverted the attention of researchers to suitable alternative materials as aggregate due to factors like technical, environmental, economic feasibility. Therefore, the use of alternative sources for replacing of natural aggregates is becoming increasingly important. For this purpose, researchers have explored variety of by-product materials which can be used as an aggregate (Asi, 2007; Asi et al., 2007; Aziz et al., 2014; Fronek, 2012; Yildirim and Prezzi, 2011). By-products may be one of the best substitutes of artificial aggregates for road construction (Oluwasola et al., 2014).

It is well-known that, metallurgical industry produce large amount of industrial byproducts, which have been treated, recycled and used worldwide (Reuter et al., 2004). Steel slag is a leftover component from the steel making process (Fronek, 2012). Steel slag has a complex chemical structure, comprising mostly of oxides and silicates that are formed through the oxidation of various additives within the steel. Moreover, steel slag has superior properties comparing to natural aggregates which are mechanical strength, stiffness, and wear resistance (Aziz et al., 2014; Oluwasola et al., 2014; Proctor et al., 2000; Yildirim and Prezzi, 2011).

Turkey is one of the biggest steel manufactures in the world with the full capacity of 50 million tons per year. A report on the production capacity of steel Turkey published by Turkish Steel Producer Association (TSPA, 2016) shows that this production is approximately 35 million tons. Production of steels with EAF constitutes approximately 72 percent (≈ 25 million tons) of total annual steel production. As we consider the 10-15 % of the total production of steel is composed as slag, it will be observed that nearly 4.5 million tons slag have been produced (Uz et al., 2014). Utilization of steel slag is important for Turkey, since great amount of road network consists of flexible pavement, and accordingly great amount of aggregate is need to be supplied at the required qualities whose requirements given in the HTS (Gürer et al., 2012; Karasahin et al., 2014; Karasahin et al., 2011; Terzi et al., 2013). This condition leads to irreparable damage to the environment on behalf of destruction the nature. However, replacing all or some portion of natural aggregates with steel slag would lead to considerable both economic and environmental benefits. Unfortunately, the usage of slags are very limited and mostly remained in theory in Turkey. This is causing to stand almost all steel slags, in particular EAF slags, to waste disposal areas. Thereof, there are needs to additional researches to determine the feasibility

of utilizing this industrial by-product, technically as aggregate in different pavement type and/or pavement layers (Gökalp et al., 2016; Uz et al., 2014; Yilmaz and Sütaş, 2008).

Slag has a wide range of uses as a replacement for part or all of the natural aggregates including road construction aggregate, railroad ballast, and filling materials, concrete aggregate (Asi et al., 2007; Aziz et al., 2014; Fronek, 2012; Motz and Geiseler, 2001; Oluwasola et al., 2014; Proctor et al., 2000; Yildirim and Prezzi, 2011). Fwa et al. (2013) have performed a study based on both in-situ and laboratory performance tests to develop an environmentally sustainable pavement mix. In the construction of a porous pavement surface course, steel slag was used to replace granite aggregates. In addition to using steel slags, the pavement was designed to provide environmental sustainability performance in terms of wet-pavement skid resistance and visibility of road markings in wet weather conditions, and reducing tyre-pavement noise. The results obtained from both field an laboratory assessment indicated that asphalt mixes with steel slags provides sufficient drainage of water, better wet-pavement skid resistance and reduction in tyre-pavement noise as compared with the others.

Sorlini et al. (2012) evaluated reusability of EAF steel slags in bituminous paving mixtures. In the study, series of tests were conducted to characterize physical, mechanical, and chemical properties, and bituminous mixtures containing up to 40% of EAF slags were designed and tested. According to the test results have shown that physical, mechanical properties complied with relevant specification limits.

Wu et al. (2007) aimed to explore the feasibility of utilizing steel slag as aggregate in stone mastic asphalt (SMA) mixtures. To evaluate properties of such asphalt mixture, X-Ray diffraction (XRD), SEM, and mercury intrusion porosimetry (MIP) were conducted. A natural aggregate, which is basalt was used in SMA mixture for comparison. The results indicated that SMA mixture with steel slag complied the related specification limits. Compared to mixture produce by basalt, some properties of SMA mixtures were improved. These were high temperature property, low temperature cracking skid resistance performance.

The performance of asphalt concrete consisting of crushed steel slag material instead of fractional fine natural aggregate were assessed by Ziari and Khabiri (2007). In addition to Marshall test, the tests including the high-temperature stability and creep stiffness of steel slag asphalt concrete were evaluated. Consequently, the researchers demonstrated that the recycling and use of waste steel slag in asphalt concrete is feasible. Similarly, Krayushkina

et al. (2012) indicated that electric furnace steel slag can be used as crushed rock aggregate and mineral powder in road structures for preparation of asphalt mixture.

Performance of asphalt wearing courses with electric arc furnace slag aggregates was conducted within a project lasting for a period of 10 years by Kehagia (2009). The researcher analyzed the outcomes of 1 year period, and presented the results as followings: (1) Skid-resistance performance of EAF slag layers was constantly higher than the natural hard aggregate mixes, (2) Loss in skid-resistance could be estimated at 10–15% after 1 year under traffic for EAF surface layers, and (3) Compared with natural aggregates, the properties occurs in the surfaces of the EAF slag aggregate such as high density, the angular shape and the irregularities provide substantial resistance to deterioration under construction, continuous traffic loading, and environmental conditions.

In a study dealing with both characterization of steel slags in terms of physical and mechanical properties and possible uses of them in construction of different pavement layers according to HTS of Turkey was conducted by Gökalp et al. (2016). The authors concluded that almost all physical and mechanical characteristics of the slags meet with the specification limits, and thus the slags could be used in construction of different pavement layers including subbase, base, wear layer, and surface coatings.

In an study dealing with utilization of ferrochromium slags as highway base material, which performed by Yilmaz and Sütaş (2008) was concluded that the slags could be used for granular pavement layers as base materials instead of natural ones due to their superior physical and mechanical properties.

Khan and Wahhab (1998) assessed and aimed to improve the performance slurry seal in the laboratory by incorporating steel slag. To prepare the samples, aggregate blend improvement technique was followed. Slurry seal samples were prepared with steel slag, limestone and mixture of two in different emulsion content. The results indicated that a significant improvement were provided in slurry seal samples with mixture consisting of slags and limestone in terms of abrasion and crashing resistance.

Moreover, utilization of artificial materials benefits environmental issues, ensures reduction of deposits and the preservation of raw materials (Reuter et al., 2004). For instances, some of the environmental impacts that could be seen from utilization the slag in pavement would be a reduction in the amount of landfill, reducing the CO_2 produced by equipment during the mining of natural aggregates, and lowering the cost of shipping if there is a steel plant closer to the construction plant than the location of the natural aggregates. Reducing the distance

the aggregate is shipped would also reduce the emissions from trucks during shipping (Fronek, 2012; Huang et al., 2007; Motz and Geiseler, 2001; Uz et al., 2014; Wu et al., 2007).

2.7 Earlier Studies About Aggregate Polishing Resistance

In this section of the thesis, earlier studies about aggregate polishing resistance have been discussed in detail. As analyzed the earlier studies, it was found different polishing methods were performed, namely Micro-Deval, Polish Stone Value, Aachen Polishing Machine, Wehner/Schulze machine, Auckland Pavement Polishing, Los Angeles, and Road Test Machine. These devices were used to evaluate aggregate abrasion resistance performance in this respect. Related studies are summarized here.

Polishing of aggregates using MD devices was implemented by many researchers. For illustration, an indirect method was developed by Crouch and Goodwin (1995) to measure polishing resistance using Micro-Deval. In the method, aggregate are polished for 9 hours via Micro-Deval test, an then the polished aggregates uncompact voids are measured, where fewer voids refers smother aggregates.

An experimental method was developed by Mahmoud and Masad (2007) for measuring aggregate resistance to polishing, abrasion and breakage. Here, the differences in micro texture of aggregate particle, before and after the Micro-Deval test were analyzed as a function of polishing duration time via Scanning Electron Microscope (SEM). In the developed method, the aggregate micro-texture degrading rate in terms of time is considered as the polishing resistance of aggregates.

At the same aspect, Xue et al. (2010) subjected the aggregates from different sources to Micro-Deval abrasion test. Before and after abrasion test, aggregate particles were evaluated by aggregate imaging systems (AMIS). It was concluded that aggregate morphology has an important role in aggregate resistance to polishing.

In another study, polishing resistance using Micro-Deval apparatus for coarse aggregates including natural aggregates such as limestone, quartz, gravel (crashed, chert), dolomite, diabase and sandstone, and by-products such as steel slags and blast furnace steel slag were analyzed via AIMS, which was used before and after different polishing time. In the study modified Micro-Deval abrasion resistance test method was used. 750 g of aggregate passing on the 12.5 mm sieved and retained on the 9.5 mm-sieve was decided for polishing at different polishing duration time, which were 15, 30, 45, 60, 75, 90, 105, 180, 210, 270 in

minutes. As presented by researchers, aggregates with different mineralogy exhibit different polishing behavior. An interesting result that researchers face with was increasing the texture index of steel slag and chert gravel while continuing to polishing, whereas the other aggregates' texture index decreasing significantly while continuing to polishing, and each aggregate reach their terminal texture in a certain polishing duration (Ortiz and Mahmoud, 2014).

An experimental-based model was developed by Rezaei and Masad (2013) for predicting the skid resistance of asphalt pavement. The aggregate samples (limestone, sandstone, gravel, and dolomite) were polished with MD apparatus for two different time durations, which are 105 and 180 minutes according to ASTM D 6928 procedure. AIMS was utilized for monitoring the polished aggregate samples, and the results highlighted by authors that skid resistance is mostly a combination of aggregate texture and gradation.

Cafiso and Taormina (2007) evaluated the texture of the aggregates (basalts obtained from different sources and limestone) being used wearing courses in asphalt pavements during polishing test. For assessing the micro-texture during polishing, PSV test, which is a time depended accelerated polishing test method was carried out. Textural analysis were performed with British Pendulum Tester (BPT), that is one part of the PSV test method after different polishing cycles at certain time interval (0, 3, 6, 9 hours). The results of the tests showed that basalts coming from different sources showed better resistance to polishing comparing to limestone, and skid resistance in terms of BPN decreases by increasing polishing time.

Wang et al. (2013) used different aggregates such as granite and diabase to prepare asphalt samples. Influence of different polishing condition on the skid resistance performance was investigated. In the research, asphalt samples were polished via Aachen Polishing Machine under various conditions using real tires. To determine the skid resistance characteristics of the samples, Wehner/Schulze machine were utilized. Polishing conditions in the content of the research were as followings: (1) Polishing duration time (16.67, 33.33, 100, 200, 300, and 600 in minute) and (2) Polishing agent with different combination of quartz powder as sand, fine and course corundum, and water. It was implied that asphalt samples show different skid resistance behavior and reach different final states under different polishing conditions.

At a similar research, two aggregates, namely, rhyolite and limestone having low and high polishing resistance, which is identified with standard test method encoded with EN 1097-8

were used to have a better understanding of the evaluation of road-surface texture due to traffic loading. Traffic loadings were simulated via Wehner/Schulze machine, and aggregates were polished with it. Skid resistances of the prepared samples have been measured at each stop, where the polishing stopped in every 1000 rotations until 15000, Afterward, stops are done at 30000, 50000, 90000, and 180000 rotations, and similarly skid resistance behavior of the samples was determined. Following each measurement of skid resistance, a laser sensor was used to characterize the surface texture. The results of the research expressed that there are two mechanism due to polishing process. One is removing globally materials, and the other one is regenerating roughness due to hardness difference between aggregate minerals (Do et al., 2009).

Kane et al. (2013) focused on the relation between mineralogical composition of three different types of aggregate, which were namely greywacke, granite and limestone and their capacity to generate adequate friction between the road surface and the tyre after the polishing action of traffic Wehner/Schulze machine has also been used to simulate action of traffic for different cycles up to 180000 revolutions on both produced asphalt and mosaic aggregates.

Woodward et al. (2004) used a modified polish stone value test method for better understanding between the laboratory prediction of aggregate skid resistance and actual performance. The arm on the accelerated polishing machine used for polish stone value test was redesigned allowing angles of 0^0, 3^0, 6^0 and 10^0 for examination. According to the results, it was concluded that up to angle of 6^0, PSV was continually decreased, while polish stone value started increase at 10^0.

Road Test Machine (RTM) testing is mentioned by the researcher as an test that subjects the test specimen to trafficking using full-scale tires rather than solid rubber tires and/or rollers due to 305 x 305 mm test specimens that provide interaction between tire and surface. Unlike other test equipment such polish stone value and Wehner/Schulze machine, the RTM uses full-scale tires to traffic test specimens in the same way every time. This allows different materials to be ranked using different measured properties (Friel and Woodward, 2013).

RTM was used for simulating an accelerated trafficking by Friel and Woodward (2013) in order to predict the development of asphalt surfacing properties in terms of skid resistance based on polishing. To achieve this, RTM was stopped at regular number of polishing passes up to 100,000 wheel passes, which is referred to 5 to 10 years trafficking. BPT was

conducted on the specimen for wet skidding resistance properties assessment depending on the type of pavement, aggregate and gradations used depending on the number of wheel passes. As a result, significant difference in skid resistance were observed.

Polishing and degradation resistance of both natural aggregates including granite, gneiss and phonolite and steel slag were evaluated via AIMS. To obtain the results of the polishing resistance and degradation of aggregates, Los Angeles (LA) abrasion equipment has been used in 500 rpm for each two aggregate sizes, which are passing on the 19 mm- sieved and retained on the 12.5 mm-sieve, passing on the 12.5 mm- sieved and retained on the 9.5 mm-sieve. With the results gathered for the selected aggregate, it was concluded that the steel slag was the most resistant to polishing and abrasion aggregate compared to other aggregates (Bessa et al., 2014).

CHAPTER 3.MATERIALS AND METHODS

3.1   Aggregates

In the scope of this thesis, a total of ten coarse aggregate samples including natural rocks and industrial by-products (slags) were collected. Aggregates were selected from nine provinces of Turkey in the Mediterranean and Southeast Region. One boulder, three types of limestone, two types of basalt, one ferrochrome slag and three types of Electric Arc Furnace (EAF) steel slag were utilized in order to have a wide range of results. All natural aggregates were supplied from the quarries operated privately. Slags were taken from the plants of metal manufacturing companies, and from disposal areas. In accordance with privacy policy, the exact names and locations of the sample and material suppliers are not presented here. The random sample identification number, material lithology, and source district of the aggregates are presented in Table 3.1 and geographic location of the sources is given in Figure 3.1.

Table 3.1 Aggregates distribution based on lithology and source district.

Sample ID	Lithology	Source District
LS-1	Limestone	Antakya - Kırıkhan
LS-2	Limestone	Mersin - Tarsus
LS-3	Limestone	Adana - Ceyhan
BS-1	Basalt	Niğde - Bor
BS-2	Basalt	Kayseri
BLD	Boulder	Kahramanmaraş - Aksu
EAF-1	EAF Slag	Antakya - İskenderun
EAF-2	EAF Slag	Osmaniye
EAF-3	EAF Slag	Antakya - İskenderun
FER	Ferrochrome Slag	Elazığ

Due to the geological structure of Turkey, limestone is the most common natural aggregate and it is widely used in construction works for different engineering purposes. Three types of limestone were chosen here for being major source of construction materials in the region. Due to their superior physical and mechanical properties basalts and boulders are the preferred natural aggregates for highway construction applications. Moreover, Turkey is one of the biggest steel manufactures in the world with the full capacity of more than 50 million

tons per year. As knowing that 10-15% of the total production of steel is composed as slag (Uz et al., 2014), approximately 4.5 million tons of slag is been produced each year. The facilities located only in the southern part of Turkey manufacture steel with the full capacity of 15.8 million tons per year, and nearly 2 million tons of slags is produced each year. Ferrochromium (FeCr) slag is another type of slag that being occurred at the end of production process of FeCr. In Turkey, there are two facilities served in Ferrochromium production. One is industrial is located in Elazığ with full capacity of 150000 tons per year in production of FeCr with high amount of carbon, and the other is located in Antalya with full capacity of 10000 tons per year in production of FeCr with low amount of carbon. Accordingly, about 200000 tons slag is produced annually in Turkey, and unfortunately almost all amount of slags is kept in waste storage plant. It is known in previous studies that, FeCr slag have superior properties comparing to natural aggregates (Erdoğan et al., 2014; Panda et al., 2013; Uz et al., 2014; Yılmaz et al., 2012).
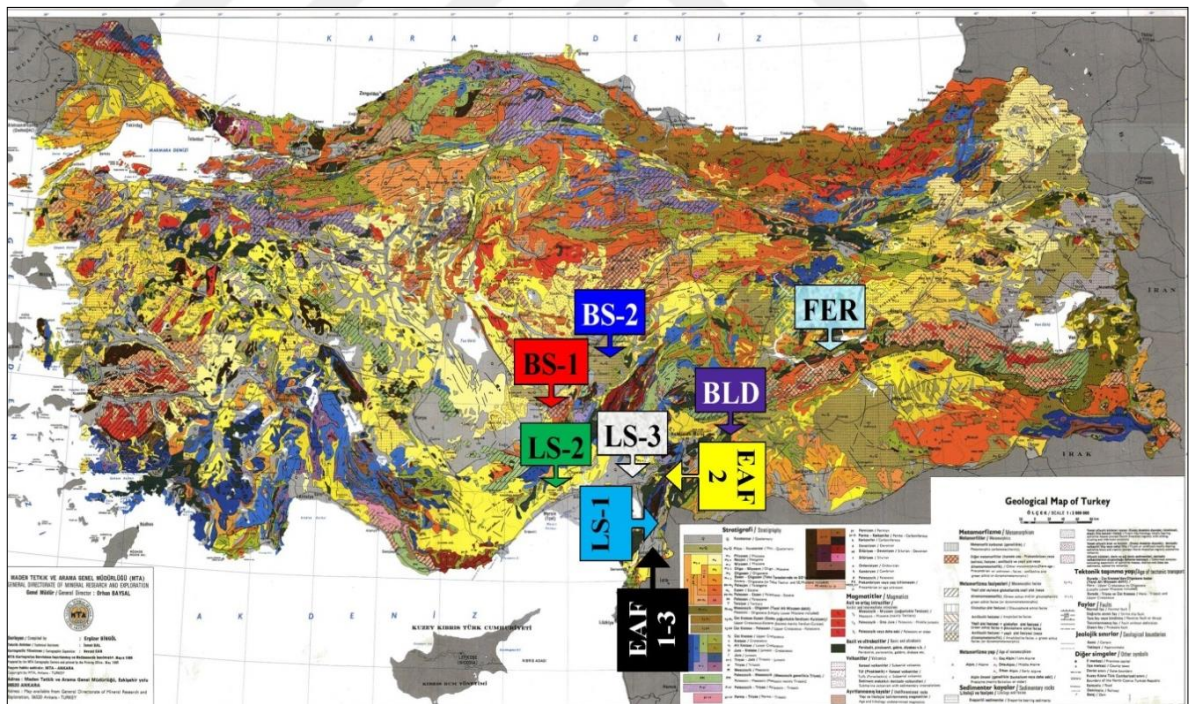
Figure 3.1 Geological map of Turkey and locations of the material sources

It is well-known that aggregate is one of the basic materials of concrete structures, road pavements and other earth constructions. Naturally, the properties of aggregates utilized in any type of pavement construction should be determined.

3.1.1 Properties of aggregates

In order to determine physical and mechanical properties of the aggregates used in this study, series of tests are conducted such as abrasion resistance with Micro-Deval apparatus, fragmentation resistance with Los-Angeles, thermal weathering resistance with $MgSO_4$ solution, dry unit weight and water absorption, and polishing resistance (PSV). Since, aggregates are used to prepare surface coatings affinity between aggregate and bitumen is determined with Vialit plate and Nicholson Striping tests. Moreover, to identify the chemical composition of each material, X-Ray Fluorescent (XRF) test method was used. To follow and make a comparative evaluation on the polishing characteristic of each aggregate, Scanning Electron Microscope (SEM) was used to get the surface images for each polishing level. In here, the test methods used are presented in briefly.

3.1.1.1 Micro-Deval abrasion resistance test

The Micro-Deval (MD) abrasion test which is a measure of abrasion resistance and durability of mineral aggregates, results from a combination of actions including abrasion and grinding with steel balls in the presence of water (Cooley Jr and James, 2003). Micro-Deval test is the most common test used for qualifying aggregates on behalf of the resistance to wear. To determine the abrasion resistance of each material, European standard encoded with EN-1097-1 (CEN, 2011a) was followed, which is suggested by HTS of Turkey (GDH, 2013).

The standard aggregate size in EN 1097-1 test method is 10/14 mm. The mass of the test sample used is 500 ± 2 g and is obtained from a sampled mass of at least 2 kg of aggregate. It is required that 60% to 70% of the test sample mass should pass through the 12.5 mm sieve. If an 11.2 mm sieve is used, the percentage changes to 30% to 40%. The test specimens are washed and dried in the oven at 110 ± 5°C to constant mass. Along with the dry aggregate, 2.5 ± 0.05 lt of water at a temperature 20 ± 5°C are added to the drum for minimum 1 hour either in the Micro-Deval drum or some other suitable container. Then, 5000 ± 5 g steel balls having a diameter of 10 ± 0.5 mm are placed into the drum. The drum is then sealed and is rotated for 12000 revolutions at 100 ± 5 rpm (Figure 3.2) After completion of the test, the aggregates are dried and sieved through the 1.6 mm sieve. The MDC is calculated with following equality.

$$MDC = \frac{500-m}{5} \qquad (1)$$

Where,

m is the mass of aggregate retained on the 1.6 mm sieve.

Figure 3.2 Micro-Deval test

3.1.1.2 Los Angeles fragmentation resistance test

Los Angeles test is one of the oldest and best known aggregate test. It determines the wear on aggregates under the influence of crushing and abrasion forces. The forces are developed during rotation of the aggregate and steel spheres in an apparatus known as the Los Angeles machine. To determine the fragmentation resistance of each material, European standard encoded with EN-1097-2 (CEN, 2010a) was followed as suggested by HTS.

The machine consists of a rotating drum with internal dimensions 508 mm (length) by 711 mm (diameter). The tested aggregate size is 10/14 mm in accordance with TS EN 1097-2. The mass of the test sample used is 5000 ± 5 g and is obtained from a sampled mass of at least 15 kg of aggregate. It is required that 60% to 70% of the test sample mass should

pass through the 12.5 mm sieve. If an 11.2 mm sieve is used, the percentage changes to 30% to 40%. Along with the dry aggregate, 11 steel spheres 45 to 49 mm in diameter and mass between 400 and 445 g each are also added (Figure 3.3). The drum is then sealed and rotated for 500 revolutions at 31 to 33 revolutions per minute (rpm). After completion of the test, the aggregates are sieved (wet sieving), then the aggregates are dried to determine the mass of material that is retained on a 1.6 mm sieve. The Los Angeles (LA) coefficient is calculated with following equality.

$$LA = \frac{5000\text{-}m}{50} \tag{2}$$

Where,

m is the mass retained on a 1.6 mm sieve.

Figure 3.3 Los Angeles Test

3.1.1.3 Thermal weathering resistance test

The thermal resistance of aggregates may be found out with freezing and thawing, boiling, drying shrinkage, thermal shocking and magnesium sulphate test (Nikolaides, 2014). Among them, magnesium sulphate test method was used to implement on aggregates

since, it is the specified test method in HTS. This test determines the resistance to weathering or disintegration of aggregate when subjected to the cyclic action of immersion in magnesium sulfate, followed by oven drying. It simulates the long-term resistance to weathering due to volume changes caused by the impact of alternating seasonal temperatures. If the aggregate is not resistant to ambient temperature change, its disintegration may cause loss of bearing capacity of the layer, cracks, potholes and pavement surface disintegration. The simulation of volume change is carried out with the crystallization and hydration of magnesium sulfate (Mg_2SO_4) within the pores of the aggregates during the drying stage of saturated aggregates. A mass of 500 g of aggregate particles between 10.00 and 14.00 mm, according to EN 1367-2 (CEN, 2011b) is immersed in a magnesium sulfate solution for 17 ± 0.5 hours. The aggregate is left to drain for a period of 2 ± 0.25 hours and then dried at 110°C ± 5°C for 24 ± 1 hours. This process is repeated for five times. The aggregates are then washed with tap water to remove any magnesium sulfate. The aggregates are then dried at 110°C ± 5°C and sieved manually using the 10.00 mm sieve (Figure 3.4).

Figure 3.4 Thermal weathering resistance test

The loss of weight attributed to wear is recorded and expressed as a percentage of the original sample mass. The mean value of two tests, rounded to the nearest integer, is reported as the magnesium sulfate value (MSV). MSV is calculated with following equality.

$$MSV = \frac{500\text{-}m}{5} \tag{3}$$

Where,

m is the mass of aggregate retained on the 10 mm sieve.

3.1.1.4 Polishing resistance test

The determination of polishing resistance of aggregates is important for selecting suitable aggregate for any type of surface layer or surface dressing application. Polishing resistance of an aggregate is determined with PSV test, and aggregates are considered to be suitable when their PSV is equal or greater than the value given by the national specification. The PSV test determines the resistance of the coarse aggregate to the polishing action under the vehicle tyres. The test consists of two parts: in the first part, test specimens are subjected to a polishing action in an accelerated polishing machine. In the second part of the test, the state of polish reached by each specimen is measured with British pendulum. The PSV is then calculated from the friction determinations. The test can carried out in accordance with European or American test standard. The key differences between the two standards are the nominal size of aggregate used, the polishing medium used, the number and the type of test wheels, the way the aggregates are subjected to polishing and the way the PSV index is calculated.

To determine the PSV of each material, European standard EN-1097-8 (CEN, 2010b) was determined followed. Approximately 36 to 46 aggregate particles of size 7.2 10 mm are carefully placed in a single layer in a standard mould with their flattest surface lying on the bottom. The interstices between the aggregates are filled with fine sand. The quantity of sand used is such that only three quarters of the depth of the interstices is filled. Then, the mould is in filled with an epoxy resin and any surplus is removed with a spatula. After the resin has hardened, the specimen is cleaned thoroughly to remove any sand and is transferred to the polishing machine. The polishing machine has a metal wheel called the road wheel. This is 406 mm in diameter and holds the test specimens and the stone control specimens around its rim. The number of specimens placed around the wheel is 14 in total (Figure 3.5). The wheel rotates at 320 revolutions per minute during the test. The rubber-tyred wheel has a static contact force with the moulds of 725 N. For the first 3 hours of the test, corn emery is fed onto the Wheel at a rate of 27 ± 7 g/min together with a sufficient amount of water. The corn emery has a gradation with 98% – 100% of the particles passing through the 0.600 mm sieve. After the first 3 h, the second rubber-tyre wheel is fitted and

the test is repeated for another 3 h using flour emery. The emery flour rate is 3 ± 1 g / min with the rate of water approximately twice that of the emery flour. On completion of the test after 6 h, the test specimens are cleaned and tested for friction using the Pendulum friction tester The PSV is determined using the following equation:

$$PSV=S+52.5-C \tag{4}$$

Where,

S is the mean value of skid resistance for the four aggregate test specimens, and

C is the mean value of skid resistance for the four PSV control stone specimens, that must range from 49.5 to 55.5 units of PSV.

Figure 3.5 Polising resistance test

3.1.1.5 Dry-unit weight and water absorption test

The basic equipment for determination of the density of coarse aggregates are as follows: a watertight tank, a balance (weighing capacity of 0.1 g) and a wire basket of suitable size that is suspended from the balance. After sampling the aggregate in accordance with EN 932-1

(CEN, 1997) and reducing the amount in accordance with EN 932-2 (CEN, 1999), a representative portion of dry coarse aggregate is placed in the wire basket, which is the minimum mass per test portion required is given in Table 3.2. After that, the aggregate particles immersed in a water tank for 24 ± 0.5 h, at 22°C ± 3°C.

Table 3.2 The minimum mass of test portions.

Sieve Size (mm)		Mass (kg)
Passing	Retained	
31.5	16	1.5
16	8	1.0
8	4	0.5

After 24 hours, the basket containing the aggregate is weighed (M2) in water at 22°C ± 3°C. The aggregate is then carefully removed from the wire basket and the empty basket is weighed in water (M3). The aggregate is placed on absorbent paper or cloth and dried until any surplus water is removed from its surface (Figure 3.6). The aggregate is then weighed (M1). Finally, the aggregate is placed in an oven at 110°C ± 5°C until it reaches constant mass (M4).

Figure 3.6 Dry-unit weight and water absorption test

The apparent density (ρa), oven dry density (ρrd) and saturated surface dry density (ρssd), in kg/m^3, are calculated as follows:

$$\rho a = \rho w \times M4 / [M4 - (M2 - M3)] \tag{5}$$

$$\rho rd = \rho w \times M4 / [M1 - (M2 - M3)] \tag{6}$$

$$\rho ssd = \rho w \times M1 / [M1 - (M2 - M3)] \tag{7}$$

Additionally, the water absorption after immersion for 24 h, WA24 can be calculated as follow:

$$WA24 = 100 \times [(M1 - M4) / (M4)] \tag{8}$$

3.1.1.6 Vialit Plate adhesion test

French Public Works Research Group developed vialit plate test in the 1960's in order to evaluate retention between aggregate and binder. After that, it was standardized in British. The vialit plate test, according to BS EN 12272-3 (BSI, 2003) determines the binder aggregate adhesivity and the influence of adhesion agents or interfacial dopes in adhesion characteristics as an aid to design binder aggregate systems for surface dressing.

In particular, BS EN 12272-3, specifies methods of measurements of the mechanical adhesion of the binder to the surface of aggregates, the active adhesivity of the binder to chippings, the improvement of the mechanical adhesion and active adhesivity by adding an adhesion agent either into the mass of the binder or by spraying the interface between binder and chippings, the wetting temperature and the fragility temperature. Overall, the adhesivity value is determined as the sum of number of aggregates remaining bonded to the plate and the number of fallen chippings that are stained by the binder. In the vialit plate test aggregates specimens is fabricated on 20x20 cm steel plates and cured at 35°C in the oven and after 24 hours a stainless ball is dropped three times from 50 cm (19.7 in.) height onto an inverted chip seal tray for 10 s. Samples weights are measured before and after the test and then the difference is calculated as a percentage (Figure 3.7).

This test method has been slightly modified throughout the years by researchers and organizations. However, it has been kept essentially the same (BSI, 2003; Jordan III and Howard, 2011; Karasahin et al., 2011; Nikolaides, 2014)

Figure 3.7 Vialit plate test processes

In Turkey, Vialit plate testing procedures 40 grams of bitumen is spread over a 20 cm x 20cm steel plate. A hundred aggregates between 9.5 mm and 19.5 mm are placed onto plate with spreader. The chip seal specimens are compacted with a 25 kg rubberized roller three times in two direction (North to South and West to East). After that specimens are put in 35°C water bath for 24 hours. Then, it is removed and placed reversely in the Vialit apparatus. An impact load of dropping metal ball is applied to the plate, three times with ten seconds intervals. After the drops, the number of fallen aggregates is recorded. Since a hundred aggregates are used to perform the test, then it is reported the percentage of the adhesion between aggregates and bitumen with the fallen amount of aggregate (GDH, 2013).

3.1.1.7 Nicholson striping test

ASTM D1664 "Test Method for Coating and Stripping Test of Bitumen Aggregate Mixture" (ASTM, 2012g) is used to evaluate the degree of stripping of asphalt mixtures. In this method, coarse aggregate (9.5 - 6.3 mm) were coated with bitumen. The loose mixture was then immersed in distilled water for 24 hours and the degree of stripping was observed under water to visually estimate the total surface area of the aggregate on which bitumen coating remains (Figure 3.8).

Figure 3.8 Nicholson striping test

According to the HTS, the percentage of the adhesion between aggregates and bitumen is required at least 60. So, performing of Nicholson stripping test is determined with different kind of bitumen just like bitumen 70/100 penetration rate (PR) and modified bitumen PR: 70/100 with %0.2 adjuvant which is peeling preventive bitumen additives.

3.1.1.8 X-Ray fluorescent test

In this thesis, Semi Quantitative XRF was used to determine the chemical elements present in the aggregates. Because, semi-quantitative processing allows the user to compare spectral data from samples in order to obtain information regarding the relative concentrations of elements from sample to sample. In Semi Quantitative XRF, a specific software package is applied suitable to perform the XRF analysis without the use of calibration curves set up with dedicated reference samples. Most of the instruments available are delivered with pre-calibrated analytical methods.

To determine the chemical elements of each samples, the standard called EN 15309 (Characterization of waste and soil - Determination of elemental composition by X-ray fluorescence) was followed. According to the specification, aggregates were prepared as powder form, which passing No:200 sieve. about 200 g. Then, the slags powders were pressed under 180 kN and the other pressed under 150 kN for 30 seconds for being a pellet in the specific pellets which has 32 mm diameter. The pellets was placed to the box and cover of box is closed. Finally, all pellets placed into the XRF machine, and software program compatible to the machine was started and the results were obtained (Figure 3.9)
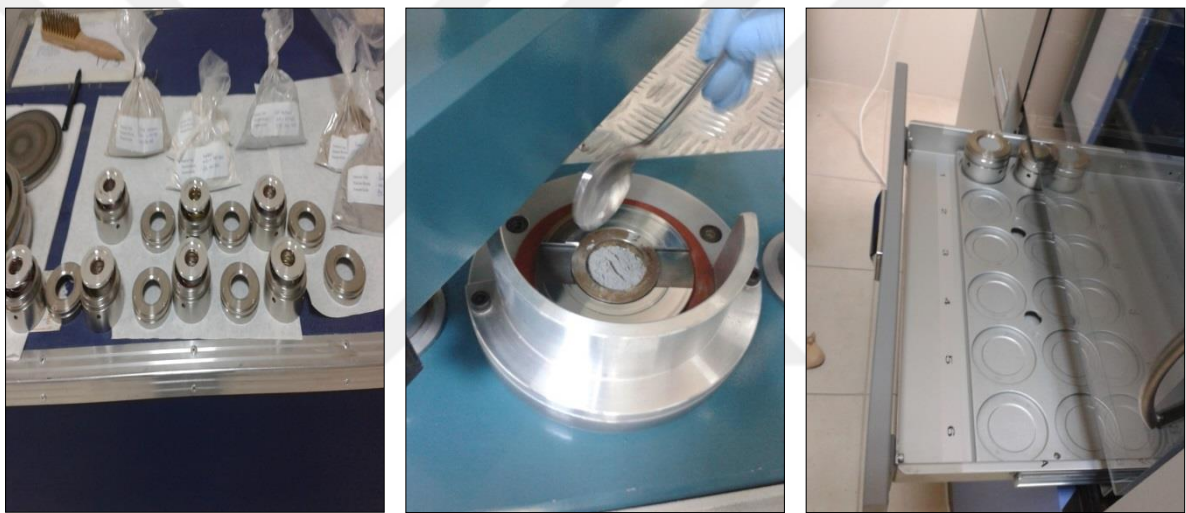
Figure 3.9 X-Ray fluorescent test

3.1.1.9 Scanning electron microscope (SEM) test

Scanning Electron Microscope (SEM) is robust magnification tool, which utilizes focused beams of electrons to obtain desired information regarding on the materials. With high-resolution, and three-dimensional images that could be produced by SEM, SEM is considered as invaluable and versatile tool in a variety of science and industry applications. Since, SEM is feasible tool owing to mentioned features to provide topographical, morphological, and compositional information. Moreover, a SEM can be utilized to detect and analyze surface fractures, to provide information in microstructures and qualitative chemical analysis, to evaluate surface contaminations, and to identify crystalline structures. Thus, it can be expressed that SEM is versatile and essential toll in the fields such as life science, biology, geology, medical and forensic science, material and metallurgy by a

majority (Goldstein et al., 2012). Basically, SEM consist of following components: Electron source, thermionic gun, field emission gun, electromagnetic and/or electrostatic lenses, vacuum chamber, sample chamber and storage, computer, secondary electron, backscatter, diffracted backscatter, and X-ray detectors. Additionally, The device requires a stable power supply, vacuum and cooling system, vibration-free space and need to be placed in an area that isolates the instrument from magnetic and electric fields (Postek, 1997).

In this study, SEM was utilized for monitoring the surface of aggregates with different origins, scientifically named as limestone, basalt, boulder, by-products including of EAF steel and ferrochromium, at four different polishing levels. To perform this process, a mini-SEM was used. The model of the SEM is SNE-4500M (Figure 3.10), which can provide high-quality SEM images, and easily magnify up to 100.000x with variable voltage (5 - 30 kW) within a short period of time (in seconds)
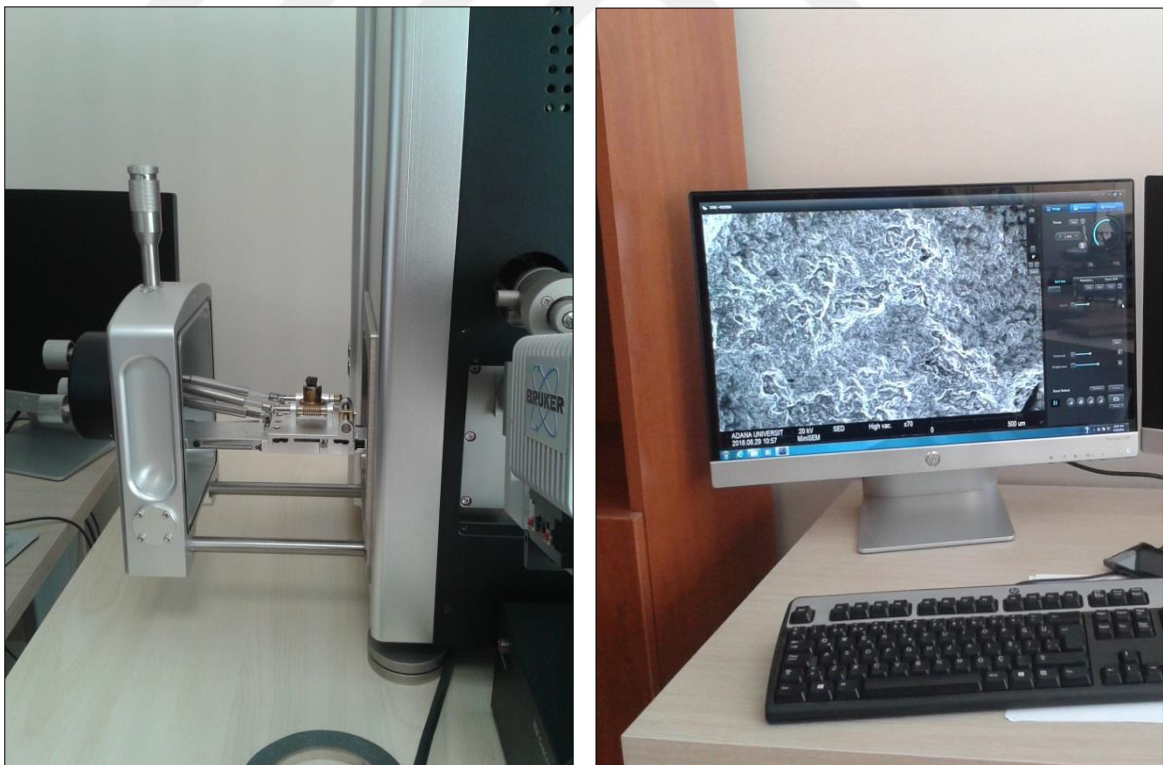
Figure 3.10 Scanning electron microscope and monitoring

The magnification process begins with an electron gun generating a beam of electrons down the column and onto a series of electromagnetic lenses, which are tubes, and wrapped in coil. Then, the coils are adjusted for focusing the incident electron beam onto samples. Controlling via computer, the operator can set the beam to control the magnification, that to determine the surface area to be scanned. Then, the beam focused onto the stage that the samples is placed. At this part of process, an interactions occurs between the incident electrons and the surface of samples via acceleration rate of incident electrons. Incident electrons no sooner came in contact with the sample than the scatter patterns made by the interaction yields information on size, shape, texture and composition of the sample. A schematic diagram (Postek, 1997) regarding on working principle is given in Figure 3.11.
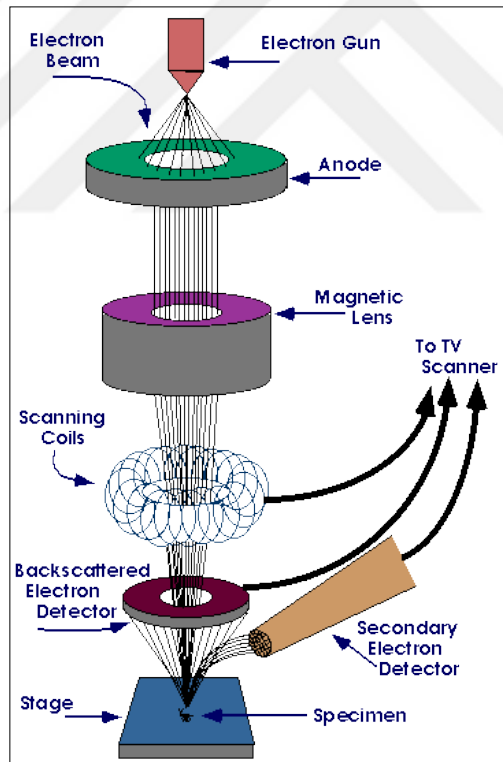
Figure 3.11 Schematic diagram for working principle of SEM

3.2 Bitumen

The bitumen types for being used in construction of chip seal applications according to the region are indicated by General Directorate of Highways Republic of Turkey (GDH, 2016) The bitumen to be used for province of Adana is identified as 70/100 penetration rate (PR).

In order to manufacture slurry seal samples, emulsion which is one type of bitumen had been used. The binder is specified as CRS-2 cationic emulsion. The recipe of the CRS-2 is given in the Table 3.3.

Table 3.3 Recipe of emulsion.

Raw Materials	Bitumen	Solutions					
		Water	Emulator	Emulato	HCl	CaCl$_2$	Adjuvant
Type	50/70	H$_2$O	Redicote Em 22/44	RC-406	HCl	CaCl$_2$	Not given
Quantity (kg)	710	290	1	2	2	1	2

3.3 Aggregate Polishing Process

Polishing of aggregates have been done with Micro-Deval apparatus conjunction with ASTM D 6928 (ASTM, 2012f).In the standard, grain size of aggregate samples is given according to aggregate maximum nominal grain size. The aggregate fractions for the test sample shall consist of material passing 19.0-mm sieve, retained on the 9.5-mm sieve or passing 12.5-mm sieve, retained on the 4.75-mm sieve or passing 9.5-mm sieve, retained on the 4.75-mm sieve, which are enumerated with MD-A, MD-B, and MD-C, respectively. Test sample' size and mass are given in Table 3.4.

Table 3.4 Sieve size and mass of the aggregates used in ASTM D-6928 test method.

Passing Sieve Size (mm)	Retained Sieve (mm)	MD-A (g)	MD-B (g)	MD-C (g)
19.0	16.0	375	-	-
16.0	12.5	375	-	-
12.5	9.5	750	750	-
9.5	6.3	-	375	750
6.3	4.75	-	375	750

The mass of the test sample used is 1500 ± 5g according to Table 3.4. The test specimens are washed and dried in oven at 110 ± 5°C to constant mass. Along with the dry aggregate, 2.0 ± 0.05 L of water at a temperature 20 ± 5°C is added either in the MD drum or to some other suitable container for minimum 1 hour. Then, 5000 ± 5g steel balls having a diameter of 10 ± 0.5 mm are placed into the drum. The drum is then sealed and rotated for 12000 ± 100 revolutions for grading 19.00 / 9.50 in mm, for 10500 ± 100 for grading 12.50 / 4.75 in mm and for 9500 ± 100 revolutions for grading 9.50 / 4.75 in mm at 100 ± 5 rpm. After completion of the test, the aggregates are dried and sieved through the 1.18 mm sieve. The MDC is calculated with the following equation.

$$MDC = (1500-m)/15 \tag{9}$$

Where m is the mass of aggregate retained on the 1.18 mm sieve.

ASTM standard test method in the part B grading size , which ranges 12.50 to 4.75 mm have been conducted on the aggregates in order to obtain the aggregates in grain sizes of 12.50 - 10.00, 10.00 -08.0 , 8.00 - 6.30, and 6.30 - 4.0 mm with different polishing levels, where polishing level is identified according to standard revolution number Table 3.5.

Table 3.5 Polishing level and case of standard revolution number.

Polishing Level	Revolution Numbers (RN)	Case of Standard RN
Original	0	Unpolished
1st	5250	Half
2nd	10500	Standard
3rd	21000	Double
4th	31500	Triple
5th	52500	Quintuple

3.4   Surface Coating Design

Two kinds of surface coating applications, which are chip seal and slurry seal were used in the scope of this thesis. Inhere, all the design procedure and manufacturing of the samples have been presented in detail.

3.4.1 Chip seal design

As previously mentioned, in total ten types of aggregate samples including natural and industrial by-products were utilized. A chip seal is generally applied with the aggregate in single size. In the scope of this thesis, different aggregate grain sizes and aggregate gradations have been decided for being utilized to prepare chip seal and slurry seal samples, respectively. The prepared chip seal samples with unpolished aggregate has seven different aggregate grain sizes range from 19.00 to 2.00 mm, whereas four different aggregate grading sizes range from 12.50 to 4.00 mm have been used in preparation of polished chip seal samples (Table 3.6).

Table 3.6 Aggregate sizes for chip seal production at different polishing levels.

Aggregate sizes (mm)	Polishing Level					
	Original	1st	2nd	3rd	4th	5th
19.0-16.0	X	-	-	-	-	-
16.0-12.5	X	-	-	-	-	-
12.5 – 10.0	X	X	X	X	X	X
10.0 – 8.0	X	X	X	X	X	X
8.0 – 6.3	X	X	X	X	X	X
6.3 – 4.0	X	X	X	X	X	X
4.75 – 2.0	X	-	-	-	-	-

Macro-texture depth is mainly depending on aggregate size, shape and placement of the aggregates on the surface. To avoid misleading in any test results, all collected aggregates were removed from such any elongated and platy aggregates according to ASTM D 4791 (ASTM, 2012c) and EN-933-3 (CEN, 2012) and cubic particles were used to prepare the test samples. For chip seals, the aggregate size which equal or lower from 6.3 mm is not necessary to be separated from platy and elongated particles (Gürer et al., 2012). Removing friable particle from aggregates is utmost important for a good adhesion between aggregate and bitumen. Thus, all aggregates were washed and then dried at 100±5 °C in the ventilated oven.

Aggregate spread rates are based on the theory of average least dimensions (ALD). ALD represents the expected chip seal thickness when the aggregate is oriented on its flattest

side (TNZ, 2005). According to the formula specified by TNZ, aggregate spreading rate was calculated with the following equation.

$$ASR = 950/ALD \qquad (10)$$

Where,

ASR is aggregate spreading rate

Since each of aggregate has different unit weight, the ASR was calculated in unit of ml/m^2. Aggregates spreading rate and flakiness sieves are summarized in the Table 3.7. The galvanized metal plate used for preparation of the specimens has been specially designed with 180 mm inner, 200 mm outer diameter, and 3 mm depth in order to keep the binder inside of plate.

Table 3.7 Aggregates spreading rate and flakiness sieves sizes.

Aggregate Gradations for Chip Seals	Flakiness Sieves	ALD	Aggregate Spreading Rates	
			Calculated*	Used
mm	mm	mm	ml/m^2	ml/m^2
19.0-16.0	10.0	17.5	512.0	510.0
16.0-12.5	8.0	14.3	416.9	420.0
12.5 – 10.0	6.3	11.3	329.2	330.0
10.0 – 8.0	5.0	9.0	263.3	260.0
8.0 – 6.3	4.0	7.2	209.2	210.0
6.3 – 4.0	-	5.15	150.7	150.0
4.75 – 2.0	-	3.4	98.8	100.0

* Aggregate spread rates were calculated for standard sample plate which has 0.025 m^2 area

In this thesis, the adhesion between bitumen and aggregates was investigated with the tests called Nicholson striping and Vialit plate test which determine the affinity and adhesion behavior of binder with aggregates. These tests are conducted with both neat bitumen and bitumen modified with adjuvant (DOP) in different percentages. According to results of the tests, the quantity of adjuvant was determined as 0.4% of the bitumen by weight.

Bitumen rate is determined related to United Kingdom's design method for surface dressing (Roberts and Nicholls, 2008). The factors to be considered in calculating the binder spread rate are traffic, existing surface, climatic conditions, and types of chips or aggregates. In the Table 3.8, the weighting factor of all these factors are presented.

Table 3.8 The factors in calculating the binder spraying rate (Roberts and Nicholls, 2008).

Traffic			Existing Surface		Climatic Condition		Aggregates	
Traffic Type	Vehicles	F	Existing Surface	F	Climatic Condition	F	Type of Chips or	F
Very Light	0-50	3	Untreated	6	Wet and Cold	2	Round / Dusty	2
Light	50-250	1	Very Lean	4	Wet and Hot	1	Cubical	0
Medium	250-500	0	Lean	0	Temperate	0	Flaky	-2
Medium-Heavy	500-1000	-1	Average	-1	Semi-Arid (Hot	-1	Pre-Coated	-2
Heavy	1500-3000	-3	Very Rich	-3	Arid (Very Hot	-2	-	-

After the determination of the overall and average least dimension of the aggregate, the binder application rate can be determined using the following equation

$$R= 0.0625 + (F×0.023) + [0.0375 + (F×0.0011)] × ALD \qquad (11)$$

where;

R is basic rate of spread rate of bitumen in unit of kg/m^2, and

F is weighting factors

In the scope of this thesis, the factors determined as following: medium for traffic, lean bituminous for existing surface, temperate for climate, and finally cubical for type of aggregates, where overall the weighting of factors (F) was calculated as zero.

For each aggregate gradation, the bitumen spraying rate were determined using above mentioned equation based on the plate size, and given in Table 3.9.

Table 3.9 Spraying rate of bitumen based on aggregate gradations

Aggregate Gradations for	The Rate of Bitumen g/m^2	
	Calculated*	Used
19.00 - 16.00	30.03	30.00
16.00 - 12.5	27.35	27.50
12.50 - 10.00	24.88	25.00
10.00 - 8.00	23.03	23.00
8.00 - 6.30	21.51	21.00
6.30 - 4.0	19.86	20.00
4.75 - 2.0	18.40	19.00

* Spraying rates were calculated for standard sample plate which has 0.025

3.4.2 Slurry seal design

Slurry seals are mentioned a mixture of asphalt emulsion, graded aggregates, mineral filler, water and other additives. Three type of slurry seals are identified by ASTM in the standard of ASTM D 3910 (ASTM, 2012b) were used in design of the samples in this thesis.

The aim of manufacturing all types of slurry samples is based on the gradation and differences in usage, where

1- Type 1 has the fines aggregate gradations and is used to fill small surface cracks and provide a thin covering on the existing pavement surface defects,

2- Type 2 has maximum aggregate size of 6.30 mm and is used to treat existing pavements had raveling due to aging, or to improve skid resistance, and the finally,

3- Type 3 has the most coarse aggregate gradations and is used to severe surface defects (Anonymus, 2016b).

The gradations percentages of materials for both advised and used in design of slurry seals samples are given in Table 3.10.

Table 3.10 Advised and used aggregate gradations for slurry seals.

Sieve Size (mm)	Passing (%)					
	Type-1		Type-2		Type-3	
	Advised	Used	Advised	Used	Advised	Used
9.50	-	-	100	100	100	100
4.75	100	100	90-100	95	70-90	80
2.36	90-100	95	65-90	77.5	45-70	57.5
1.18	65-90	77.5	45-70	57.5	28-50	39
0.600	40-60	50	30-50	40	19-34	26.5
0.300	25-42	33.5	18-30	24	12-25	18.5
0.150	15-30	22.5	10-21	15.5	7-18	10.5
0.075	10-20	15	5-15	10	5-15	10

Amount of aggregate for slurry seals have been specified as 4±1, 8±1, 10±1.5 in kg/m^2 for Type 1, Type 2 and Type 3, respectively (ASTM, 2012b). Depending on the area of the plate which is 0.025 m^2; 100, 200, 250 g natural aggregates have been used in total for Type 1, Type 2 and Type 3, respectively. Since the unit weight of EAF slags is higher than the natural ones, slurry seal samples with slags required an arrangement. The amount of slags used to manufacture slurry seal samples were determine according reference limestone (LS-1), and presented in Table 3.11

Table 3.11 The amount of slags used for production slurry seal samples.

Sample ID	Type-1		Type-2		Type-3	
	Calculated	Applied	Calculated	Applied	Calculated	Applied
	g	g	g	G	g	g
EAF-1	127.3	130	254.7	260	318.3	320
EAF-2	127	130	254.0	260	317.4	320
EAF-3	123.9	130	247.9	250	309.9	310
FER	109.7	110	219.4	220	274.3	280

The emulsion application rate is identified depending on the type of slurry seal with percentage of dry aggregate weight. Accordingly, the advised and used application rates of emulsion for each slurry seal type were identified (Table 3.12)

Table 3.12 Application rate of emulsion.

Unit	% Dry Aggregate					
Types	Type-1		Type-2		Type-3	
Application	Advised	Applied	Advised	Applied	Advised	Applied
Rate	10.0-16.0	16.0	7.5-13.5	13.5	6.5-12.0	12.0

3.5 Preparation of Surface Coating Samples

Surface coating samples have been prepared in two ways depending on the types (Chip Seal, Slurry Seal). Chip seal samples were prepared with single size aggregates at different polishing levels. However, slurry seal samples were prepared only with unpolished aggregate. In here, manufacturing processes for both type of samples is explained step by step.

3.5.1 Manufacturing process of chip seal samples

In order to product the chip seal samples, following steps were tracked. Also, some images taken during manufacturing are given in Figure 3.12.

1- Measuring the amount of aggregates in terms of volume, and placing aggregates in a metal box for heating;

2- Heating the plate in an oven at 100±5 ^{o}C;

3- Weighting the amount of bitumen according to aggregate gradations;

4- Heating the bitumen at 145±5 ^{o}C;

5- Pouring the bitumen on the plate, and laying via spatula;

6- Spreading the aggregate uniformly on the bituminous plate;

7- Rolling the sample with a rubber cylinder in both directions for three passes.

8- Curing the samples at room temperature for 24 hours

Figure 3.12 Images in manufacturing process of chip seal samples

3.5.2 Manufacturing process of slurry seal samples

In order to product the slurry seal samples, following steps were tracked. Also, some images taken during manufacturing are given in Figure 3.13.

1- Lining the plate to avoid in any kind of adhesive problems,

2- Weighting the amount of aggregates and emulsion,

3- Conditioning of emulsion in a water bath at temperature 60 $^{\circ}$C for 1 hour,

4- Wetting the aggregates in metals box with a sprayer.

5- Mixing the aggregates and bitumen in a metal box.

6- Paving the prepared mixture on the lined plate.

7- Rolling with a rubber cylinder in both directions for three passes.

8- Curing the samples at room temperature for 24 hours.

Figure 3.13 Images in manufacturing process of slurry seal samples

3.6   Macro Texture Measurements

In this thesis, two different measuring methods have been utilized to determine macro texture depth of each samples. The first method, Sand Patch (SP) Test and the second method is Outflow Meter (OFM) Test method. Both of test methods are relatively simple, and inexpensive method. In here, both of two methods have been presented in detail based on the ASTM standards.

3.6.1   Sand patch test method

Sand Patch is one of the most known and used method for determining the macro texture of pavement surface. The implementation of this test varies due to standards published by different agencies or institutions. In this study, ASTM E 965 (ASTM, 2012d) was used to operate the sand patch test.

In this test method, the volume of materials which is mostly sand that fills the surface voids determines the surface macro-texture depth. The test is implemented on the samples prepared in the laboratory as followings; firstly, a known volume of sand is poured onto a

cleaned surface and spread out in a circular motion with the sand spreader. This spreading motion has been continued until the diameter of circle stabilizes, and sand particles have completely filled the voids, and the sand patch is leveled to the highest points on the surface. After those described processes, the diameter of the circle is measured at four evenly spaced directions. Finally, the average of four readings is determined and the mean texture depth calculated by using following equation Some images taken during manufacturing are given in Figure 3.14.

$$MTD=4V/\pi D^2 \qquad (12)$$

Where,

MTD is mean texture depth,

V is volume, and

D is average diameter.

Figure 3.14 Sand patch apparatus and test operation

3.6.2 Outflow meter test method

The test method is specified by ASTM E 2380 (ASTM, 2012e). This test method covers the connectivity of the texture as it relates to the drainage capability of the pavement through its surface and subsurface voids. It is performed with a specific device which shows how long time takes a known quantity of water to escape through voids in the pavements texture of the structure being tested under gravitational pull.

The main body of the device is a vertical cylinder for containing water. The cylinder has an open top and rubber ring mounted centrally round the orifice or opening on the bottom of the device. Water discharge is through the opening in the center of the seal and is controlled by a spring loaded of cylinder. Upper and lower float switches are suspended from the cap into the cylinder and mounted vertically. An electronic timer which has 0.01 precision is provided and wired to the float switches (Figure 3.15). This property of the instrument benefits to get more accurate and to obtain more sensitive results (ASTM, 2012e).

The procedure for estimating texture depth with this method is briefly given as follows.

1-The device is placed on the samples with the plunger sealing the water discharge opening.

2-Sufficient amount of water is poured in the transparent cylinder to raise the switch floats to their top position, which is prevent the electronic timer from operating.

3-The timer is reset to zero and the plunger is released to allow discharge of the water.

4-As water flows out from the opening of the device through the pavement voids, the water level in the cylinder falls past the upper float switch, which activates the electronic timer to begin counting. As water level continues to fall past the level of the lower float switch, the lower float switch then stop the timer. The time required for the water level in the cylinder to fall from the level of the upper float switch to the level of the lower switch is indicated on the timer (Hydrotimer, 2016).

It is important to mention that performing the more tests provide the better information. Thus, a minimum of four randomly spaced tests are performed, and arithmetic average of the test results being presented as the average time for the sample. Finally, mean texture depth is calculated via following equation.

$$\text{MTD}= \left(\frac{3.114}{\text{OFT}}\right) +0.636 \tag{13}$$

Where,

OFT is average outflow time.

Figure 3.15 Hydrotimer device and test operation.

3.7 Skid Resistance Measurements

British Pendulum Skid Resistance Tester (BPT) is a dynamic pendulum impact-type tester used to measure the energy loss when a rubber slider edge is propelled over a test surface had been used due to their simplicity, low cost and portability. BPT was developed by the British Road Research Laboratory, and consists of following apparatus: pendulum, rubber sliders, thermometer, gauge, water spray bottle, if necessary wind guard, brush, measuring equipment. In this study, ASTM E 303 standard test method was followed in measurement of skid resistance (ASTM, 2012a). This test method provides a measure of a frictional property, micro-texture, of surfaces, either in the field and/or in the laboratory. The results are reported as British Pendulum Numbers (BPNs). To implement the test method on the sample surface the procedure described at bellow which is divided into four steps, which are (1) Preparation the test site and/or sample surface, (2) Zero adjustment, (3) Slide length adjustment, and finally (4) Operation. Herein, all steps is presented in detail.

(1) Preparation of Test Site and/or Sample Surface: It is the first step needed to do. The selected samples (if in the laboratory) or the test site (if in the field) must be swept by the operator to ensure it is free from loose particles. After sweeping, test operator places the BPT on the sample, and levels the device accurately by turning leveling screws until the bubble is centered in the spirit level.

(2) Zero Adjustment: This step is virtually kind of calibration step. It is quiet important to do right. The operator raises the pendulum mechanism via loosening locking knob. Then

turning either of pair of head movement knobs at the center of tester to let the slider to swing free of test surface. After tighten locking knob, the pendulum is placed in release position and rotated the drag pointer counter clockwise until it comes to rest against adjustment screw on the pendulum arm. The pendulum is released and the operator notes the pointer reading. If reading is not zero, the operator loses locking ring and rotates friction ring on bearing spindle slightly and locks again. The operator need to repeat the test and adjust friction ring until the pendulum swing carries pointer to zero.

(3) Length Adjustment: The operator raises slider by lifting handle, moves pendulum to right lower slider, and allows pendulum to move slowly to left until edge of slider touches surface. Then, placing gage beside slider and parallel to direction of swing to verify length of contact path is necessary to determine the first contact point. This is repeated for other edge. If the length of the contact path is not between 124 and 127 mm (47⁄8 and 5.0 in.) on flat test specimens or between 75 and 78 mm (215⁄16 and 31⁄16 in.) on curved polishing-wheel specimens, it is needed to adjust by raising or lowering the instrument with the front leveling screws. Placing the pendulum in release position and rotate the drag pointer -clockwise until it comes to rest against adjustment screw on pendulum arm.

Figure 3.16 Slide length adjustment.

(4) Operation: The last step is performing the test. Before starting the test, it is necessary to wet surface of samples. Thus, the operator wets the pavement surface and slider with water via spray. Then, he/she pushes the release button and allows the pendulum arm to swing freely through its arc, it should be taken into consideration that the operators have to catch the arm on its return swing before the slider touches the sample surface. Without any

delaying, four more swings should be repeated with rewetting the test area each time and finally recording the results (ASTM, 2012a).
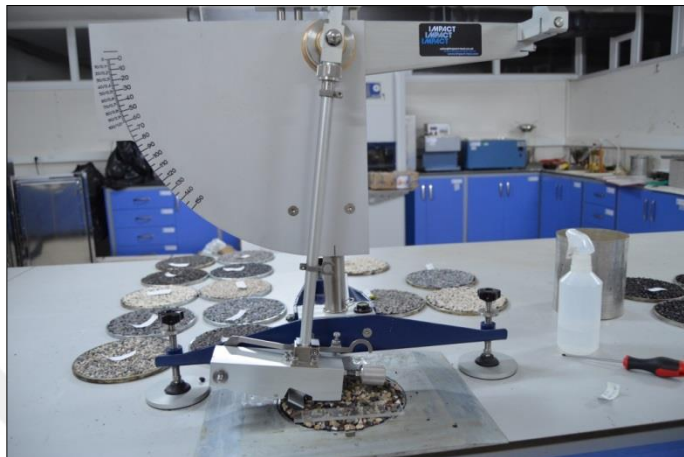
Figure 3.17 Image in operation the test on sample surface.

CHAPTER 4. RESULTS AND DISCUSSION

4.1   Properties of Aggregates

Physical and mechanical of aggregates have been determined in terms of abrasion, fragmentation, weathering, and polishing resistance, and dry unit weight and water absorption for each materials. In addition to physical and mechanical properties, chemical properties via XRF standard test method for each materials were identified. In this section, the results are presented.

4.1.1   Physical and mechanical properties

Physical and mechanical properties of any type of aggregate may vary depending on their geological formations. While lithological characteristic of a material changes, then it is expected that abrasion, fragmentation, weathering, and polishing resistance performance of the material change. In Table 4.1, mechanical and physical properties of natural aggregates and the slags are presented.

Table 4.1 Mechanical and physical properties of natural aggregates and the slags

Tests, Methods & Units		Abrasion Resistance (EN 1097-1)	Fragmentation Resistance (EN 1097-2)	Weathering Resistance (EN 1367-2)	Polishing Resistance (EN 1097-8)	Dry Unit Weight (EN 1097-6)	Water Absorption (EN 1097-6)
		(%)	(%)	(%)	(PSV)	(g/cm^3)	(%)
	LS-1	10.6	24.4	2.4	41.2	2.67	0.44
	LS-2	16.2	21.3	3.0	43.2	2.69	0.24
	LS-3	11.7	24.4	8.1	41.6	2.69	0.28
Sample ID & Test results	BS-1	10.4	12.0	6.9	61.0	2.61	2.00
	BS-2	9.4	25.9	9.4	52.4	2.67	1.44
	BLD	11.3	17.5	6.2	57.9	2.73	0.90
	EAF-1	9.5	22.9	2.3	76.1	3.40	1.79
	EAF-2	8.8	25.3	8.3	59.0	3.39	2.46
	EAF-3	12.3	29.7	3.7	54.1	3.31	2.92
	FER	7.6	16.5	6.1	61.7	2.93	1.10

As seen in Table 4.1, physical and mechanical properties of the selected aggregates are quite variable depending on their sources as expected. Abrasion resistance performance of LS-2 was found out as the worst (16.2%), whereas abrasion resistance of FER was determined as the best (7.6%) among all aggregates. Fragmentation resistance value for BS-1 is 12.0% and for EAF-3 is 29.7%, where may referred as the best and the worst aggregate in terms of fragmentation resistance. Thermal weathering resistance test results vary for each material. Compared to natural aggregates, by-products have better polishing resistance except for BS-1. Slags have higher water absorption percentage, and dry unit weight. As the test results compared with the limitations given in Highway Technical Specifications, a compatibility was observed.

4.1.2 Chemical properties

It is also important to identify the chemical composition of the materials. Thus, the chemical elemental composition for each material was determined by X-ray fluorescence depending on EN-15309 test standard. The results derived from the average results of at least double repetition is presented in Table 4.2

Table 4.2 Chemical compositions of aggregates

No	Components	Materials and Amount of Components in mg/kg									
		LS-1	LS-2	LS-3	BS-1	BS-2	BLD	EAF-1	EAF-2	EAF-3	FER
1	CaO	47.60	48.90	47.50	8.51	7.50	31.00	25.60	21.80	22.60	4.54
2	CO_2	47.00	47.20	46.50	5.64	5.48	28.90	17.50	37.90	18.10	22.00
3	Fe_2O_3	0.42	0.01	0.26	7.35	6.00	4.70	28.70	15.40	26.00	1.35
4	SiO_2	1.37	0.88	1.18	49.90	56.80	22.70	10.60	10.30	12.10	23.80
5	Al_2O_3	0.58	0.15	0.64	18.10	16.00	5.62	5.77	4.45	6.10	14.90
6	MgO	0.46	0.32	0.76	3.27	1.60	4.01	1.65	2.51	4.50	28.30
7	Others	2.58	2.54	3.16	7.23	6.62	3.07	10.18	7.64	10.60	5.11

As known that limestone comprises of chemical elementals such as CaO and CO_2. In this regard, the great amount chemical components for limestone, which obtained from three different quarries was found via XRF test method in the range of 47.00 to 48.90 mg/kg. The great amount chemical component of basalts was determined as SiO_2 49.90 and 56.80 mg/kg. Boulder involved three main chemical components, which are CaO, CO_2 and SiO_2 with amount of 31.00, 28.90, and 22.70 mg/kg, respectively. In addition to CaO, CO_2 and SiO_2 chemical components, Fe_2O_3 was found naturally in chemical compositions of EAF slags. And finally, four main chemical elements have been specified in Ferrochrome slags. These are CO_2, SiO_2, MgO, and Al_2O_3, which constitute 89.00% of chemical component. Therefore, it can be concluded that chemical components naturally vary based on geological formation and manufacturing process of the materials.

4.2   SEM Analysis of Aggregates

As aforementioned that ten types of aggregates were utilized in this study. The origin of them are limestone, basalt, boulder and slags, where obtained from two different sources, steel and ferrochromium. Five of aggregates that representing the aggregates all type of origin were selected for surface monitoring via SEM at different polishing level. The selected aggregates were with sample ID of LS-3, BS-2, BLD, EAF-1, and FER.

Polishing levels of aggregate have chosen at four levels, which are unpolished, 2nd, 3rd and 5th, which identified 0, 10500, 21000, and 52500 revolutions numbers (RNs), respectively. All aggregate samples were chosen randomly from a couple of cubical ones in grain size of 8.00 - 10.00 mm. SEM images for these different kind of aggregates at different polishing levels are given separately at the followings tables.

The first aggregate is limestone, the most common natural aggregate and it is widely used in construction works for different engineering purposes in Turkey, since the geological structure of Turkey conforms the formations of this kind of rocks. Limestone is a

sedimentary rock, which principle composed of carbonate. As mentioned that three types of limestone were chosen for being major source of construction materials. It was decided to examine the surface of limestone encoded with LS-3 for which it was provided at the closest quarry in Adana.

RNs	SEM Images	RNs	SEM Images
0	 a	10500	 b
21000	 c	52500	 d
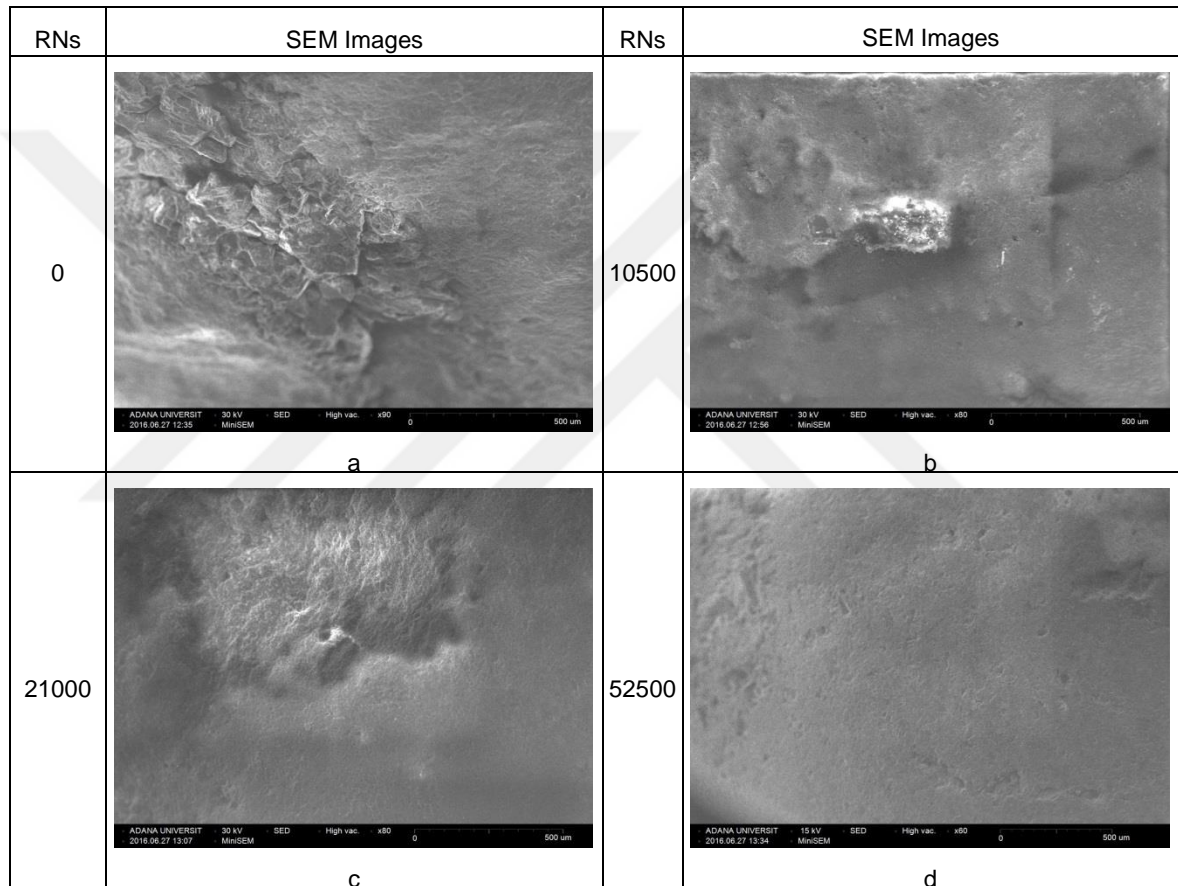
Figure 4.1 SEM images for limestone (LS-3) at different polishing levels

As examining the images given in Figure 4.1, it can be easily to see the polishing process depending on the RNs. To illustrate, the surface micro-texture is obvious in case of unpolished, whereas the surface micro-texture is relatively diminished in case of polishing with 10500, and 21000 RNs via Micro-Deval apparatus. In addition to these, increasing in the number of revolutions up to 52500 RNs, cause continuing to polishing of aggregate surface. As seen in Image "d" that, the aggregate particle is almost completely polished, and a smooth surface were occurred.

The second aggregate is basalt, which is a common extrusive igneous rock formed by the rapid cooling of basaltic lava exposed at or very near the surface of Earth and principally composed of silica. Basalt is a very resistant material in terms of abrasion, fragmentation, freezing-thawing impacts and friction as being presented in the Table 4.1. As mentioned that two types of basalt were chosen. It was decided to examine the surface of limestone encoded with BS-2. Following images given in Figure 4.2 show the changes in the surface characteristics of aggregate depending on polishing.

RNs	SEM Images	RNs	SEM Images
0	a	10500	b
21000	c	52500	d
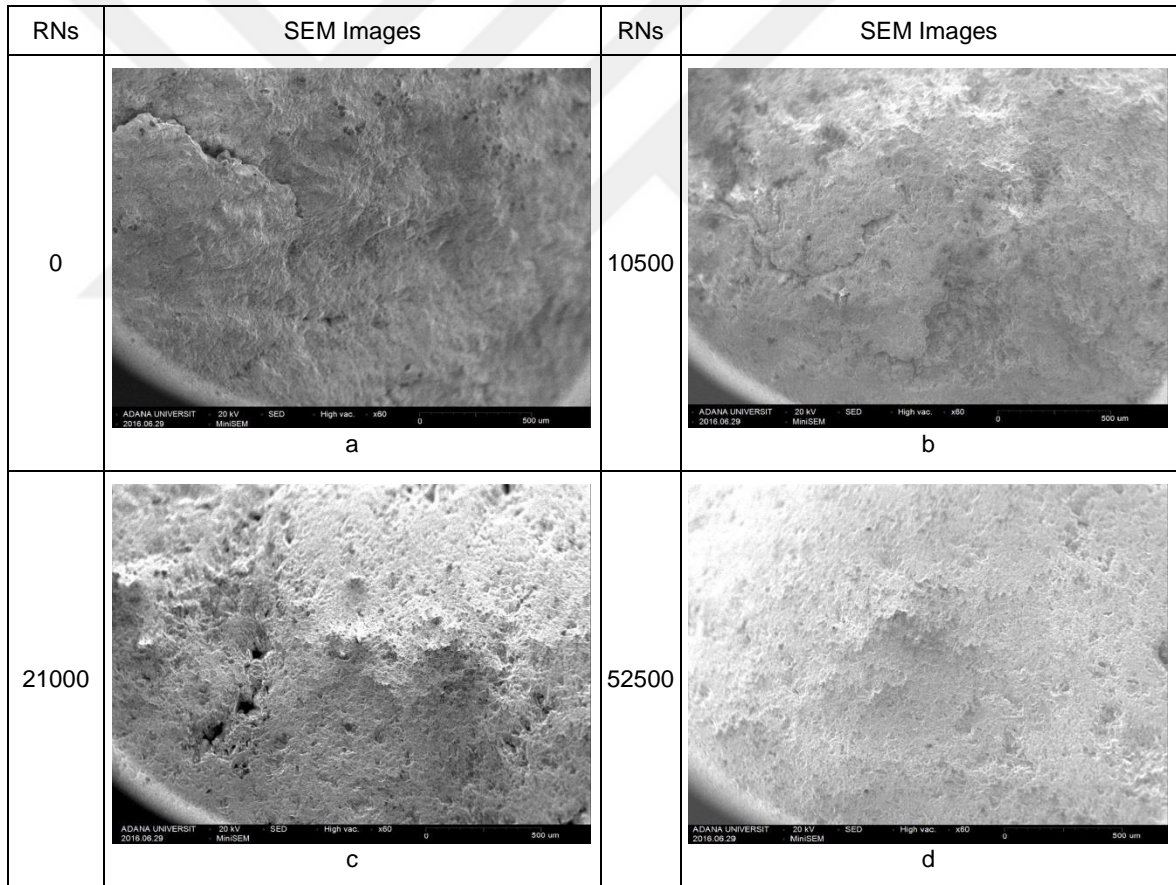
Figure 4.2 SEM images for basalt (BS-2) at different polishing levels

As analyzing the images given in Figure 4.2 depending on polishing at different RNs, there were shown significant differences on the surface of the aggregate, where from the

unpolishing level up to the highest polishing level, the surface was observed quite flattened. Additionally, the porous structure of the basalts can be clearly observed at the SEM images.

Boulder is a material with high quality features in terms of abrasion, fragmentation, freezing-thawing impacts and polishing as being presented in the Table 4.1. Following images given in Figure 4.3 show the changes in the surface characteristics of aggregate depending on polishing.

RNs	SEM Images	RNs	SEM Images
0	a	10500	b
21000	c	52500	d
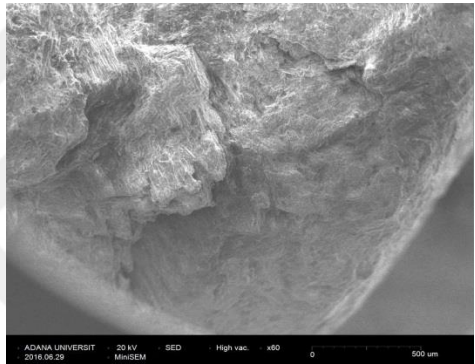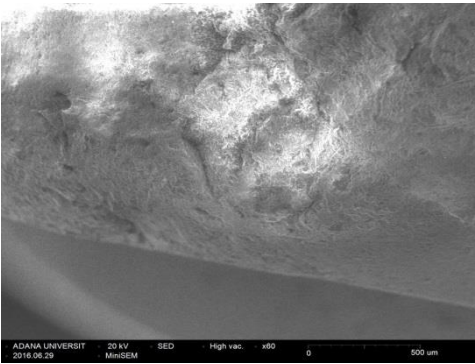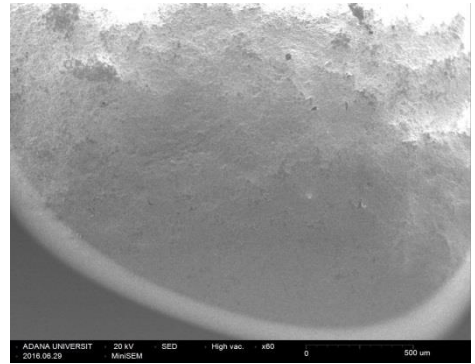
Figure 4.3 SEM images for boulder (BLD) at different polishing levels

As have been examined thoroughly the images given in Figure 4.3, micro-texture aggregate has disappeared, dramatically depending on the polishing levels. In the first (a) and second (b) polishing level, the surface roughness is visible, however is significantly disappeared for the third (c) and fifth (d) polishing level.

As expressed that Turkey is the one of biggest steel producer in the world with the capacity of approximately 50 million tones and EAF comprises 75% of all steel productions (Gökalp

et al., 2016; Uz et al., 2014). Due to huge amount of production, the waste called by-products or slags are emerged in large quantities. Based on relevant studies, it could be indicated that slags have some better properties compared to natural aggregates, and could be used in construction works. One of the superior properties of slags is expressed as resistance to polishing. Following images given in Figure 4.4 show the changes in the surface characteristics of aggregate depending on polishing levels.

RNs	SEM Images	RNs	
0		10500	
21000		52500	
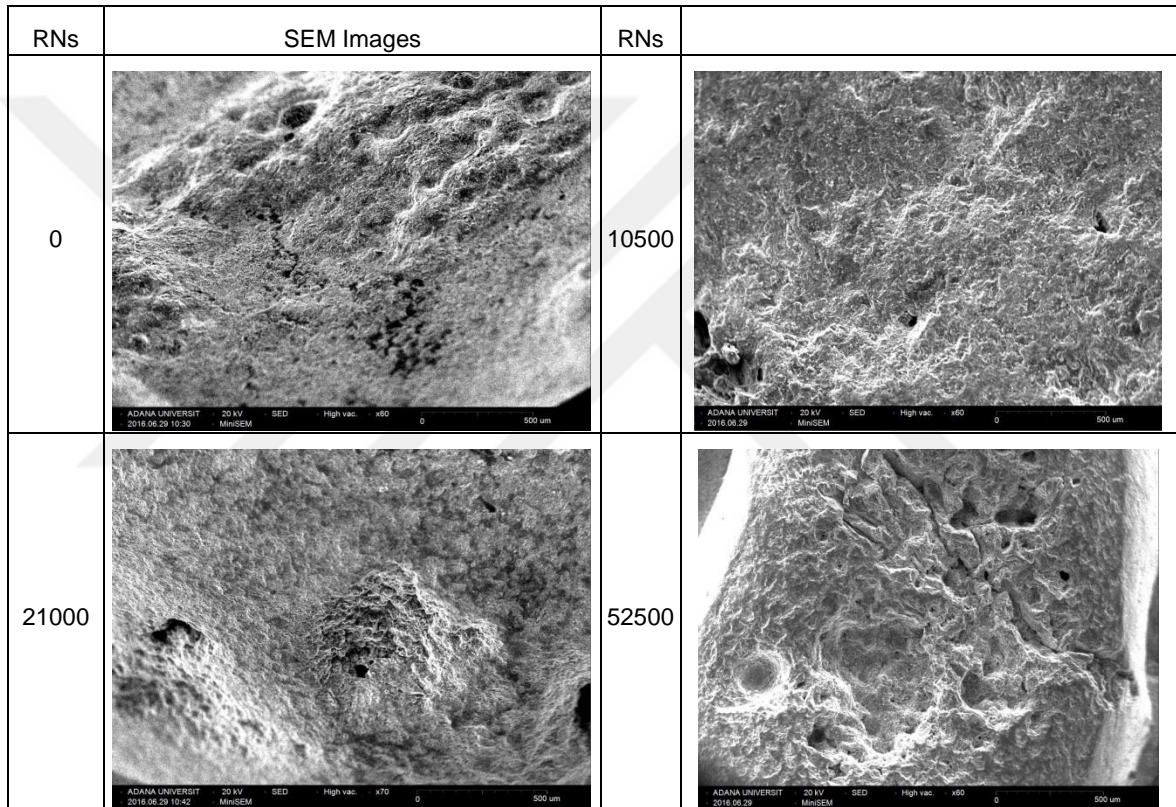
Figure 4.4 SEM images for steel slag (EAF-1) at different polishing levels

The SEM images given in Figure 4.4 show this case, explicitly. As a result of further polishing, micro-texture of the slag particle is decreased. Comparing to polishing resistant slags show better performance than the natural aggregate samples the in each polishing level. For instances, surface roughness of slags at fifth polishing level was seemed to be the same or better than the unpolished level of natural aggregates including limestone, basalt and boulder. Furthermore, an interesting result was encountered at 5th polishing level, where RNs is equal to 52500. In this polishing level, continues cracks were observed unlike

the case observed in other aggregates. Additionally, the porous structure of the slag can be clearly observed at the SEM images.

Ferrochromium slag is another by-product considered for being utilized in the scoped of this study for surface coatings. Similar to EAF slags, it has some of superior compared to by-products by means of abrasion and polishing resistance. To monitor polishing characteristics, SEM were used to obtain the surface images. Following images given in Figure 4.5 show the changes in the surface characteristics of aggregate depending on polishing levels.

RNs	SEM Images	RNs	SEM Images
0	a	10500	b
21000	c	52500	d
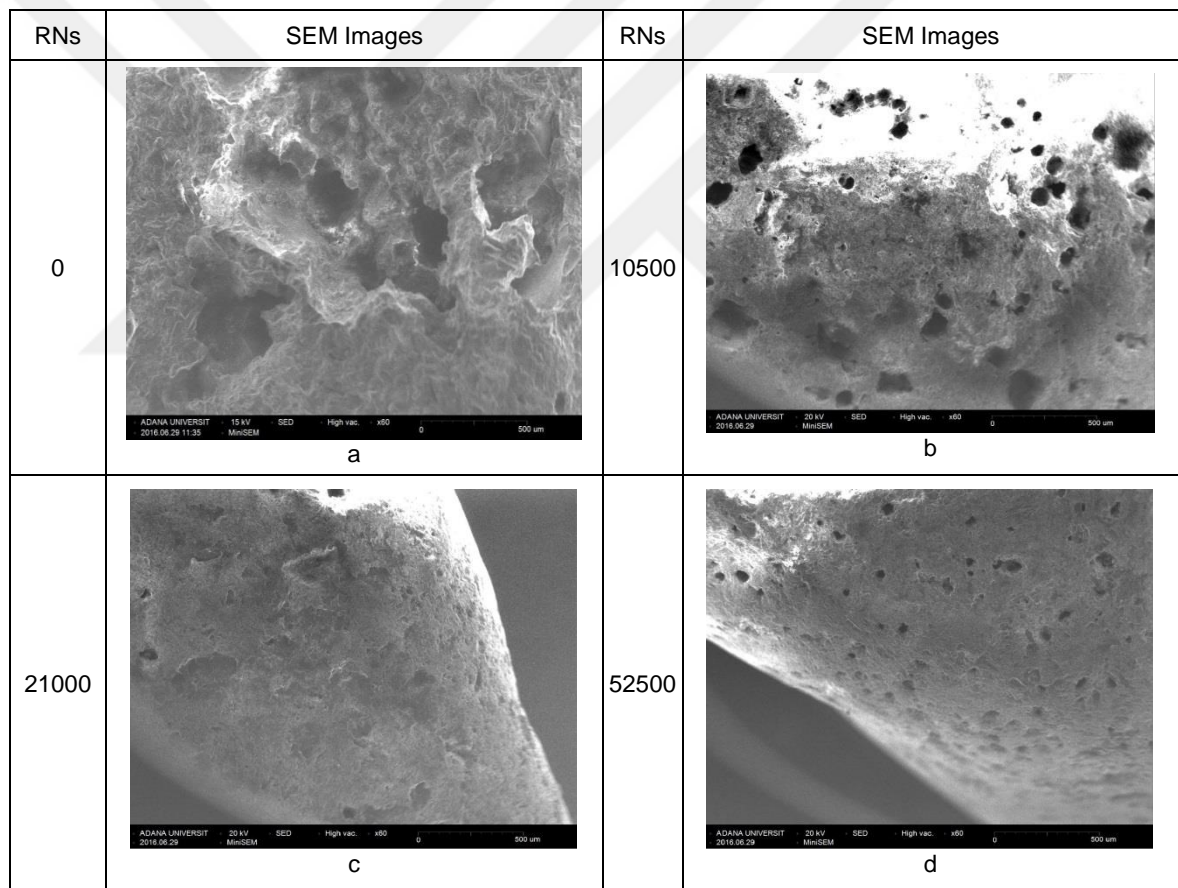
Figure 4.5 SEM images for Ferrochromium slag (FER) at different polishing levels

The SEM based images presented in Figure 4.5 satisfies the superior properties (abrasion and polishing resistance) of the Ferrochromium slag. Comparing with polishing resistant slags show better performance than the natural aggregate samples in each polishing level, whereas comparing with EAF slag, it displays less performance. For instances, surface

roughness of slags even at fifth polishing level was seemed to be better than the first polishing level of other natural aggregate samples. Unlike EAF slags at fifth polishing level, continues cracks were not observed and as the basalt aggregate the porous structure was also observed at FER slag.

4.3   Properties of Bitumen

The selected bitumen for this thesis was considered based on the map published by GDH for usage of bitumen for different regions of Turkey. Depending on the map, the bitumen with 70/100 penetration rate (PR) was used for the Mediterranean region in chip seal applications. To identify some specific properties of the bitumen, a series of tests were conducted. These tests are penetration, softening point before and after ageing, mass change, retained penetration, flash point, and solubility test. The test methods, and results are presented in Table 4.3.

Table 4.3 Properties of bitumen.

Properties	Unit	Test Methods	Test Results
Penetration	× 0.1 mm	EN 1426	76
Softening Point	^{0}C	EN 1427	48
Mass change	%	EN 12607-1	0.8
Retained penetration	%	EN 1426	46
Softening point after hardening	^{0}C	EN 1427	45
Flash Point	^{0}C	EN ISO 2592	230
Solubility	wt %	EN 12592	99

It is crucial to determine the adhesion characteristic between aggregate and bitumen. If there is no adequate adhesion between aggregates and bitumen, retention of aggregates may be possible. In this study, steel plate was utilized to manufacture surface coating samples. Thus, it is utmost important to provide good adhesion between bitumen and aggregates Based on this case, Vialit plate and Nicholson stripping was conducted on materials. In this regard, neat and modified bitumen were utilized. Bitumen was modified with a kind of adjuvant namely DOP in quantity 0.1% and 0.2% by weight. The results of the tests with neat and modified bitumen (0.2%) are given in Table 4.4.

Table 4.4 Affinity characteristics of aggregates with bitumen.

Sample ID	Vialit Plate Test with NB	Vialit Plate Test with MB	Stripping Test with NB	Stripping Test with MB
	%	%	%	%
LS-1	4	3	80-85	85-90
LS-2	3	1	80-85	95-100
LS-3	4	1	85-90	70-95
BS-1	2	1	60-65	85-90
BS-2	2	1	75-80	95-100
BLD	3	2	60-65	95-100
EAF-1	4	1	50-55	80-85
EAF-2	4	1	45-50	80-85
EAF-3	2	1	55-60	80-85
FER	2	1	85-90	90-95

NB: Neat Bitumen, MB: Modified Bitumen (0.2%)

It can easily be seen that affinity between aggregates and bitumen is low with neat bitumen. Although modification of bitumen with 0.2% adjuvant (DOP) is sufficient according to the HTS limits for both tests, for preventing loss of aggregates during the BPT test and to provide better adhesion 0.4% additive by weight was considered to use for all chip seal productions.

4.4   Macro-Texture Measurement

In this thesis, macro texture depths (MTDs) of surface coating samples including chip seals and slurry seals were evaluated with two standard volumetric test methods The volumetric standard test methods are as aforementioned that sand patch test and outflow meter test methods, which are specified in ASTM E 965-12, ASTM E 2380-12, respectively. MTDs derived by sand patch (SP) and outflow meter (OFM) test methods for chip seal and slurry seal samples are given in this section.

4.4.1   Sand patch test

MTDs have been determined for each type of aggregate, grading size and polishing level for both surface coatings (chip seal and slurry seal). As looking the MTDs results given in Table

4.5, the smaller MTDs were obtained on samples produced with natural aggregates, while the bigger MTDs were found out on samples manufactured with slags throughout all grain sizes. For examples, MTDs for the samples produced with BLD is the lowest (2.39 mm) and with EAF-3 is identified as the highest (3.44 mm) for 4.75- 2.00 mm. On the other hand, MTDs for the samples produced with LS-2 is the lowest (7.70 mm) and with EAF-3 is identified as the highest (10.56 mm) for 19.00 – 16.00 mm chip size. In addition, the MTDs increase while grain sizes increase for all type of aggregates.

Table 4.5 MTDs for chip seal samples with unpolished aggregate.

Grain Sizes (mm)	Sample ID and MTDs (mm)									
	LS-1	LS-2	LS-3	BS-1	BS-2	BLD	EAF-1	EAF-2	EAF-3	FER
4.75 – 2.00	2.69	2.61	2.52	2.87	3.34	2.39	2.56	3.30	3.44	3.17
6.30 – 4.00	2.93	2.88	2.60	3.36	3.58	3.11	3.44	4.05	3.32	3.40
8.00 – 6.30	4.14	3.51	4.11	4.33	4.09	3.85	4.72	4.90	4.90	4.54
10.00 – 8.00	4.64	4.36	4.70	5.02	4.51	4.76	5.24	5.82	5.04	5.22
12.50 – 10.00	5.11	5.11	5.22	5.86	6.05	5.66	6.24	6.97	6.85	6.42
16.00 – 12.50	7.92	6.65	7.44	7.40	7.94	6.86	8.84	8.67	8.90	8.09
19.00 – 16.00	8.81	7.70	8.53	9.05	9.53	8.55	10.11	9.40	10.56	10.01

Slurry seal is another type of surface coating. Three types of gradations were used for producing slurry seal samples with unpolished aggregates based on related standard method for all aggregates types. MTDs have been determined for each type of gradations (Table 4.6).

Table 4.6. MTDs for slurry seal samples.

Types	Sample ID and MTDs(mm)									
	LS-1	LS-2	LS-3	BS-1	BS-2	BLD	EAF-1	EAF-2	EAF-3	FER
Type-1	0.65	0.68	0.59	0.83	0.71	0.65	0.59	0.87	0.59	0.67
Type-2	0.86	0.70	0.64	0,98	0.82	0.77	0.87	1.02	0.74	0.97
Type-3	1.06	0.92	0.76	1.09	0.97	1.03	1.51	2.18	1.45	1.59

In Table 4.6, as it was expected that, MTDs for all samples was found as the lowest in Type1 and as the highest in Type3 samples, where samples with slags have higher MTDs. This results may be caused due to their gradations. Since, Type 1 has the finest gradation, whereas Type 3 has the coarsest gradation.

Four different aggregate particle sizes in range of 12.50 – 4.00 mm used to generate chip seals at different polishing levels. Because, polishing of aggregates was performed via Micro-Deval apparatus considering simulating the polishing under traffic loads, which specified in ASTM D 6928 within nominal aggregate size of 12.50 mm.

In Table 4.7 MTDs for chip seal samples manufactures with polished aggregate at different level have been presented, and a statistical analysis was conducted in terms of standard deviation and average MTDs regarding on the samples. As analyses the MTDs results, it is obvious that there is no continually decrease or increase in MTDs depending on both aggregate size and type.

An interesting results was pointed out that standard deviations computed of surface coating samples produced with natural aggregates at different polishing level was lower (ranges 0.07 to 0.45 in mm) than of the samples produced slags at different polishing level (ranges 0.12 to 0.56 in mm). Also, standard deviation is decreasing significantly, while grain size is decreasing.

Table 4.7 MTDs for chip seal samples with polished aggregate

Grain Sizes (mm)	Polishing Level	Sample ID and MTDs (mm)									
		LS-1	LS-2	LS-3	BS-1	BS-2	BLD	EAF-1	EAF-2	EAF-3	FER
12.50 – 10.00	1st	4.95	4.86	4.93	5.19	4.93	5.22	5.84	6.63	6.17	5.34
	2nd	4.78	4.41	4.95	4.57	4.93	5.09	6.05	5.84	5.75	5.40
	3rd	4.45	4.09	4.73	4.33	4.68	4.65	5.84	5.52	5.26	5.02
	4th	4.10	3.55	3.86	4.25	4.50	4.21	4.90	5.09	5.30	4.68
	5th	4.68	4.57	4.62	4.59	4.68	4.48	5.66	5.77	5.33	4.97
Average MTDs		4.59	4.59	4.30	4.62	4.59	4.74	4.73	5.66	5.77	5.56
Standard Deviations		0.29	0.29	0.45	0.40	0.33	0.17	0.38	0.40	0.50	0.35
10.00 – 8.00	1st	4.22	4.00	4.39	4.70	4.48	4.80	5.54	5.08	4.59	4.15
	2nd	4.28	3.52	4.38	3.90	4.06	4.00	4.80	4.81	4.76	4.33
	3rd	3.80	3.18	3.76	3.77	4.02	3.89	5.22	4.59	4.53	4.10
	4th	3.63	2.99	3.44	4.01	3.64	3.58	4.70	5.02	4.81	3.98
	5th	3.53	3.72	3.15	3.56	4.09	4.02	5.33	4.71	4.82	4.02
Average MTDs		3.89	3.48	3.82	3.99	4.06	4.06	5.12	4.84	4.70	4.12
Standard Deviations		0.31	0.36	0.50	0.39	0.27	0.40	0.32	0.18	0.12	0.12
8.00 – 6.30	1st	2.99	3.48	3.31	3.27	3.92	3.46	4.21	4.22	4.10	3.61
	2nd	3.08	3.10	3.37	2.98	3.01	3.44	3.84	3.86	4.00	3.26
	3rd	3.68	2.76	3.29	3.43	3.44	3.25	3.73	3.79	3.96	3.71
	4th	2.90	2.56	2.80	3.17	3.00	2.89	4.09	3.84	3.48	3.44
	5th	2.75	3.18	2.77	3.35	3.45	3.39	3.78	4.16	4.04	3.45
Average MTDs		3.08	3.02	3.11	3.24	3.36	3.29	3.93	3.97	3.92	3.49
Standard Deviations		0.32	0.32	0.27	0.16	0.34	0.21	0.19	0.18	0.22	0.15
6.30 – 4.00	1st	2.26	2.28	2.29	2.50	3.09	2.55	3.10	3.04	3.24	3.03
	2nd	2.27	2.53	2.70	2.53	2.48	2.34	2.65	3.36	3.31	2.71
	3rd	2.10	1.99	2.17	2.63	2.69	2.24	2.58	2.93	2.95	2.33
	4th	2.17	1.85	2.52	2.57	2.66	2.12	2.38	2.83	2.70	2.28
	5th	2.63	2.82	2.58	2.69	2.93	2.70	3.30	2.96	3.11	2.20
Average MTDs		2.29	2.29	2.45	2.58	2.77	2.39	2.80	3.02	3.06	2.51
Standard Deviations		0.18	0.35	0.19	0.07	0.21	0.21	0.34	0.18	0.22	0.31

4.4.2 Outflow meter test (OFM)

MTDs have been determined for each type of aggregate and their grading sizes and polishing level also with OFM test method. In Table 4.8, MTDs for unpolished aggregates 19.00-2.00 mm chip sizes are presented. Similar to SP test methods, the MTDs obtained with OFM increases with increasing particle sizes. However, for samples in grain size of 19.00-16.00 mm, OFM test could not be applied, due to very fast water discharge.

Table 4.8 MTDs for chip seal samples with unpolished aggregate.

Grain Sizes	Sample ID and MTDs (mm)									
(mm)	LS-1	LS-2	LS-3	BS-1	BS-2	BLD	EAF-1	EAF-2	EAF-3	FER
4.75 – 2.00	1.96	1.70	1.72	1.88	2.16	1.59	1.69	2.31	2.39	2.28
6.30 – 4.00	2.01	2.22	1.97	2.86	2.42	2.29	2.71	2.62	2.22	2.98
8.00 – 6.30	3.14	2.47	3.27	3.00	3.26	3.17	3.31	3.14	3.47	3.26
10.00 – 8.00	3.86	3.42	3.40	3.47	4.02	3.85	3.58	3.92	4.11	4.26
12.50 – 10.00	4.11	4.76	4.64	4.14	5.20	4.36	5.60	4.91	5.35	4.56
16.00 – 12.5	6.82	5.50	6.38	5.60	6.49	4.70	6.32	6.67	7.07	5.10
19.00 – 16.00	FM	FM	FM	FM	FM	FM	FM	FM	FM	FM

FM : Fail in Measurement

MTDs for all slurry seal samples were also determined by OFM standard test method. In Table 4.9, the MTDs results were summarized for all type of aggregates. As seen in Table 4.9, similar results were gathered such as the lowest in Type 1, and the highest in Type 3 samples. Also, the higher MTDs values were obtained on the samples produced with slags.

Table 4.9 MTDs for slurry seal samples.

Types	Sample ID and MTDs (mm)									
	LS-1	LS-2	LS-3	BS-1	BS-2	BLD	EAF-1	EAF-2	EAF-3	FER
Type-1	0.89	0.74	0.79	0.83	0.87	0.78	0.75	0.78	0.73	0.72
Type-2	1.08	0.81	0.82	0,98	1.11	0.84	0.85	1.31	1.07	0.91
Type-3	1.37	1.05	1.06	1.09	1.24	0.94	1.73	2.07	1.51	1.71

Another analysis (Table 4.10) has been performed to identify the relative differences of MTD results between the two test methods for all samples. Depending on the results, it can be concluded that, the relative differences between the results of the two methods change according to aggregate type and gradations. Thus, a constant change was not observed. Although, Aktaş et al. (2011) quoted that the differences between the two methods for chip seals was higher than 30%, in this study approximately 70% of chip seal sample results were calculated lower than 30%.

Table 4.10 Relative Differences in MTDs (%) between SP and OFM methods

Sample ID	Chip Seal (mm)						Slurry Seals		
	2.0-4.75	4.0-6.3	6.3-8.0	8.0-10.0	10.0-12.5	12.5-16.0	Type-1	Type-2	Type-3
LS-1	31.6	24.3	20.5	27.7	11.2	14.3	34.5	29.0	39.0
LS-2	27.3	31.4	24.2	16.7	19.6	13.9	36.6	26.3	29.3
LS-3	34.8	23.0	29.7	21.6	7.0	17.2	9.0	15.2	14.4
BS-1	35.3	32.4	20.1	10.9	14.0	18.3	21.4	36.4	27.8
BS-2	34.6	14.9	30.8	31.0	29.3	24.4	21.3	23.3	8.9
BLD	33.5	26.6	17.7	19.3	23.0	31.5	21.2	9.3	8.9
EAF-1	34.0	21.4	29.9	31.7	10.4	28.6	28.0	2.3	14.7
EAF-2	30.2	35.3	36.0	32.6	29.5	23.0	11.1	28.0	5.2
EAF-3	30.7	33.3	29.1	18.4	21.9	20.6	24.3	45.7	4.0
FER	28.0	12.5	27.9	18.5	29.0	36.6	7.6	5.4	7.8
Average	32.0	25.5	26.6	22.8	19.5	22.9	21.5	22.1	16.0
σ (SD)	2.7	7.4	5.5	7.1	8.0	7.1	9.5	13.2	11.3

In Table 4.11, MTDs for chip seal samples manufactured with polished aggregate, within four different aggregate particle sizes in range of 12.50 – 4.00 mm. A statistical analysis was conducted in terms of standard deviation and average MTDs regarding on the samples. Similar to MDTs obtained via sand patch standard methods, no continually decrease or increase was observed in MTDs based on both aggregate grain sizes and aggregate types. Also, standard deviation is decreasing significantly, while grain size is decreasing.

Table 4.11 MTDs for chip seal samples with polished aggregate

Grain Sizes (mm)	Polishing Level	Sample ID and MTDs (mm)									
		LS-1	LS-2	LS-3	BS-1	BS-2	BLD	EAF-1	EAF-2	EAF-3	FER
12.50 – 10.00	1st	3.94	4.29	3.86	3.87	3.96	3.79	4.79	4.32	4.67	4.07
	2nd	3.91	3.64	4.33	3.98	4.39	4.38	4.23	4.10	4.58	4.04
	3rd	3.87	3.37	4.09	3.34	4.03	3.62	4.64	4.01	4.67	4.18
	4th	3.73	3.05	3.60	4.07	4.65	3.81	3.99	3.87	3.65	4.44
	5th	3.8	3.71	3.97	3.82	4.29	4.01	4.24	4.08	4.24	4.27
Average MTDs		3.85	3.85	3.61	3.97	3.82	4.26	3.92	4.38	4.08	4.36
Standard Deviations		0.08	0.08	0.41	0.24	0.25	0.25	0.26	0.29	0.15	0.39
10.00 – 8.00	1st	3.55	3.21	3.36	3.46	3.33	3.41	3.42	3.69	3.77	3.71
	2nd	3.47	3.33	3.42	3.40	3.51	3.83	3.60	3.84	3.81	3.85
	3rd	3.14	3.16	3.22	2.91	3.34	3.26	3.83	3.58	3.35	3.37
	4th	3.41	2.81	3.29	3.67	3.76	3.35	3.65	3.43	3.48	3.91
	5th	3.36	3.55	2.63	3.34	3.62	3.54	4.04	3.81	3.64	3.68
Average MTDs		3.39	3.21	3.18	3.36	3.51	3.48	3.71	3.67	3.61	3.70
Standard Deviations		0.14	0.24	0.28	0.25	0.16	0.20	0.21	0.15	0.17	0.19
8.00 – 6.30	1st	2.62	2.30	2.74	2.94	3.19	2.84	3.01	2.59	3.14	3.04
	2nd	2.64	2.92	2.94	2.66	3.10	3.21	3.22	3.05	2.88	3.40
	3rd	2.66	2.87	2.69	2.72	2.95	2.66	3.12	3.15	3.05	2.91
	4th	2.17	2.10	2.14	2.55	2.49	2.62	2.78	2.72	2.65	3.39
	5th	2.58	2.47	2.51	2.88	2.88	3.11	2.91	3.55	3.06	3.08
Average MTDs		2.53	2.53	2.60	2.75	2.92	2.89	3.01	3.01	2.96	3.16
Standard Deviations		0.18	0.32	0.27	0.14	0.24	0.24	0.15	0.34	0.17	0.20
6.30 – 4.00	1st	1.94	1.89	2.00	2.12	2.32	1.85	2.36	2.43	2.15	2.28
	2nd	2.29	2.06	2.66	1.97	2.53	2.16	2.39	2.62	2.52	2.66
	3rd	2.10	2.03	1.94	2.27	2.43	2.03	2.53	2.52	2.41	2.02
	4th	1.82	1.80	1.91	2.07	2.23	2.04	2.20	2.14	2.31	2.10
	5th	2.77	2.48	2.33	2.08	2.67	2.47	2.42	2.43	2.32	1.81
Average MTDs		2.18	2.05	2.17	2.10	2.44	2.11	2.38	2.43	2.34	2.17
Standard Deviations		0.33	0.23	0.29	0.10	0.15	0.21	0.11	0.16	0.12	0.29

4.4.3 Comparative evaluations of macro texture depths test methods

MTDs evaluated according to aggregate type, grading size for chip seal and slurry seal with two different test methods. The results were compared and best-fit lines were drawn and coefficient of regressions (R^2) were computed. In the Figure 4.6, MTD distribution according to aggregate type for chip seal and slurry seal samples is given. It can be clearly seen in Figure 4.6 that, both test results for all types of aggregates are closing to each other when MTDs are low, whereas aparting from each other when MTDs are high.
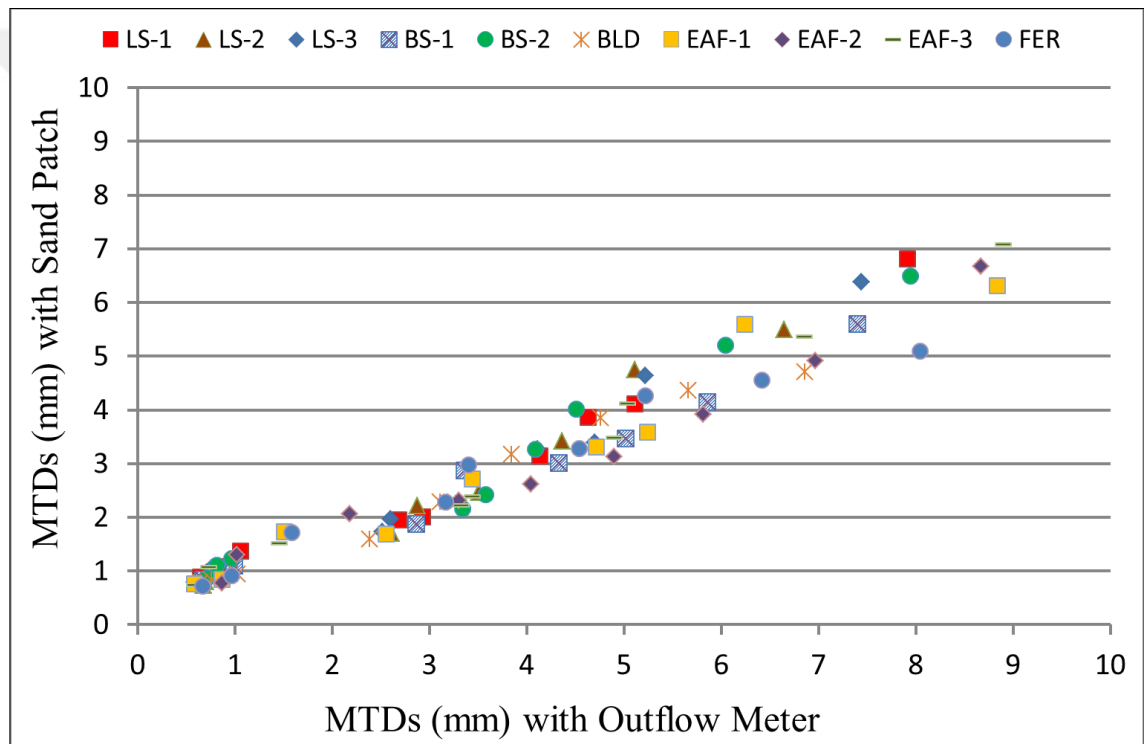
Figure 4.6 Comparison of MTDs for SP and OFM test methods

Additional figures were also drawn to express the relation between the MTDs obtained with the two test methods for each surface coating applications. The graphs given in Figure 4.7 that there is a strong correlation between the SP and OFM test method throughout all samples. The coefficient (R^2) was computed nearly 96% considering all samples. On the other hand, R^2 values were computed for chip and slurry seal samples nearly 93% and 88%, respectively as given Figure 4.8 and Figure 4.9.
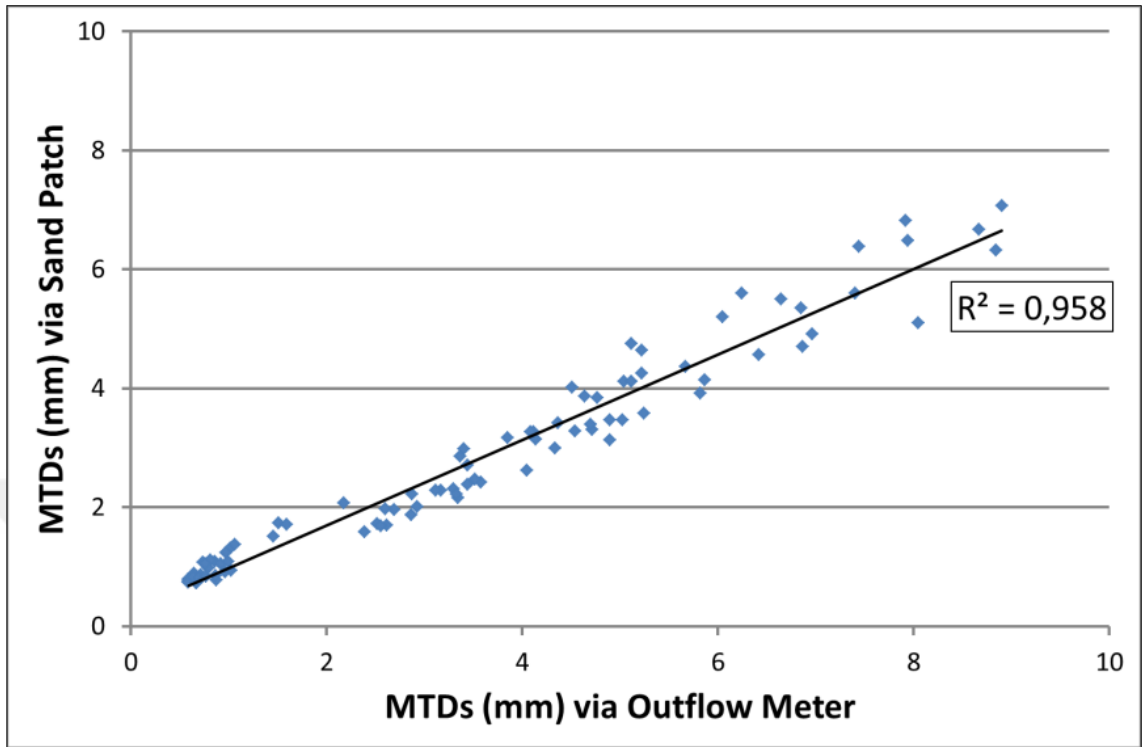
Figure 4.7 Linear regression analysis considering all samples
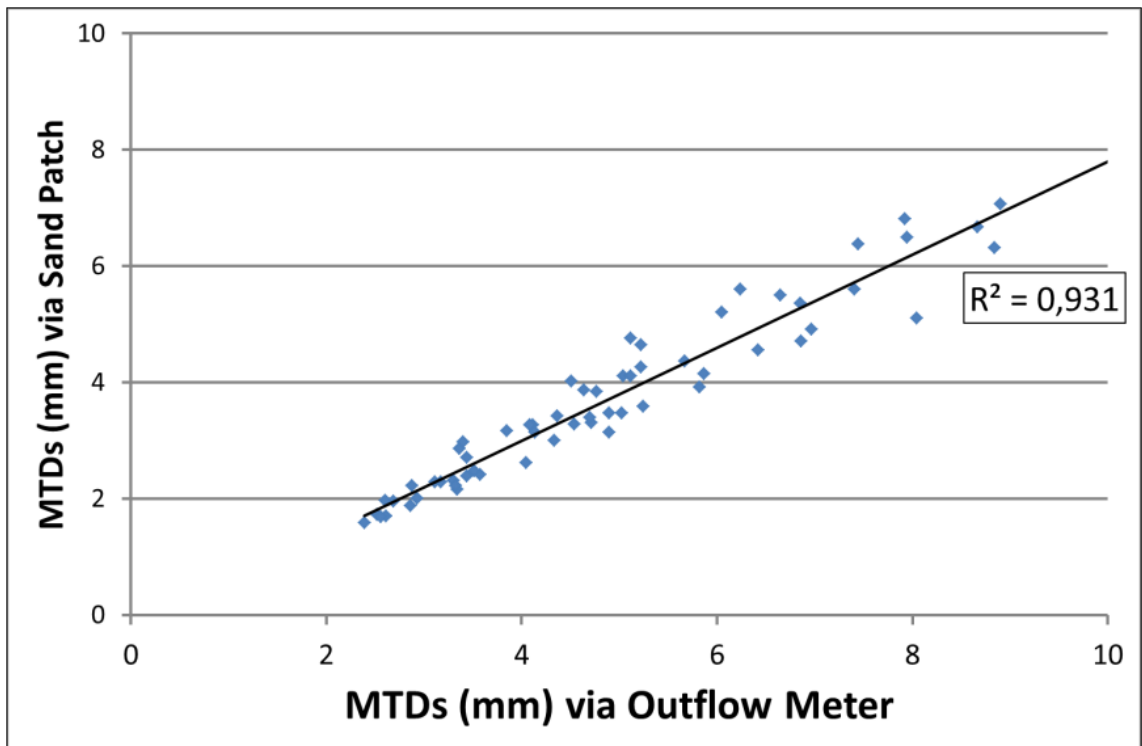
Figure 4.8 Linear regression analysis considering chip seal samples
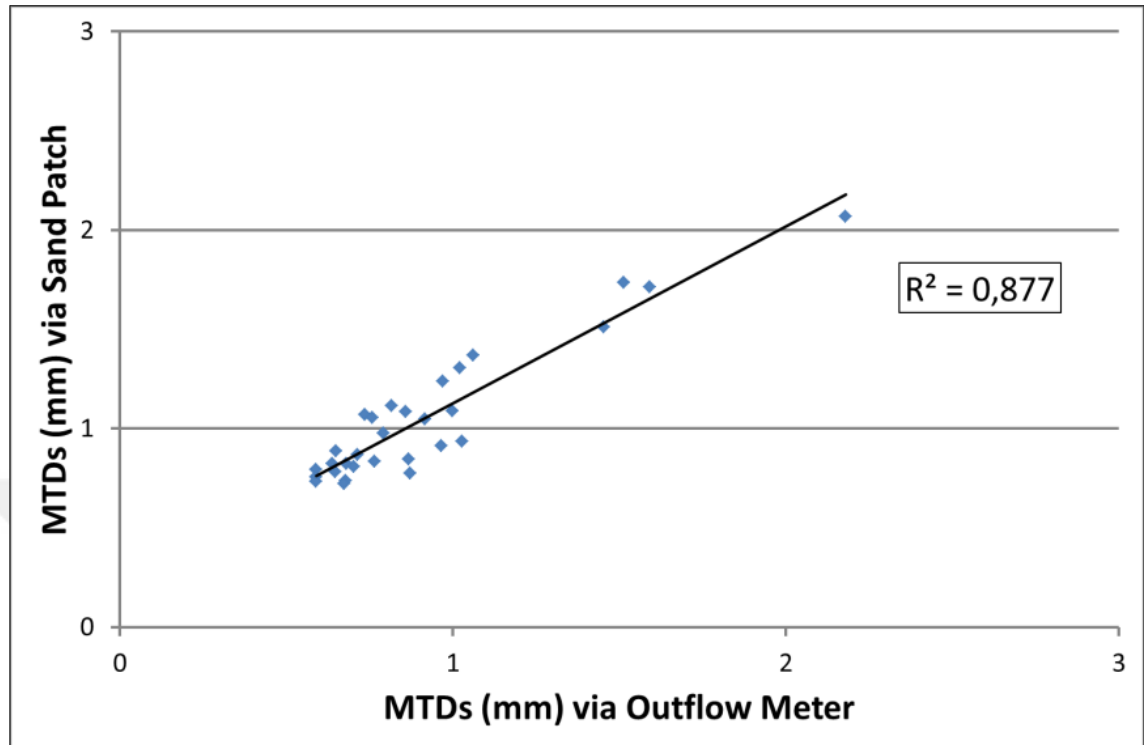
Figure 4.9 Linear Regression analysis considering slurry seal samples

Based on the all computations, applicability of both sand patch and outflow meter test method was examined for each surface coating. As a result, MTD relative differences of SP and OFM test results for all chip seal samples were determined as 21% in average. Additionally, each test method is able to specify the MTDs with increasing aggregate sizes; but 6 mm MTD can be identified as a threshold for implementation of OFM test method.

4.5   Skid Resistance Measurement

In this section of this thesis, skid resistance (SR) has been evaluated for both samples manufactured with unpolished and polished aggregates. Therewithal, comparative analysis was performed to see the relationships between SR and MTDs for both of two surface coating samples in case of unpolished level.

4.5.1   Skid resistance variations respect to polishing levels

Chip seals have been manufactured with unpolished and polished aggregates at four different chip sizes in range of 12.50 – 4.00 mm. The following figures (from Figure 4.10 to Figure 4.13) were drawn in order to express the SR performance of each aggregates in the same aggregate grain sizes, but at different polishing levels in the same labels.
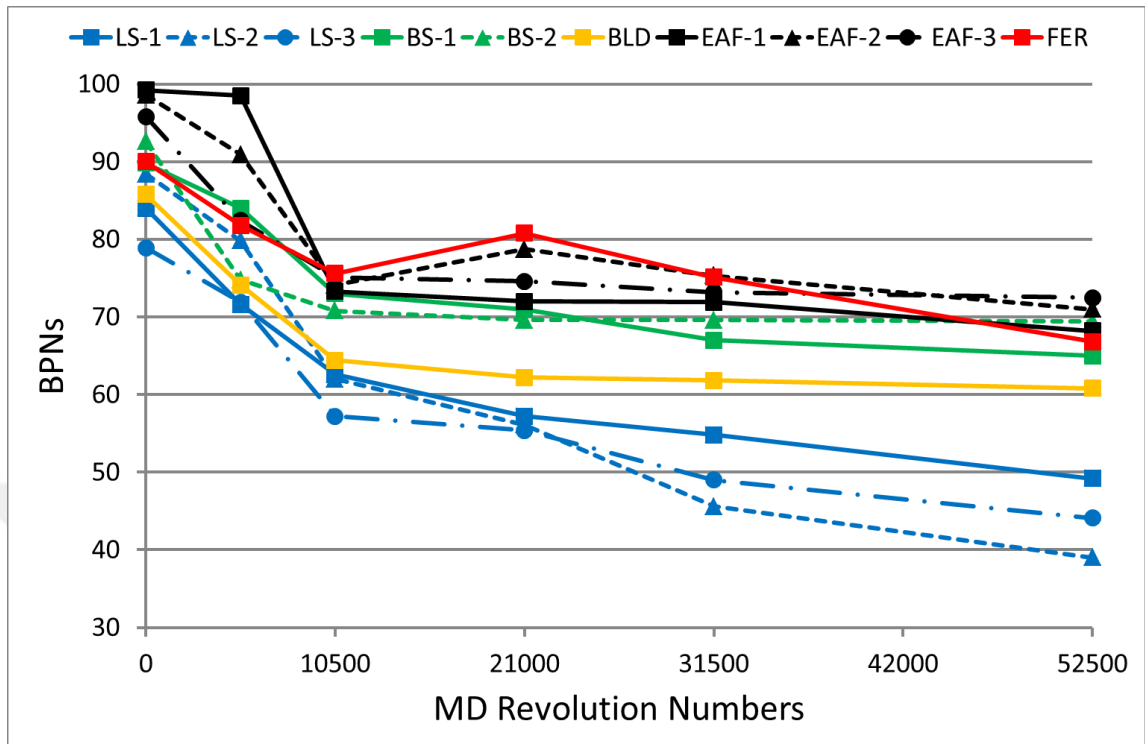
Figure 4.10 BPNs for 12.50-10.00 mm chip seal samples at different polishing levels

Figure 4.11 BPNs for 10.00-8.00 mm chip seal samples at different polishing levels

Figure 4.12 BPNs for 8.00-6.30 mm chip seal samples at different polishing levels

Figure 4.13 BPNs for 6.30-4.00 mm chip seal samples at different polishing levels

As analyzing the figures obtained for each material, we can indicate the following results.

1. Generally, skid resistance (SR) decreases as polishing level (respect to RNs) increases. In exceptional, this tendency changes particularly in the slags at 10500, 21000 RNs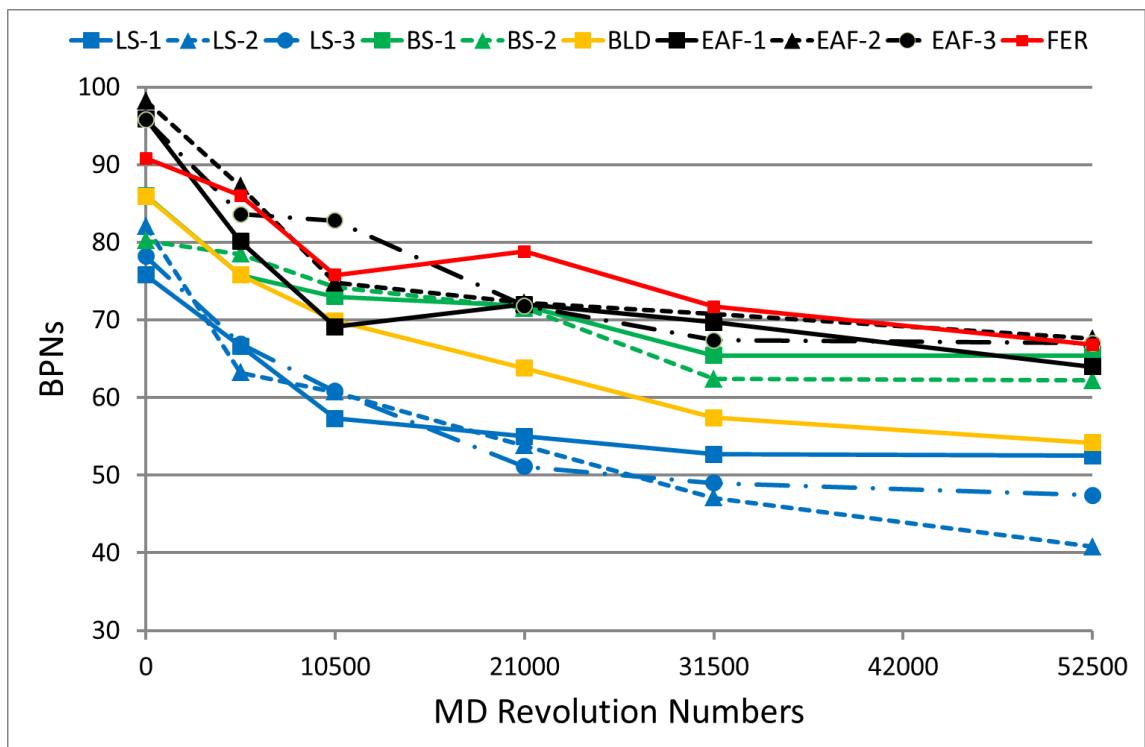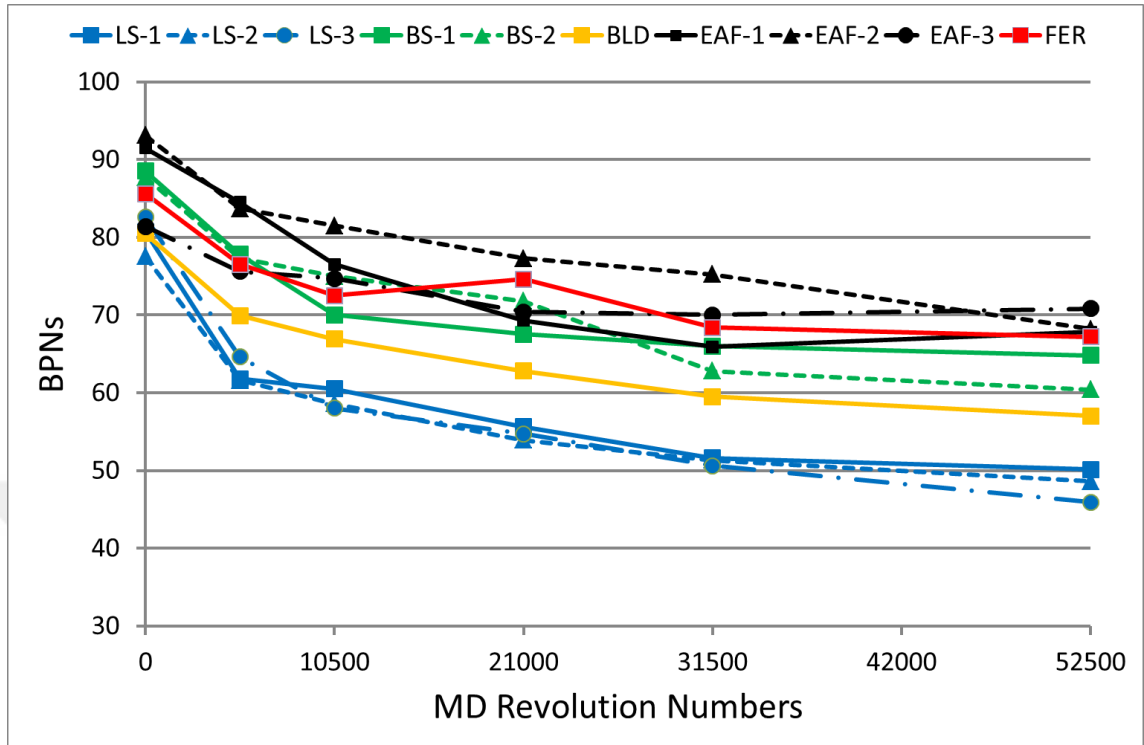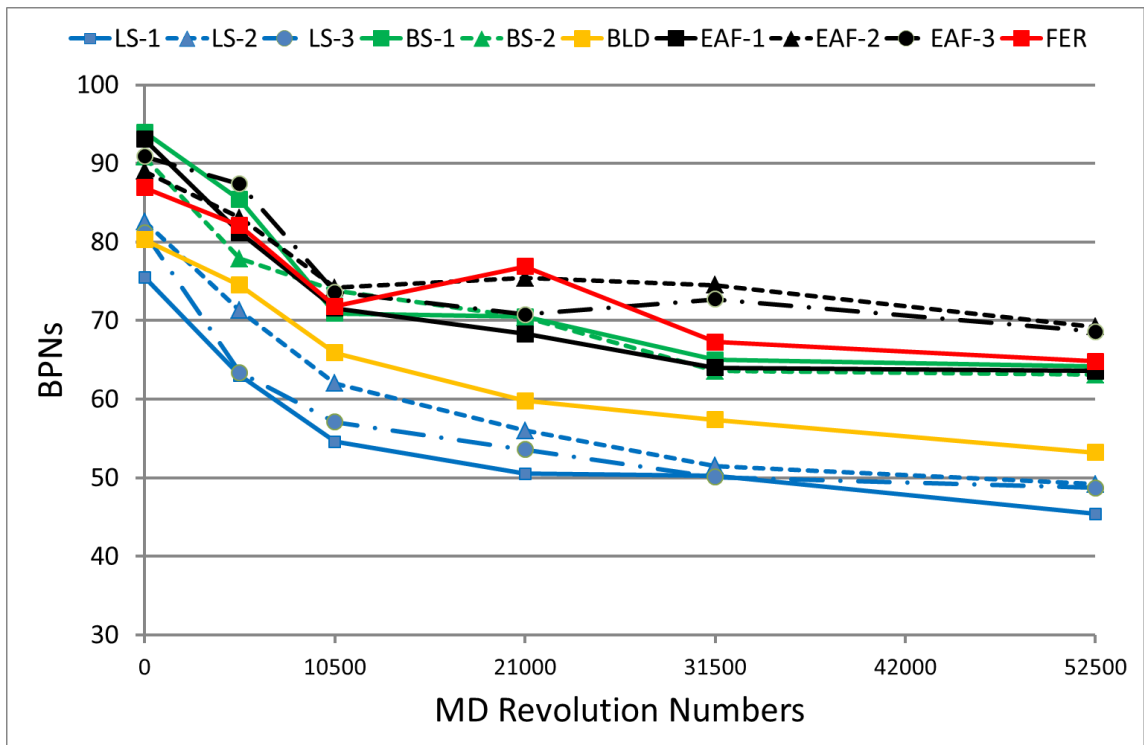. Skid resistance is normally supposed to decrease in these polishing level, however an increase was observed in these levels. The reason of this may be attributed with porous structure of the slags. Due to porous structure, new texture reveals as polishing continues.

2. As will be seen from the results, the lowest SR performance were observed in limestone both at unpolished and polished levels. SR performance followed by limestone can be given in order of boulder, basalts, EAF slag and Ferrochromium slags from the lowest to highest, respectively. An interesting results were occurred that skid resistance of all aggregates except of limestone at different polishing level tend to be constant. A continuous decreasing in SRs was observed throughout all chip sizes of limestone depending on RNs or polishing level.

3. Slags have better resistance to polishing as aforementioned. Accordingly, the results support this aspect. Since, BPN gathered at the highest polishing level (RNs:52500) is approximately 70, which is close to the BPNs gathered at the unpolished and/or second polishing level of natural aggregates.

4.5.2 Comparative evaluation of MTDs and SR measurements

To manufacture chip seals and slurry seals with unpolished state, seven different chip sizes and three type of aggregate gradations were utilized, respectively. In this section of this thesis, comparative evaluations have been performed. The aim is to reveal the relationship of the MTDs with SR in terms of BPNs. To achieve this, following figures (from Figure 4.14 to Figure 4.16) were presented. As will be seen that, the materials have been grouped in to three class such as limestone, basalts and boulder, and slags.

In Figure 4.14, MTDs and BPNs for the first group of aggregates, which includes LS-1, LS-2 and LS-3 are given. The figure shows that MDTs are decreasing with decreasing in grain sizes for chip seals, and changing with respect to gradations for slurry seals. As expected that, MTDs for Type-3 slurry seal samples as the greatest, and for Type-1 as the lowest. Although a continuous decreasing has observed in MTDs with the decreasing aggregate sizes, this tendency were not observed in BPNs. BPNs change significantly according to aggregate sizes in an irregular manner.
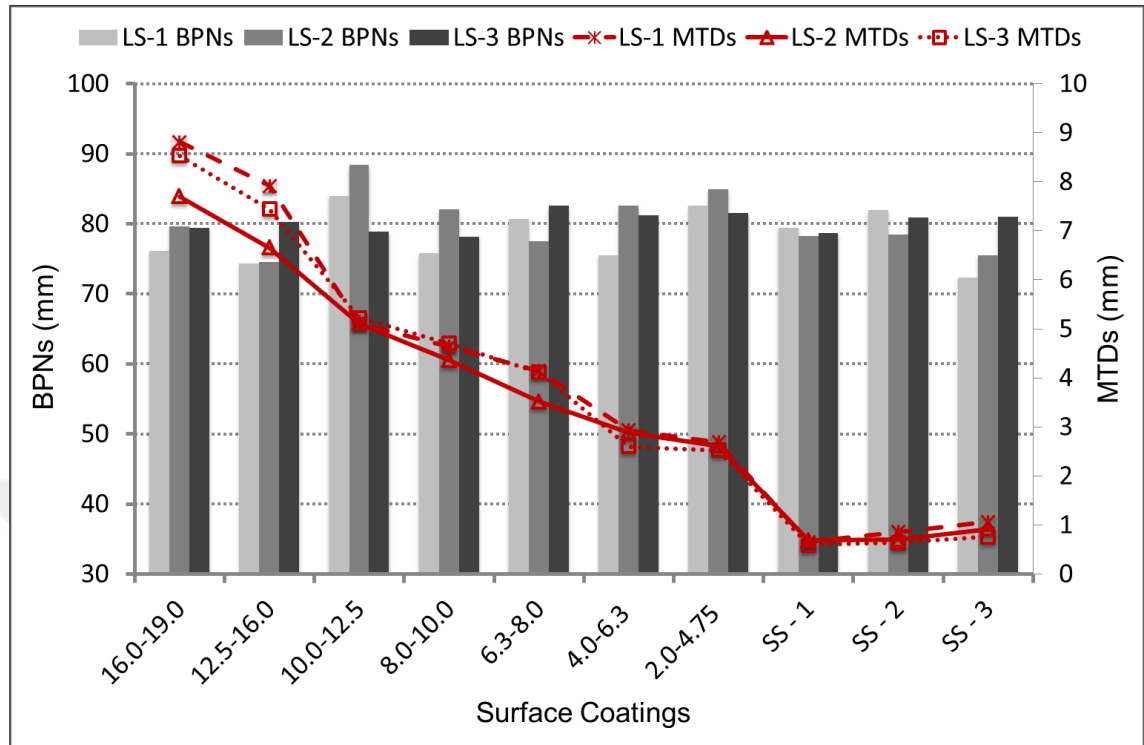
Figure 4.14 Comparative analyses of MTDs and BPNs for limestone

In Figure 4.15, MTDs and BPNs for the second group of aggregates, which includes BS-1, BS-2 and BLD are given. Similar to the first group of aggregates, MTDs tend to decrease with decreasing aggregate grain sizes, and tend to increase with aggregate gradations, which have more coarse amount of aggregate. It is apparent that, an irregular distribution of BPNs have been observed based on not only grading size, but also aggregate types, and gradations.

The final group consists of slags. Herein, BPNs for each of the four slags have been compared with MTDs of them (Figure 4.16). A surprising result was not observed in this evaluations as well. The MTDs are inclined to decrease as grading sizes decreases, and no regular differences between the BPNs results based on aforementioned variables. It is clearly shown that, an irregular distribution of BPNs have been observed based on not only grading size, but also slag types, and gradations. Also, comparing with natural aggregates in terms of BPNs, it may be implied that slags have significant superior skid resistance performance in both type of surface coatings.
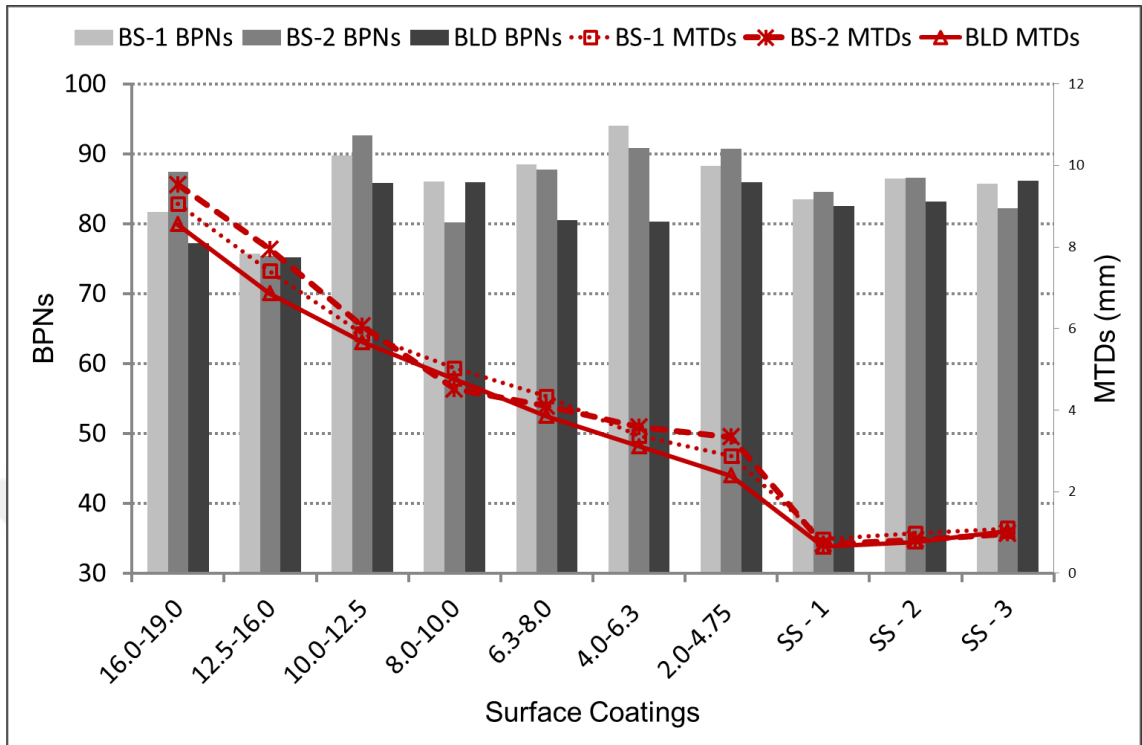
Figure 4.15 Comparative analyses of MTDs and BPNs for basalts and boulder
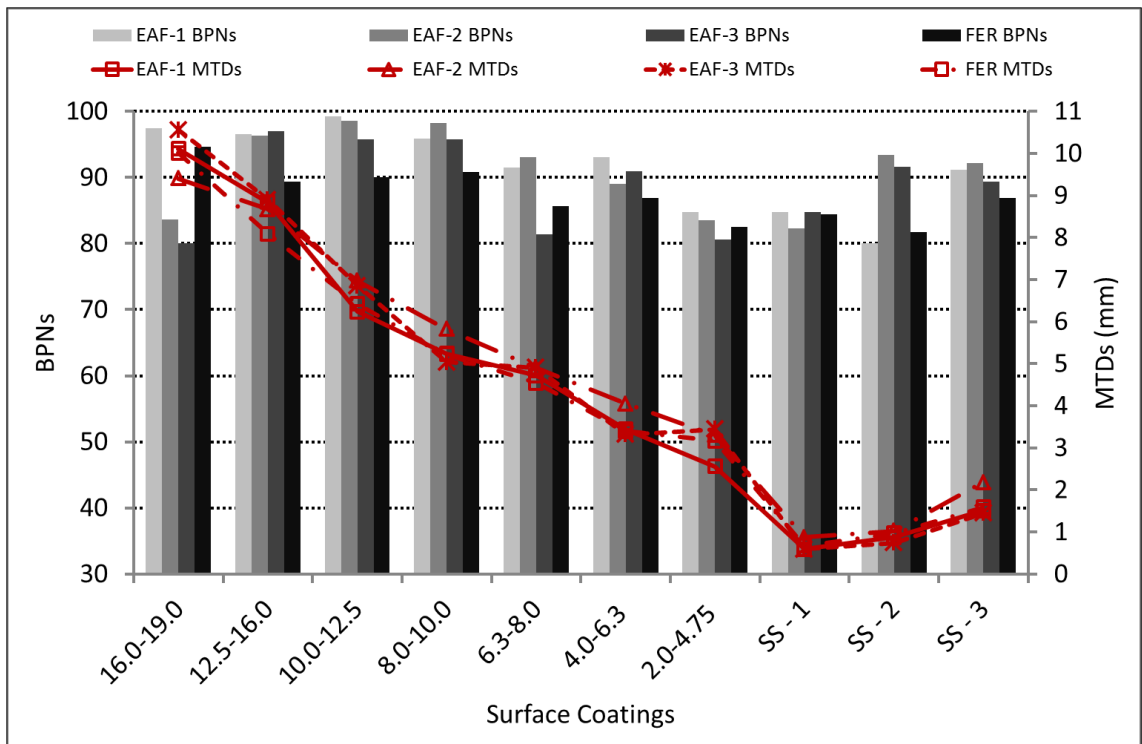
Figure 4.16 Comparative analyses of MTDs and BPNs for slags

CHAPTER 5. CONCLUSION

In this thesis, skid resistance performance of surface coatings, which were manufactured with different aggregate types, gradations, particle sizes and polishing levels at laboratory were evaluated. In this respect, six natural aggregates within three different origins (limestone, basalt and boulder) and four slags within two different sources (Electric Arc Furnace and Ferrochrome slags) were utilized for manufacturing surface coatings. To identify physical, mechanical and chemical properties of each aggregates, series of tests were conducted according to related standard test method. Additionally, for monitoring differences the surface of aggregate SEM was used. Though this study, seven different particle sizes consist of 2.00 - 19.00 mm at unpolished or original state, and four different particle sizes ranges from 4.00 to12.50 mm at different polishing state were specified for chip seal samples. Also, slurry seal samples were prepared within three type of aggregate gradations. Polishing of aggregate was performed via Micro-Deval apparatus according to a standard test method, specified in ASTM D 6928. Polishing levels was determined according to Micro-Deval standard revolution numbers (RNs), which ranges from 5250 for first polishing level to 52500 for the quintuplicate polishing level. In order to measure macro texture of each samples, two well-known standard volumetric test methods (Sand Patch and Outflow Meter) were conducted. To determine skid resistance of each samples, British Pendulum Tester which is a widely used, low speed, relatively inexpensive and portable device were utilized.

Within the scope of this thesis, some parametrical and statistical analyses were carried out. In respect to all of the analyses, following conclusions may be listed.

1. In terms of physical and mechanical properties of aggregate, slags have both superior an poorer properties comparing to natural aggregates. For example, slags have higher water absorption percentage, and dry unit weight may be considered poorer features, depend on the purpose of usage. On the other hand, resistance to abrasion, fragmentation, weathering, and importantly resistant to polishing are significantly superior features of slags compared with natural aggregate.

2. The results of the adhesion and affinity tests show that aggregate rupture, which is seen much in slags with virgin bitumen highly. This is a kind of undesirable deterioration in the surface coating. To avoid any loss of chips, the bitumen should be modified with appropriate adjuvant.

3. Resistance to polishing characteristics of each aggregate have been monitored via SEM. The acquired images support the polishing method utilized in this study, which is Micro-Deval. At each polishing level, the differences on surface micro-texture can be obviously seen. Furthermore, the SEM images have showed clearly that surface texture of slags at the highest polishing level is similar to the surface texture of natural aggregates at the unpolished level.

4. In general, skid resistance decreases as polishing level (respect to RNs) increases, In exceptional, this tendency changes in the slags, in particular, at the second and third polishing levels, referred to 10500, 21000 RNs. Skid resistance is normally supposed to decrease in these polishing level, an increase was observed. The reason of this may be attributed with porous structure of the slags. As compared the skid resistance performance of materials among themselves, limestone has the lowest value both at the unpolished and the highest polishing level. The other natural aggregates, boulder and basalts have better skid resistance performance than limestone. On the other hand, both type of slags have superior skid resistance performance compared to all natural aggregates.

5. Recovering slags ensure benefits in environmental and economic aspects. In point of economic view, utilization of steel slag as road construction aggregate may reduce the cost of extracting and processing natural aggregates. This reduces the initial investment cost of road constructions. Also, the steel producers may also reduce their cost for treating and disposing the vast number of steel slag stockpiles. In point of the environment view, utilization slags as aggregate in pavement construction may directly reduce natural aggregate consumption. Depending on the geological structure of Turkey, especially in southern region of Turkey, supplying of aggregate at the desired quality is sometimes not possible. Even if possible to supply, it is prohibitively expensive. Moreover, incorporating the slags, for examples, in road construction may reduce the area as landfill or waste storage.

6. Comparing to the skid resistance of surface coatings which produced with slags show better performance than the natural aggregates in each polishing level. Thereof, utilizing slags in surface coating applications provides high skid resistant and long lasting pavement surface. This ensures a reduction in maintenance and rehabilitation due to loss of skid resistance. Moreover, it is expected that slip-type traffic accidents decreases, dependently reduces the loss of life and property.

7. It can be expressed that, skid resistance of a pavement, particularly surface coatings for this study were not clearly found as a function of macro-texture, but strongly as a function of micro-texture. As known from earlier studies that, to observe the effect of macro-texture on skid resistance performance, a high speed measurement device, where effect of macro texture becomes clear at high speed.

8. Depending on linear regression analyses performed for both chip seal and slurry seal with wide range of macro-texture depths, a strong correlation between the sand patch and outflow meter test methods were observed. Moreover, surface characteristics of aggregates has significant role in measuring macro-texture depth of chip seal samples when the aggregate size are low, but the effect of surface characteristic are decreasing as the grading sizes increases.

It is important notify that, deterioration types including bleeding, polishing, rutting, stripping, raveling etc. may be observed in the field for a surface coating. In this study, deterioration type is limited only with polishing. Dependently, the effect of this parameter (polishing) on skid resistance performance of surface coatings were evaluated. To evaluate the MTDs and BPNs for different kind of deterioration, further study should be performed for better understanding. Also, to evaluate the skid resistance performance of each surface coating, BPT, which is low speed device was used and significant relationship between MTDs and BPNs were not observed. Further studies may be conducted using different high skid resistance measurement devices such as DFT, to reveal the effects of macro-texture on skid resistance.

REFERENCES

Adams, J.M. and Richard Kim, Y., 2014. Mean profile depth analysis of field and laboratory traffic-loaded chip seal surface treatments. International Journal of Pavement Engineering, 15(7): 645-656.

Aeron-Thomas, A., Astrop, A. and Jacobs, G., 2000. Estimating global road fatalities. 445, Department for Interantional Development, Old Wokingham Road, Crowthorne, Berkshire.

Ahammed, M.A., 2009. Safe, quiet and durable pavement surfaces. Doctor of Philosophy Thesis, University of Waterloo, Waterloo, Ontario, Canada, 292 pp.

Aktaş, B., Gransberg, D., Riemer, C. and Pittenger, D., 2011. Comparative Analysis of Macrotexture Measurement Tests for Pavement Preservation Treatments. Transportation Research Record: Journal of the Transportation Research Board(2209): 34-40.

Andriejauskasa, T., Vorobjovasa, V. and Mielonasb, V., 2014. Evaluation of skid resistance characteristics and measurement methods.

Anonymus, 2016a. Chip Seal. A-1-Chipseal., http://www.a-1chipseal.com., Access Date: 10.02.2016

Anonymus, 2016b. Slurry Seals. Pavement Interactive, http://www.pavementinteractive.org/article/slurryseals/. Access Date: 13.05.2016

Arribas, I., Santamaria, A., Ruiz, E., Ortega-Lopez, V. and Manso, J.M., 2015. Electric arc furnace slag and its use in hydraulic concrete. Construction and Building Materials, 90: 68-79.

Artamendi, I., Phillips, P., Allen, B. and Woodward, D., 2013. Development of UK Propietary Asphalt Surfacing Skid Resistance and Texture Airfield and Highway Pavement 2013@ sSustainable and Efficient Pavements. ASCE, pp. 865-874.

Aschuri, I. and Yamin, A., 2011. The use of by-product waste materials on road pavement conctruction in Indonesia, Proceedings of the Eastern Asia Society for Transportation Studies. Eastern Asia Society for Transportation Studies, pp. 283-283.

Asi, I.M., 2007. Evaluating skid resistance of different asphalt concrete mixes. Building and Environment, 42(1): 325-329.

Asi, I.M., Qasrawi, H.Y. and Shalabi, F.I., 2007. Use of steel slag aggregate in asphalt concrete mixes. Canadian Journal of Civil Engineering, 34(8): 902-911.

ASIRT, 2016. Annual Global Road Crash Statistics, http://asirt.org/. Access Date: 12.06.2016

ASTM, 2012a. ASTM E 303 Standard test method for measuring surface frictional properties using the British Pendulum Tester.

ASTM, 2012b. Standard Practices for Design, Testing, and Construction of Slurry Seal, ASTM D3910 – 11, pp. 8.

ASTM, 2012c. Standard Test Method for Flat Particles , Elongated Particles , or Flat and Elongated Particles in Coarse Aggregate, ASTM D 4791.

ASTM, 2012d. Standard Test Method for Measuring Pavement Macrotexture Depth Using a Volumetric Technique, ASTM E 965-12.

ASTM, 2012e. Standard Test Method for Measuring Pavement Texture Drainage Using an Outflow Meter, ASTM E 2380-12.

ASTM, 2012f. Standard Test Method for Resistance of Coarse Aggregate to Degradation by Abrasion in the Micro-Deval Apparatus, ASTM 6928-10

ASTM, 2012g. Test Method for Coating and Stripping Test of Bitumen Aggregate Mixture, ASTM D1664.

Austroads, 2002. Road Safety Audit. Austroads Inc., Sydney, Australia.

Aziz, M., Hainin, M., Yaacob, H., Ali, Z., Chang, F.-L. and Adnan, A., 2014. Characterisation and utilisation of steel slag for the construction of roads and highways. Materials Research Innovations, 18(sup6): S6-255-S6-259.

Ball, G., 2005. Effect of binder hardness on rate of texture change in chipseals. 284, Land Transport New Zealand Research Report.

Bazlamit, S.M. and Reza, F., 2005. Changes in asphalt pavement friction components and adjustment of skid number for temperature. Journal of Transportation Engineering, 131(6): 470-476.

Bessa, I.S., Castelo Branco, V.T.F. and Soares, J.B., 2014. Evaluation of polishing and degradation resistance of natural aggregates and steel slag using the aggregate image measurement system. Road Materials and Pavement Design, 15(2): 385-405.

Bitelli, G., Simone, A., Girardi, F. and Lantieri, C., 2012. Laser scanning on road pavements: A new approach for characterizing surface texture. Sensors, 12(7): 9110.

BSI, 2003. Surface dressing test methods: Determination of binder aggregate adhesivity by the Vialit plate shock test method, BS EN 12272-3 24.

Cafiso, S. and Taormina, S., 2007. Texture analysis of aggregates for wearing courses in asphalt pavements. International Journal of Pavement Engineering, 8(1): 45-54.

CEN, 1997. Test for general properties of aggregates: Part 1-Method for sampling, EN 932-1.

CEN, 1999. Test for general properties of aggregates: Part 2- Methods for reducing laboratory samples, EN 932-2

CEN, 2010a. Tests for mechanical and physical properties of aggregates - Part 2: Methods for the determination of resistance to fragmentation, EN 1097-2

CEN, 2010b. Tests for mechanical and physical properties of aggregates - Part 8: Determination of the polished stone value, EN 1097-8

CEN, 2011a. Tests for mechanical and physical properties of aggregates - Part 1: Determination of the resistance to wear (Micro-Deval), EN 1097-1

CEN, 2011b. Tests for thermal and weathering properties of aggregates - Part 2: Magnesium sulfate test, EN 1367-2

CEN, 2012. Tests for geometrical properties of Aggregates – Part 3: Determination of particle shape - Flakiness index, EN 933-3

Cenek, P.D. and Jamieson, N.J., 2005. Sensitivity of in-service skid resistance performance of chipseal surfaces to aggregate and texture characteristics, Proceedings of the 1st International Surface Friction Conference, pp. 1-4.

Chang, L.-Y. and Wang, H.-W., 2006. Analysis of traffic injury severity: An application of non-parametric classification tree techniques. Accident Analysis & Prevention, 38(5): 1019-1027.

Cooley Jr, L. and James, R., 2003. Micro-Deval testing of aggregates in the southeast. Transportation Research Record: Journal of the Transportation Research Board(1837): 73-79.

Crouch, L. and Goodwin, W., 1995. Identification of aggregates for Tennessee bituminous surface courses.

Cui, X., Zhou, X., Lou, J., Zhang, J. and Ran, M., 2015. Measurement method of asphalt pavement mean texture depth based on multi-line laser and binocular vision. International Journal of Pavement Engineering: 1-13.

Davis, R.M., 2001. Comparison of surface characteristics of hot-mix asphalt pavement surfaces at the Virginia Smart Road. PhD Thesis, Virginia Polytechnic Institute and State University, Blacksburg, Virginia, 245 pp.

Do, M.-T. and Cerezo, V., 2015. Road surface texture and skid resistance. Surface Topography: Metrology and Properties, 3(4): 043001.

Do, M.-T., Tang, Z.-d., Kane, M. and De Larrard, F., 2009. Evolution of road-surface skid-resistance and texture due to polishing. Wear, 266(5): 574-577.

Do, M. and Roe, P., 2008. Deliverable 04: Report on state-of-the-art of test methods, Tyre and Road Surface Optimisation for Skid Resistance and Further Effects (TYROSAFE), Forum of European National Highway Research Laboratories (FEHRL).

Doty, R.N., 1975. Study of the sand patch and outflow meter methods of pavement surface texture measurement, Surface Texture Versus Skidding: Measurements, Frictional Aspects, and Safety Features of Tire-Pavement Interactions. ASTM International.

Ech, M., Morel, S., Yotte, S., Breysse, D. and Pouteau, B., 2009. An original evaluation of the wearing course macrotexture evolution using the abbot Curve. Road Materials and Pavement Design, 10(3): 471-494.

Ech, M., Yotte, S., Morel, S., Breysse, D. and Pouteau, B., 2007. Laboratory evaluation of pavement macrotexture durability. Revue européenne de génie civil, 11(5): 643-662.

Edwards, J.B., 1999. The relationship between road accident severity and recorded weather. Journal of Safety Research, 29(4): 249-262.

Elias, M., 2014. The balance between environmental impacts and traffic safety on roads Master Thesis, Delft University of Technology, 130 pp.

Erdoğan, A., Gök, M.S. and Kocabaş, F., 2014. Ferrokrom cürufunun mikro ölçekli abrazyon testi İle aşındırma özelliklerinin araştırılması. Mühendislik ve Teknoloji Bilimleri Dergisi, 2(1): 30-49.

Fisco, N. and Sezen, H., 2013. Comparison of surface macrotexture measurement methods. Journal of Civil Engineering and Management, 19(sup1): S153-S160.

Freitas, E.F., Pereira, P.A., Antunes, M. and Domingos, P., 2008. Analysis of test methods for texture depth evaluation applied in Portugal. Seminário Avaliação das Características de Superfície dos pavimentos.

Friel, S. and Woodward, D., 2013. Predicting the development of asphalt surfacing properties in Ireland, Airfield and Highway Pavement 2013: Sustainable and Efficient Pavements. ASCE, pp. 829-840.

Fronek, B.A., 2012. Feasibility of expanding the use of Steel Slag as a concrete pavement aggregate. MSc Thesis, Cleveland State University, 205 pp.

Fwa, T.-F., Yoong, C.-C., Than, T.-N. and See, S.-L., 2013. Development of environmentally sustainable pavement mix. International Journal of Pavement Research and Technology, 6(4): 440-446.

Fwa, T., Choo, Y. and Liu, Y., 2003. Effect of aggregate spacing on skid resistance of asphalt pavement. Journal of transportation engineering, 129(4): 420-426.

Fwa, T., Choo, Y. and Liu, Y., 2004. Effect of surface macrotexture on skid resistance measurements by the British Pendulum Test. Journal of Testing and Evaluation, 32(4): 1-6.

Fwa, T. and Ong, G.P., 2008. Wet-pavement hydroplaning risk and skid resistance: analysis. Journal of Transportation Engineering, 134(5): 182-190.

GDH, 2013. Highway technical specifications. General Directorate of Highways (GDH), Republic of Turkey Ankara, Turkey.

GDH, 2016. BSK Kaplamalı Yollar İçin Bitüm Sınıfı Seçim Haritaları. Karayolları Genel Müdürlüğü, Türkiye, http://www.kgm.gov.tr , Access Date:17.06.2016

Goldstein, J., Newbury, D.E., Echlin, P., Joy, D.C., Romig Jr, A.D., Lyman, C.E., Fiori, C. and Lifshin, E., 2012. Scanning electron microscopy and X-ray microanalysis: a text for biologists, materials scientists, and geologists. Springer Science & Business Media.

Goodman, S.N., 2009. Quantification of pavement textural and frictional characteristics using digital image analysis. PhD Thesis Thesis, Carleton University, Ottawa, 324 pp.

Gökalp, İ., Uz, V.E., Saltan, M. and Ergin, B., 2016. Physico-mechanical Characterization of steel slags produced by the facilities in southern of Turkey and usability as coarse aggregate in different pavement layer according to Turkish HTS, EurAsia 2016 Waste Management Symposium, İstanbul, Turkey, pp. 259-266.

Gransberg, D. and James, D., 2005a. Chip Seal Best Practices: A Synthesis of Highway Practice. National Cooperative Highway Research Program.

Gransberg, D., Pidwerbesky, B. and James, D.M., 2005a. Analysis of New Zealand chip seal design and construction practices, Transportation Research Circular No. E-C078: Roadway Pavement Preservation 2005: Papers from the First National Conference on Pavement Preservation, Kansas City, Missouri October 31– November 1, pp. 3-15.

Gransberg, D., Pidwerbesky, B., Stemprok, R. and Waters, J., 2005b. Measuring chip seal surface texture with digital imagery, International Surface Friction Conference, Christchurch, New Zeland.

Gransberg, D.D., 2007. Using a New Zealand performance specification to evaluate US chip seal performance. Journal of Transportation Engineering, 133(12): 688-695.

Gransberg, D.D. and James, D.M., 2005b. Chip seal best practices, Transportation Research Board, Washington DC, USA.

Gundersen, B., 2008. Chipsealing Practice in Nwe Zealand, 1st Sprayed Sealing Conference- Cost Effective High Performance Surfacing, Adelaide, Australia, pp. 13.

Gürer, C., Karaşahin, M., Çetin, S. and Aktaş, B., 2012. Effects of construction-related factors on chip seal performance. Construction and Building Materials, 35: 605-613.

Hall, J., Smith, K.L., Titus-Glover, L., Wambold, J.C., Yager, T.J. and Rado, Z., 2009. Guide for pavement friction. NCHRP Project: 1-43.

Hall, K.T., Correa, C.E., Carpenter, S.H. and Elliot, R.P., 2001. Rehabilitation strategies for highway pavements. National Cooperative Highway Research Program, Web Document, 35.

Hegmon, R.R. and Mozoguchi, M., 1970. Pavement texture measurement by the sand patch and outflow meter methods. 67-11, Federal Highway Administration, Washington DC, USA.

Henry, J.J., 2000a. Evaluation of pavement friction characteristics. National Academy Press, Washington, D.C.

Henry, J.J., 2000b. Evaluation of pavement friction characteristics, 291. Transportation Research Board.

Hicks, R., Dunn, K. and Moulthrop, J., 1997. Framework for selecting effective preventive maintenance treatments for flexible pavements. Transportation Research Record: Journal of the Transportation Research Board(1597): 1-10.

Híjar, M., Carrillo, C., Flores, M., Anaya, R. and Lopez, V., 2000. Risk factors in highway traffic accidents: a case control study. Accident Analysis & Prevention, 32(5): 703-709.

Huang, Y., Bird, R.N. and Heidrich, O., 2007. A review of the use of recycled solid waste materials in asphalt pavements. Resources, Conservation and Recycling, 52(1): 58-73.

Hydrotimer, 2016. Manuel Book for Hydrotimer. www.hydrotimer.com. Access Date: 18.07.2016

Jianwen, J., 2006. Discussion on Application of Modified Slurry Sealing Technology in Road Maintenance [J]. Technology of Highway and Transport, 4: 018.

Jordan III, W.S. and Howard, I.L., 2011. Applicability of Modified Vialit Adhesion Test for Seal Treatment Specifications. Journal of Civil Engineering and Architecture, 5(3).

Kai-bing, W., 2013. Factors Influencing the Construction Quality of Slurry Seal and Control Measures. Value Engineering, 7: 057.

Kane, M., Artamendi, I. and Scarpas, T., 2013. Long-term skid resistance of asphalt surfacings: correlation between Wehner–Schulze friction values and the mineralogical composition of the aggregates. Wear, 303(1): 235-243.

Karasahin, M., Aktas, B., Gungor, A., Orhan, F. and Gurer, C., 2014. Laboratory and In Situ Investigation of Chip Seal Surface Condition Improvement. Journal of Performance of Constructed Facilities, 29(2): 04014047.

Karasahin, M., Aktas, B. and Gurer, C., 2011. Determining Precoated Aggregate Performance on Chip Seals Using Vialit Test, Transportation Research Board 90th Annual Meeting.

Kehagia, F., 2009. Skid resistance performance of asphalt wearing courses with electric arc furnace slag aggregates. Waste Management & Research, 27(3): 288-294.

Kelvin, L.Y.P., 2005. Analyzing laboratory skid resistance test using finite element modeling. PhD Thesis Thesis, Nationaly University of Singapore, 236 pp.

Khan, M.I. and Wahhab, H.A.-A., 1998. Improving slurry seal performance in Eastern Saudi Arabia using steel slag. Construction and Building Materials, 12(4): 195-201.

Kim, Y.R. and Lee, J., 2005. Optimizing gradations for surface treatments. FHWA/NC/2005-15.

Kodippily, S., Henning, T.F. and Ingham, J.M., 2011. Detecting flushing of thin-sprayed seal pavements using pavement management data. Journal of Transportation Engineering, 138(5): 665-673.

Kogbara, R.B., Masad, E.A., Kassem, E., Scarpas, A.T. and Anupam, K., 2016. A state-of-the-art review of parameters influencing measurement and modeling of skid resistance of asphalt pavements. Construction and Building Materials, 114: 602-617.

Kokkalis, A., Tsohos, G. and Panagouli, O., 2002. Consideration of fractals potential in pavement skid resistance evaluation. Journal of Transportation Engineering, 128(6): 591-595.

Krayushkina, K., Prentkovskis, O., Bieliatynskyi, A. and Junevičius, R., 2012. Use of steel slags in automobile road construction. Transport, 27(2): 129-137.

Krugler, P.E., Freeman, T.J., Wirth, J.E., Wikander, J.P., Estakhri, C.K. and Wimsatt, A.J., 2012. Performance Comparison of Various Seal Coat Grades Used in Texas, Citeseer.

Kucharek, A.S., Keith Davidson, J., Moore, T. and Linton, T., 2010. Performance Review of Micro Surfacing and Slurry Seal Applications in Canada, CTAA Annual Conference Proceedings-Canadian Technical Asphalt Association, pp. 311.

Kucharek, A.S., Moore, T., Linton, P., Keith Davidson, J. and Phillips, T., 2011. Optimizing the Effectiveness of High Performance Chip Seals in Ontario, CTAA Annual Conference Proceedings-Canadian Technical Asphalt Association, pp. 243.

Kumar, P., 2014. Laboratory Base Pavement Surface Analysis Based on Materials Characterization. International Journal of Emerging Trends in Science and Technology, 1(07): 8.

Lee, D. and Orhan, O., 1984. Slurry seal texture as affected by aggregate gradation. Bulletin of the International Association of Engineering Geology-Bulletin de l'Association Internationale de Géologie de l'Ingénieur, 30(1): 89-92.

Lee, D.Y., 1977. Laboratory stduy of slurry seal coats. ISU-ERI-Ames-78188, Iowa DOT.

Lindenmann, H., 2006. New findings regarding the significance of pavement skid resistance for road safety on Swiss freeways. Journal of safety research, 37(4): 395-400.

Loprencipe, G. and Cantisani, G., 2013. Unified analysis of road pavement profiles for evaluation of surface characteristics. Modern Applied Science, 7(8): 1.

Mahmoud, E. and Masad, E., 2007. Experimental methods for the evaluation of aggregate resistance to polishing, abrasion, and breakage. Journal of Materials in Civil Engineering, 19(11): 977-985.

Martino, M.M. and Weissmann, J., 2008. Evaluation of Seal Coat Performance Using Macro-texture Measurements. FHWA/TX-08/0-5310-3 Texas Department of Transportation.

Mayora, J.M.P. and Piña, R.J., 2009. An assessment of the skid resistance effect on traffic safety under wet-pavement conditions. Accident Analysis & Prevention, 41(4): 881-886.

Meyer, W., 1991. Pavement Texture Significance and Measurement-Why Are Pavements Slippery When Wet? ASTM Standardization News, 19(2).

Motz, H. and Geiseler, J., 2001. Products of steel slags an opportunity to save natural resources. Waste Management, 21(3): 285-293.

Nikolaides, A., 2014. Highway Engineering: Pavements, Materials and Control of Quality. CRC Press.

Oluwasola, E.A., Hainin, M.R. and Aziz, M.M.A., 2014. Characteristics and utilization of steel slag in road construction. Jurnal Teknologi, 70(7): 117-123.

Ong, G.P. and Fwa, T., 2007. Wet-pavement hydroplaning risk and skid resistance: modeling. Journal of Transportation Engineering, 133(10): 590-598.

Ortiz, E.M. and Mahmoud, E., 2014. Experimental procedure for evaluation of coarse aggregate polishing resistance. Transportation Geotechnics, 1(3): 106-118.

Pakgohar, A., Tabrizi, R.S., Khalili, M. and Esmaeili, A., 2011. The role of human factor in incidence and severity of road crashes based on the CART and LR regression: a data mining approach. Procedia Computer Science, 3: 764-769.

Panda, C., Mishra, K., Panda, K., Nayak, B. and Nayak, B., 2013. Environmental and technical assessment of ferrochrome slag as concrete aggregate material. Construction and Building Materials, 49: 262-271.

PIARC, 1987. Technical Committee Report: Road Tunnels.

Pidwerbesky, B., Waters, J., Gransberg, D. and Stemprok, R., 2006. Road surface texture measurement using digital image processing and information theory. 290, Land Transport New Zealand.

Postek, M.T., 1997. The scanning electron microscope. Handbook of Charged Particle Optics: 363-399.

Praticò, F.G., Vaiana, R. and Iuele, T., 2015. Macrotexture modeling and experimental validation for pavement surface treatments. Construction and Building Materials, 95: 658-666.

Proctor, D., Fehling, K., Shay, E., Wittenborn, J., Green, J., Avent, C., Bigham, R., Connolly, M., Lee, B. and Shepker, T., 2000. Physical and chemical characteristics of blast furnace, basic oxygen furnace, and electric arc furnace steel industry slags. Environmental Science & Technology, 34(8): 1576-1582.

Reuter, M., Xiao, Y. and Boin, U., 2004. Recycling and environmental issues of metallurgical slags and salt fluxes, VII International conference on molten slags fluxes and salts, The South African Institute of Mining and Metallurgy, pp. 349-356.

Rezaei, A. and Masad, E., 2013. Experimental-based model for predicting the skid resistance of asphalt pavements. International Journal of Pavement Engineering, 14(1): 24-35.

Rezaei, A., Masad, E. and Chowdhury, A., 2011. Development of a model for asphalt pavement skid resistance based on aggregate characteristics and gradation. Journal of transportation engineering, 137(12): 863-873.

Roberts, C. and Nicholls, J.C., 2008. Road Note 39 : Desing Guied for Road Surface Dressing. IHS, pp. 76.

Sandberg, U. and Descornet, G., 1980. ROAD SURFACE INFLUENCE ON TIRE/ROAD NOISE--1, Proceedings of the International Conference Noise Control Engineering, Noise Control for the 80's, Inter-Noise 80, Vol. 1, Miami, Florida, December 8-10, 1980.

Saplioglu, M., Yuzer, E., Aktas, B. and Eriskin, E., 2013. Investigation of the Skid Resistance at Accident Occurred at Urban Intersections. Journal of traffic and transportation engineering (Valley Cottage, NY), 1(1): 19-29.

Sarsam, S. and Al Shareef, H., 2015. Assesment of texture and skid varibles at pavement surface. Applied Research Journal, 1(8): 422-432.

Sarsam, S.I. and Ali, A.M., 2015. Assessing Pavement Surface Macrotexture Using Sand Patch Test and Close Range Photogrammetric Approaches. International Journal of Materials Chemistry and Physics, 1(2): 124-131.

Saykin, V.V., Zhang, Y., Cao, Y., Wang, M.L. and McDaniel, J.G., 2012. Pavement Macrotexture Monitoring through Sound Generated by a Tire-Pavement Interaction. Journal of Engineering Mechanics.

Sengoz, B., Topal, A. and Tanyel, S., 2012. Comparison of pavement surface texture determination by sand patch test and 3D laser scanning. Periodica Polytechnica. Civil Engineering, 56(1): 73.

Sheng-fei, G., 2011. Application of Slurry Seal Coat in Asphalt Pavement Preventive Maintenance. China Municipal Engineering, 1: 002.

Song, W., Chen, X., Smith, T. and Hedfi, A., 2006. Investigation of hot mix asphalt surfaced pavements skid resistance in Maryland state highway network system, TRB 85th Annual Meeting, Transportation Research Board.

Sorlini, S., Sanzeni, A. and Rondi, L., 2012. Reuse of steel slag in bituminous paving mixtures. Journal of hazardous materials, 209: 84-91.

Sugg, R., 1979. An Investigation into Measuring Runway Surface Texture by the Grease Patch and Outflow Meter Methods. DRIC-BR-70263, DTIC Document, England.

Terzi, S., Karaşahin, M., Saltan, M., Yilmaz, A., Saplioğlu, M., Ertem, S., Özgüngördü, M. and Taciroğlu, M.V., 2013. Physical properties of multi-layer seal surfacing in Turkey, Proceedings of the Institution of Civil Engineers-Transport. Thomas Telford Ltd, pp. 137-143.

Thenoux, G., Allen, W. and Bell, C., 1996. Study of aircraft accident related to asphalt runway skid resistance. Transportation Research Record: Journal of the Transportation Research Board(1536): 59-63.

TNZ, 2005. Chipsealing in New Zealand. Transit New Zealand, New Zealand.

TSPA, 2016. Steel Map of Turkey. Turkish Steel Producer Association, http://www.dcud.org.tr/. Access Date: 18.07.2016

Uz, V.E., Gökalp, I., Epsileli, S.E. and Tepe, M., 2014. Karayollari teknik şartnamesinde (KTŞ) yer alan pürüzlendirme uygulaması ve bu uygulamada endüstriyel atıkların kullanılabilirliği, , Karayolları 3. Ulusal Kongresi, Ankara, Turkey, pp. 123–135.

Wallman, C.-G. and Åström, H., 2001. Friction and traffic safety, Swedish National Road and Trasnport Research Institue, Linköping, Sweden.

Wambold, J.C. and Henry, J., 1994. International PIARC Experiment to Compare and Harmonize Texture and Skid Resistance Measurement. Nordic Road and Transport Research.

Wang, D., Chen, X., Yin, C., Oeser, M. and Steinauer, B., 2013. Influence of different polishing conditions on the skid resistance development of asphalt surface. Wear, 308(1): 71-78.

Woodward, D., Woodside, A. and Jellie, J., 2004. Improved prediction of aggregate skid resistance using modified PSV tests.

WSDOT, 2016. Waht is Chip Seal?, http://www.wsdot.wa.gov/Regions/Eastern/ChipSeal/. Access Date: 11.04.2016

Wu, S., Xue, Y., Ye, Q. and Chen, Y., 2007. Utilization of steel slag as aggregates for stone mastic asphalt (SMA) mixtures. Building and Environment, 42(7): 2580-2585.

Xiao, J., Kulakowski, B. and EI-Gindy, M., 2000. Prediction of risk of wet-pavement accidents: fuzzy logic model. Transportation Research Record: Journal of the Transportation Research Board(1717): 28-36.

Xue, W., Druta, C., Wang, L. and Lane, D.S., 2010. Assessing the polishing characteristics of coarse aggregates using micro-deval and imaging system, GeoShanghai 2010 International Conference.

Yildirim, I.Z. and Prezzi, M., 2011. Chemical, mineralogical, and morphological properties of steel slag. Advances in Civil engineering, 2011: 1-13.

Yılmaz, A., Saltan, M. and Akıllı, A., 2012. Göller Yöresinde İşletilen Kireçtaşı Agregalarının Yol İnşaatı Malzemesi Olarak Kullanılabilirliğinin Araştırılması. Pamukkale Üniversitesi Mühendislik Bilimleri Dergisi, 18(3): 199-207.

Yilmaz, A. and Sütaş, İ., 2008. Ferrokrom Cürufunun Yol Temel Malzemesi Olarak Kullanımı. İMO Teknik Dergi, 20084455: 4470.

Ziari, H. and Khabiri, M.M., 2007. Preventive maintenance of flexible pavement and mechanical properties of steel slag asphalt. Journal of Environmental Engineering and Landscape Management, 15(3): 188-192.

Zoghi, M., Ebrahimpour, A. and Pothukutchi, V., 2010. Performance Evaluation of Chip Seals in Idaho.

APPENDIX

Table 1. BPNs for chip seals produced with unpolished aggregate

Grain Size (mm)	LS-1	LS-2	LS-3	BS-1	BS-2	BLD	EAF-1	EAF-2	EAF-3	FER
16.00-19.00	76.2	79.7	79.4	81.7	87.4	77.2	97	83.6	80.0	94.6
12.50-16.00	74.4	74.6	80.3	75.7	75.4	75.2	96.5	96.3	97.0	89.4
10.00-12.50	84.0	88.4	78.9	89.8	92.6	85.8	99.2	98.6	95.8	90.0
8.00-10.00	75.8	82.1	78.2	86.0	80.2	85.9	95.9	98.2	95.8	90.8
6.30-8.00	80.7	77.5	82.6	88.5	87.7	80.5	91.5	93.1	81.4	85.6
4.00-6.30	75.5	82.6	81.2	94.0	90.8	80.3	93.1	89.0	90.9	86.9
2.00-4.75	82.6	85.0	81.6	88.3	90.7	85.9	84.8	83.5	80.6	82.5

Table 2. BPNs for slurry seals produced with unpolished aggregate

Grain Size (mm)	LS-1	LS-2	LS-3	BS-1	BS-2	BLD	EAF-1	EAF-2	EAF-3	FER
SS - Type - 1	79.5	78.3	78.7	83.5	84.5	82.5	84.7	82.3	84.8	84.4
SS - Type - 2	82.0	78.5	80.9	86.5	86.6	83.2	80.0	93.4	91.6	81.7
SS - Type - 3	72.4	75.5	81.0	85.7	82.2	86.1	91.2	92.2	89.4	86.9

Table 3. BPNs for 12.50-10.00 mm grain sizes

Sample ID	Polishing Level with RNs					
	Unpolished	1st	2nd	3rd	4th	5th
LS-1	84.0	71.6	62.6	57.2	54.8	49.2
LS-2	88.4	79.8	62	56.1	45.6	39.0
LS-3	78.9	71.9	57.2	55.4	49	44.1
BS-1	89.8	84.0	73.0	71.0	67.0	65.0
BS-2	92.6	74.8	70.8	69.6	69.6	69.4
BLD	85.8	74.1	64.4	62.2	61.8	60.8
EAF-1	99.2	98.5	73.3	72.0	71.9	68.2
EAF-2	98.6	90.9	74.1	78.7	75.3	71.0
EAF-3	95.8	82.4	75.1	74.6	73.2	72.5
FER	90.0	81.8	75.6	80.8	75.1	66.8

Table 4. BPNs for 10.00-8.00 mm grain sizes

Sample ID	Polishing Level with RNs					
	Unpolished (0)	1st (5250)	2nd (10500)	3rd (21000)	4th (31500)	5th (52500)
LS-1	75.8	66.6	57.3	55.0	52.7	52.5
LS-2	82.1	63.2	60.7	53.8	47.1	40.8
LS-3	78.2	66.9	60.8	51.1	49.0	47.4
BS-1	86.0	75.8	73.0	71.8	65.4	65.4
BS-2	80.2	78.5	74.2	71.5	62.4	62.2
BLD	85.9	75.8	69.9	63.8	57.4	54.2
EAF-1	95.9	80.1	69.1	72.0	69.7	64.0
EAF-2	98.2	87.2	74.8	72.2	70.8	67.6
EAF-3	95.8	83.6	82.8	71.8	67.4	67.0
FER	90.8	86.0	75.8	78.8	71.7	66.8

Table 5. BPNs for 8.00-6.30 mm grain sizes

Sample ID	Polishing Level with RNs					
	Unpolished (0)	1st (5250)	2nd (10500)	3rd (21000)	4th, (31500)	5th (52500)
LS-1	80.7	61.8	60.5	55.6	51.6	50.1
LS-2	77.5	61.6	58.6	53.9	51.3	48.6
LS-3	82.6	64.6	58.0	54.7	50.6	45.9
BS-1	88.5	77.8	70.0	67.5	66.0	64.8
BS-2	87.7	77.3	75.0	71.8	62.8	60.4
BLD	80.5	69.9	66.9	62.8	59.5	57.0
EAF-1	91.5	84.5	76.5	69.3	65.9	67.8
EAF-2	93.1	83.7	81.5	77.3	75.2	68.2
EAF-3	81.4	75.6	74.7	70.4	70.0	70.8
FER	85.6	76.5	72.5	74.6	68.4	67.2

Table 6. BPNs for 6.30-4.00 mm grain sizes

Sample ID	Polishing Level with RNs					
	Unpolished (0)	1st (5250)	2nd (10500)	3rd (21000)	4th (31500)	5th (52500)
LS-1	75.5	63.0	54.6	50.5	50.3	45.4
LS-2	82.6	71.3	62.0	56.0	51.5	49.2
LS-3	81.2	63.4	57.1	53.6	50.1	48.7
BS-1	94.0	85.4	70.9	70.5	65.0	64.2
BS-2	90.8	77.9	73.8	70.4	63.6	63.1
BLD	80.3	74.5	65.9	59.8	57.4	53.2
EAF-1	93.1	81.2	71.6	68.3	64.0	63.6
EAF-2	89.0	83.1	74.2	75.4	74.5	69.2
EAF-3	90.9	87.4	73.6	70.8	72.7	68.6
FER	86.9	82.1	71.8	76.9	67.3	64.8

Figure 1. BPNs for LS-1 at different polishing levels
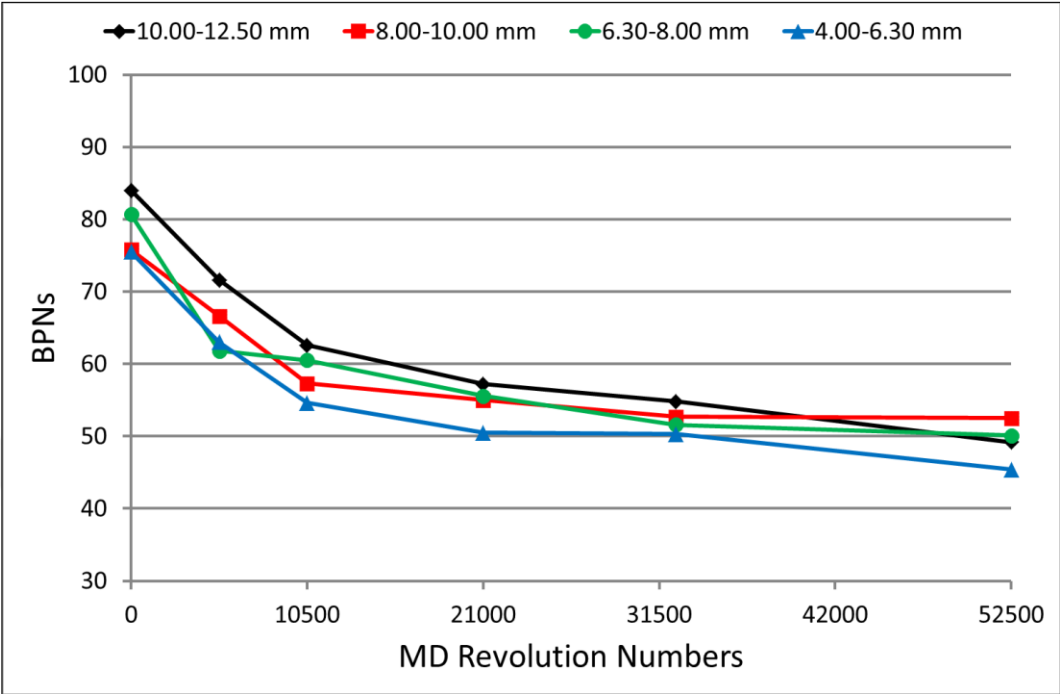
Figure 2. BPNs for LS-2 at different polishing levels
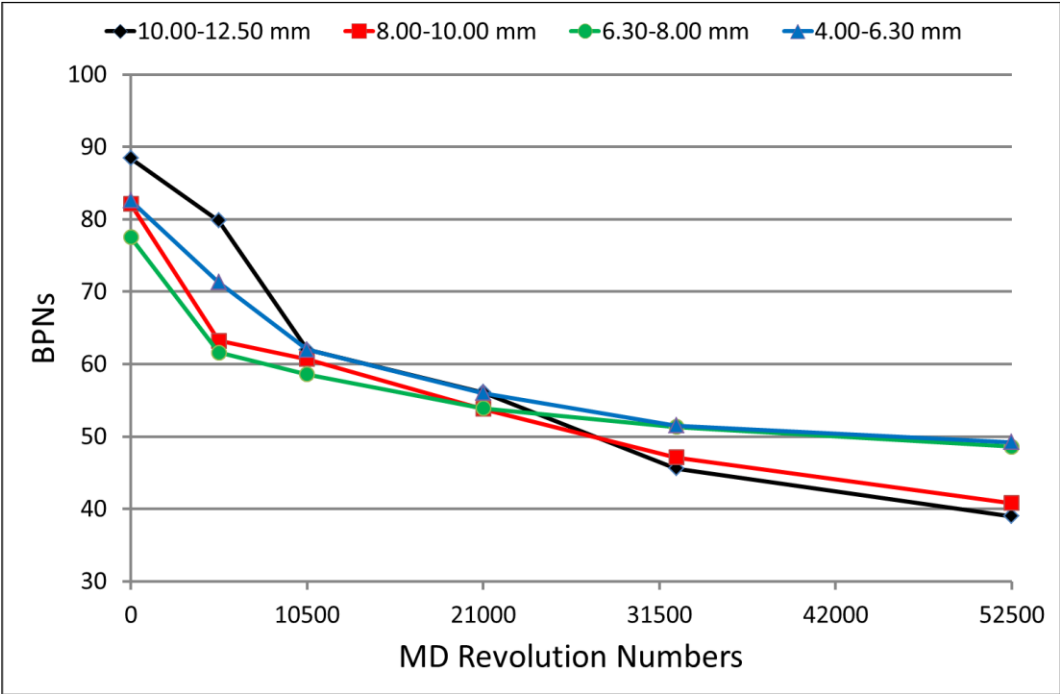
Figure 3. BPNs for LS-3 at different polishing levels
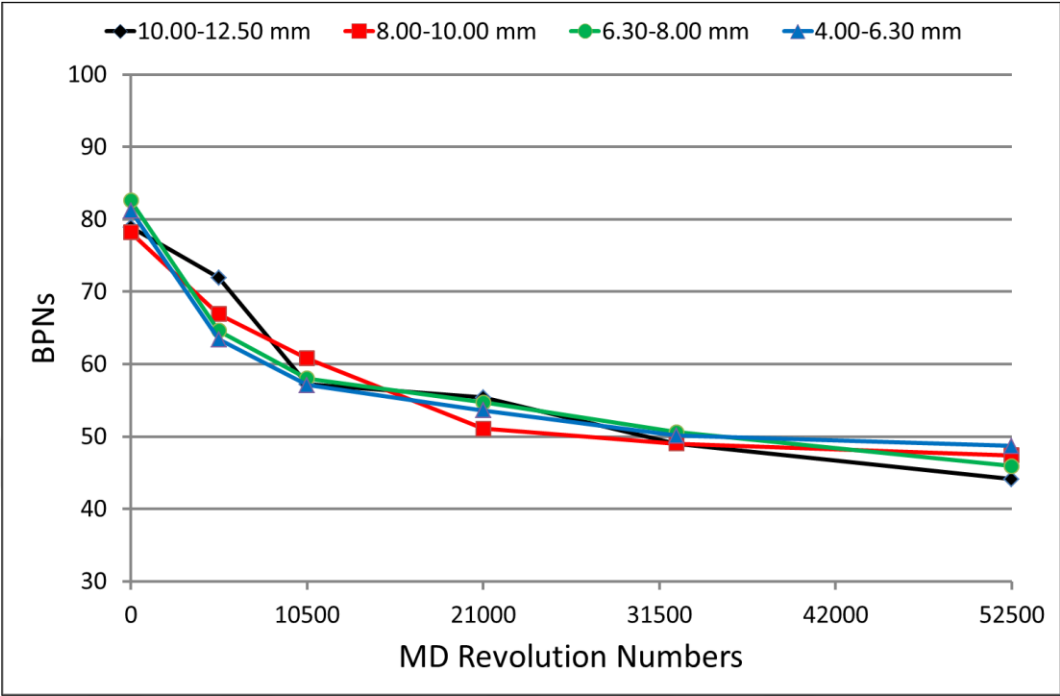
Figure 4. BPNs for BS-1 at different polishing levels
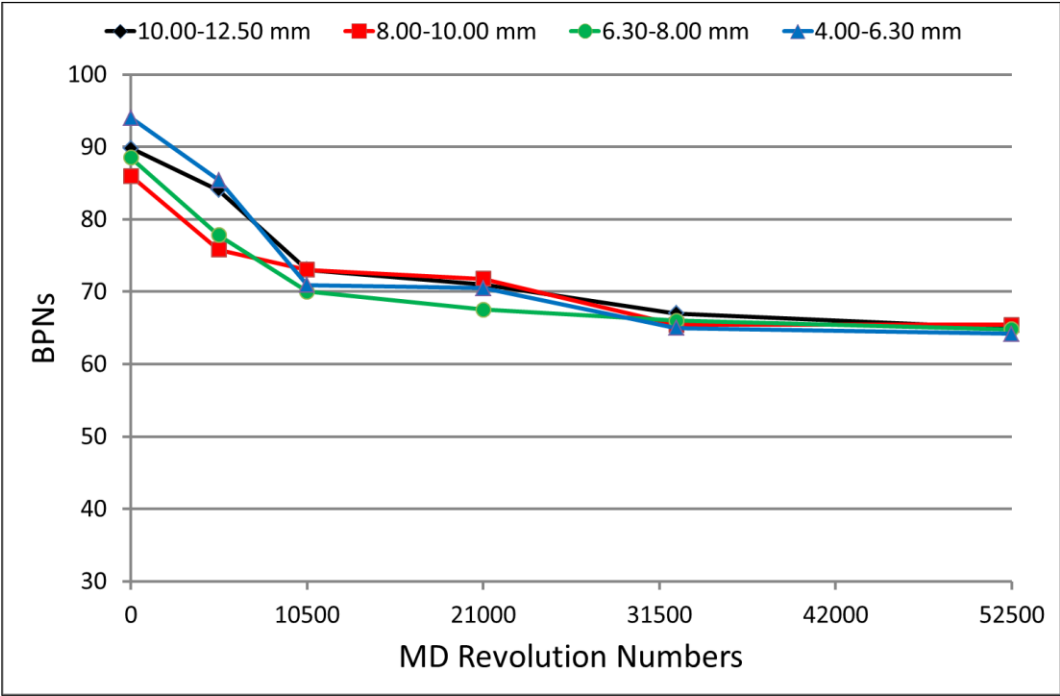
Figure 5. BPNs for BS-2 at different polishing levels
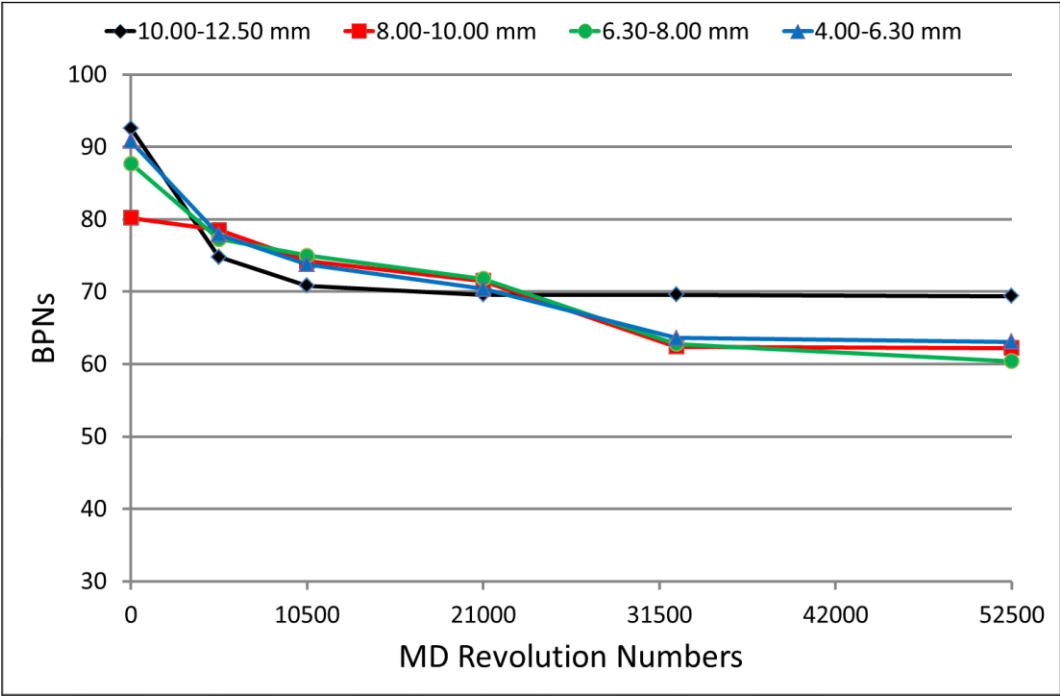
Figure 6. BPNs for BLD at different polishing levels
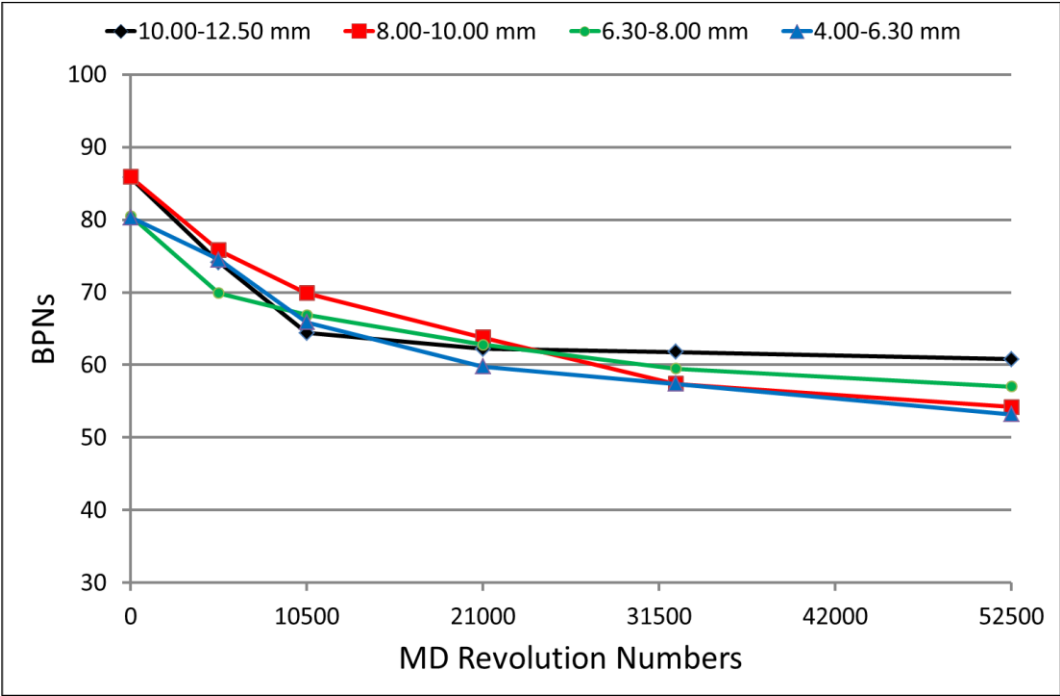
Figure 7. BPNs for EAF-1 at different polishing levels
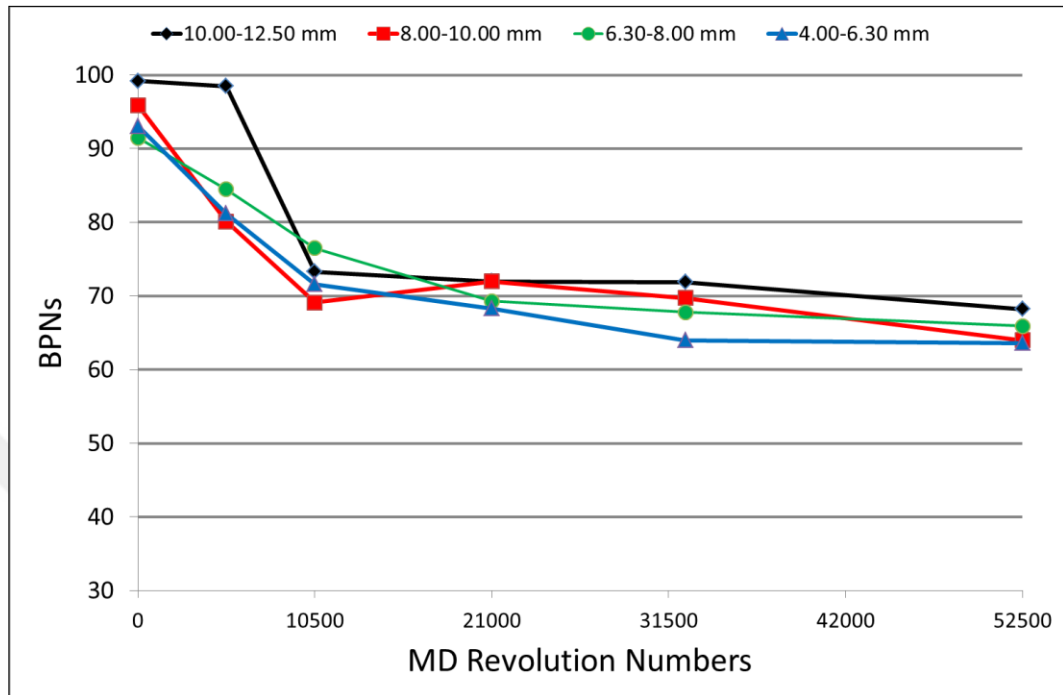
Figure 8. BPNs for EAF-2 at different polishing levels
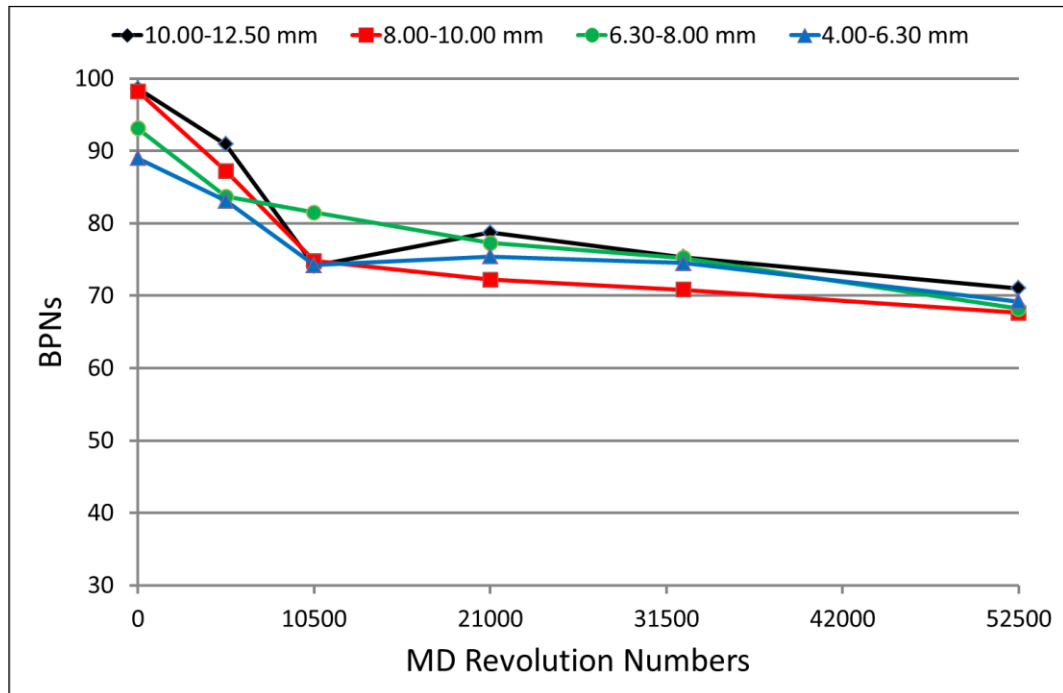
Figure 9. BPNs for EAF-3 at different polishing levels
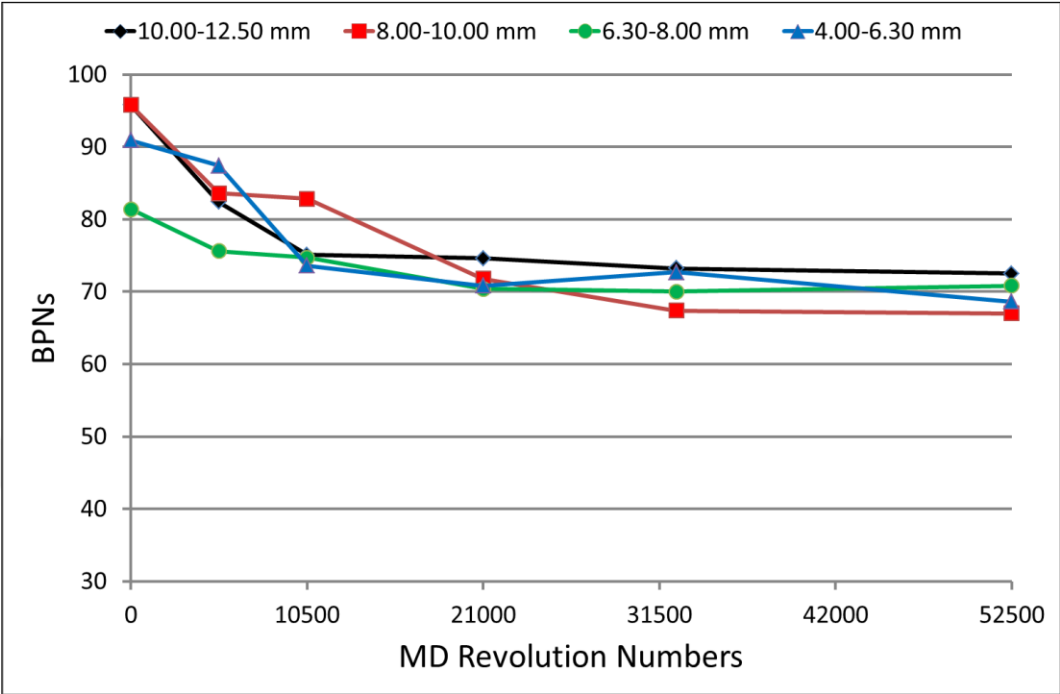
Figure 10. BPNs for FER at different polishing levels

Figure 11. Images for chip seal samples with unpolished aggregates

LS1 (4.75-2.0 mm)	LS1 (6.3-4.0 mm)	LS1 (8.0-6.3 mm)	LS1 (10.0-8.0 mm)
LS1 (12.5-10.0 mm)	LS1 (12.5-16.0 mm))	LS1 (19.0 -16.0 mm)	LS2 (4.75-2.0 mm)
LS2 (6.3-4.0 mm)	LS2 (8.0-6.3 mm)	LS2 (10.0-8.0 mm)	LS2 (12.5-10.0 mm)
LS2 (12.5-16.0 mm)	LS2 (19.0 -16.0 mm)	LS3 (4.75-2.0 mm)	LS3 (6.3-4.0 mm)
LS3 (8.0-6.3 mm)	LS3 (10.0-8.0 mm)	LS3 (12.5-10.0 mm)	LS3 (12.5-16.0 mm

LS3 (19.0-16.0 mm)	BLD (4.75-2.0 mm)	BLD (6.3-4.0 mm)	BLD (8.0-6.3 mm)
BLD (10.0-8.0 mm)	BLD (12.5-10.0 mm)	BLD (12.5-16.0 mm)	BLD(19.0-16.0 mm
BS1 (6.3-4.0 mm)	BS1 (8.0-6.3 mm)	BS1 (10.0-8.0 mm)	BS1 (12.5-10.0 mm)
BS2 (4.75-2.0 mm)	BS2 (6.3-4.0 mm)	BS2 (8.0-6.3 mm)	BS2 (10.0-8.0 mm)
BS2 (12.5-10.0 mm)	BS2 (12.5-16.0 mm)	BS2 (19.0-16.0 mm	EAF1 (4.75-2.0 mm)

EAF1 (6.3-4.0 mm)	EAF1 (8.0-6.3 mm)	EAF1 (10.0-8.0 mm)	EAF1 (12.5-10.0 mm)
EAF1 (12.5-16.0 mm)	EAF1 (19.0-16.0 mm)	EAF2 (4.75-2.0 mm)	EAF2 (6.3-4.0 mm)
EAF2 (8.0-6.3 mm)	EAF2 (10.0-8.0 mm)	EAF2 (12.5-10.0 mm)	EAF2 (12.5-16.0 mm)
EAF2 (19.0-16.0 mm)	EAF3 (4.75-2.00 mm)	EAF3 (6.3-4.0 mm)	EAF3 (8.0-6.3 mm)
EAF3 (10.0-8.0 mm)	EAF3 (12.5-10.0 mm)	EAF3 (12.5-16.0 mm)	EAF3 (19.0-16.0 mm)

FER (4.75-2.0 mm)	FER (6.3-4.0 mm)	FER (8.0-6.3 mm)	FER (10.0-8.0 mm)

FER (12.5-10.0 mm)	EAF3 (16.0-12.5 mm)	EAF3 (19.0-16.0 mm)

Figure 12. Images for chip seal samples with polished aggregates at 1st polishing level

LS1 (6.3-4.0 mm)	LS1 (8.0-6.3 mm)	LS1 (10.0-8.0 mm)	LS1 (12.5-10.0 mm)
LS2 (6.3-4.0 mm)	LS2 (8.0-6.3 mm)	LS2 (10.0-8.0 mm)	LS2 (12.5-10.0 mm)
LS3 (6.3-4.0 mm)	LS3 (8.0-6.3 mm)	LS3 (10.0-8.0 mm)	LS3 (12.5-10.0 mm)
BLD (6.3-4.0 mm)	BLD (8.0-6.3 mm)	BLD (10.0-8.0 mm)	BLD (12.5-10.0 mm)
BS1 (6.3-4.0 mm)	BS1 (8.0-6.3 mm)	BS1 (10.0-8.0 mm)	BS1 (12.5-10.0 mm)

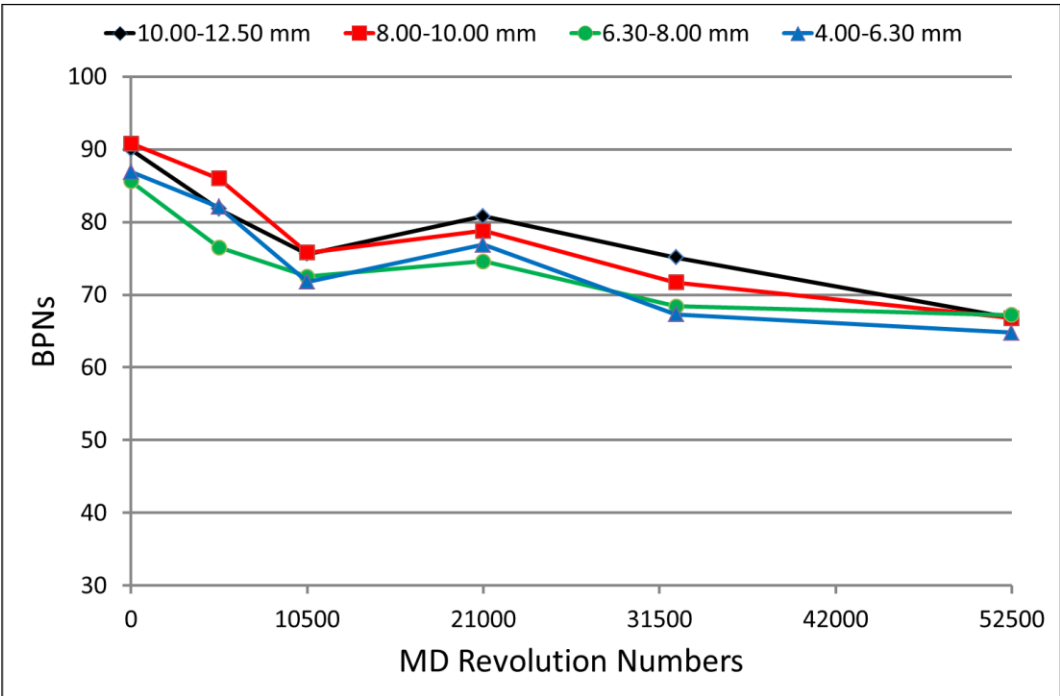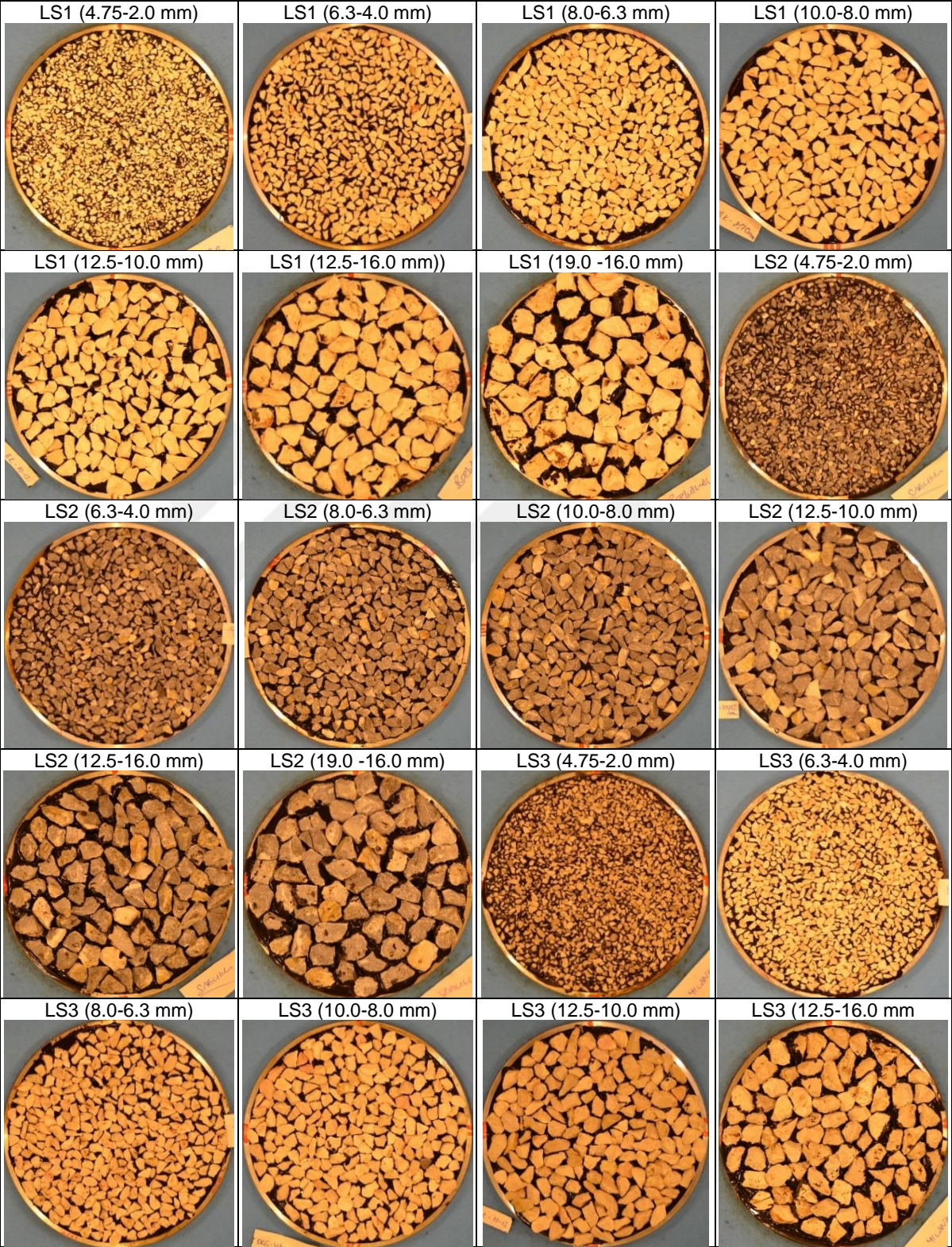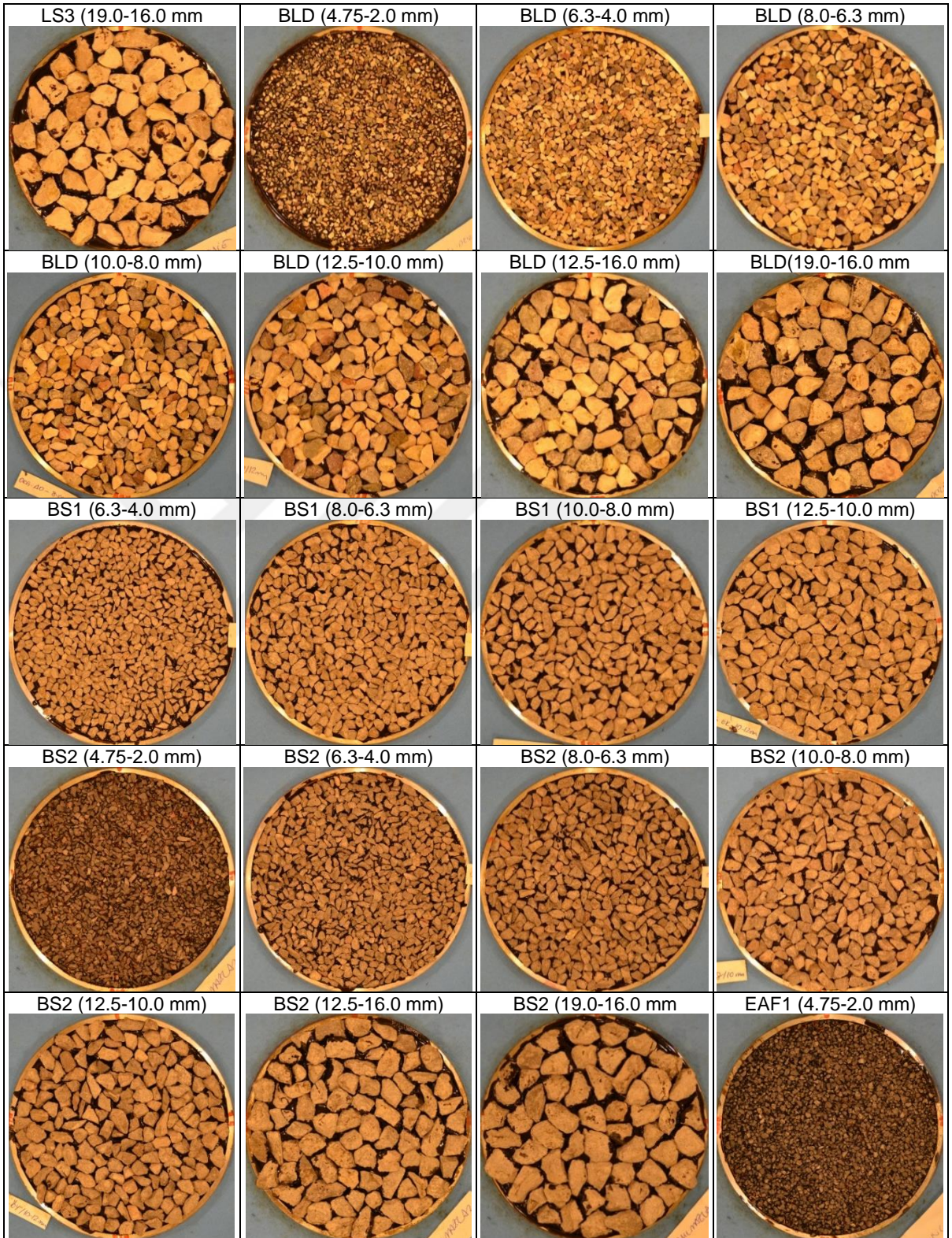| BS2 (6.3-4.0 mm) | BS2 (8.0-6.3 mm) | BS2 (10.0-8.0 mm) | BS2 (12.5-10.0 mm) |
EAF1 (6.3-4.0 mm)	EAF1 (8.0-6.3 mm)	EAF1 (10.0-8.0 mm)	EAF1 (12.5-10.0 mm)
EAF2 (6.3-4.0 mm)	EAF2 (8.0-6.3 mm)	EAF2 (10.0-8.0 mm)	EAF2 (12.5-10.0 mm)
EAF3 (6.3-4.0 mm)	EAF3 (8.0-6.3 mm)	EAF3 (10.0-8.0 mm)	EAF3 (12.5-10.0 mm)
FER (6.3-4.0 mm)	FER (8.0-6.3 mm)	FER (10.0-8.0 mm)	FER (12.5-10.0 mm)

Figure 13. Images for chip seal samples with polished aggregates at 2nd polishing level

LS1 (6.3-4.0 mm)	LS1 (8.0-6.3 mm)	LS1 (10.0-8.0 mm)	LS1 (12.5-10.0 mm)
LS2 (6.3-4.0 mm)	LS2 (8.0-6.3 mm)	LS2 (10.0-8.0 mm)	LS2 (12.5-10.0 mm)
LS3 (6.3-4.0 mm)	LS3 (8.0-6.3 mm)	LS3 (10.0-8.0 mm)	LS3 (12.5-10.0 mm)
BLD (6.3-4.0 mm)	BLD (8.0-6.3 mm)	BLD (10.0-8.0 mm)	BLD (12.5-10.0 mm)
BS1 (6.3-4.0 mm)	BS1 (8.0-6.3 mm)	BS1 (10.0-8.0 mm)	BS1 (12.5-10.0 mm)

BS2 (6.3-4.0 mm)	BS2 (8.0-6.3 mm)	BS2 (10.0-8.0 mm)	BS2 (12.5-10.0 mm)
EAF1 (6.3-4.0 mm)	EAF1 (8.0-6.3 mm)	EAF1 (10.0-8.0 mm)	EAF1 (12.5-10.0 mm)
EAF2 (6.3-4.0 mm)	EAF2 (8.0-6.3 mm)	EAF2 (10.0-8.0 mm)	EAF2 (12.5-10.0 mm)
EAF3 (6.3-4.0 mm)	EAF3 (8.0-6.3 mm)	EAF3 (10.0-8.0 mm)	EAF3 (12.5-10.0 mm)
FER (6.3-4.0 mm)	FER (8.0-6.3 mm)	FER (10.0-8.0 mm)	FER (12.5-10.0 mm)

110
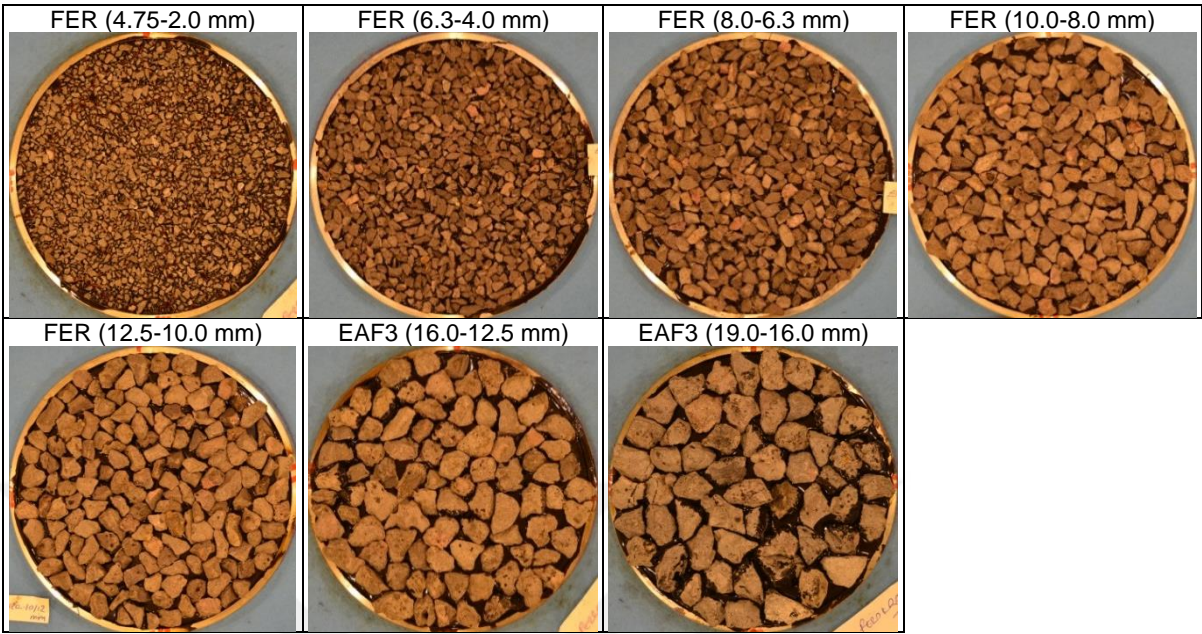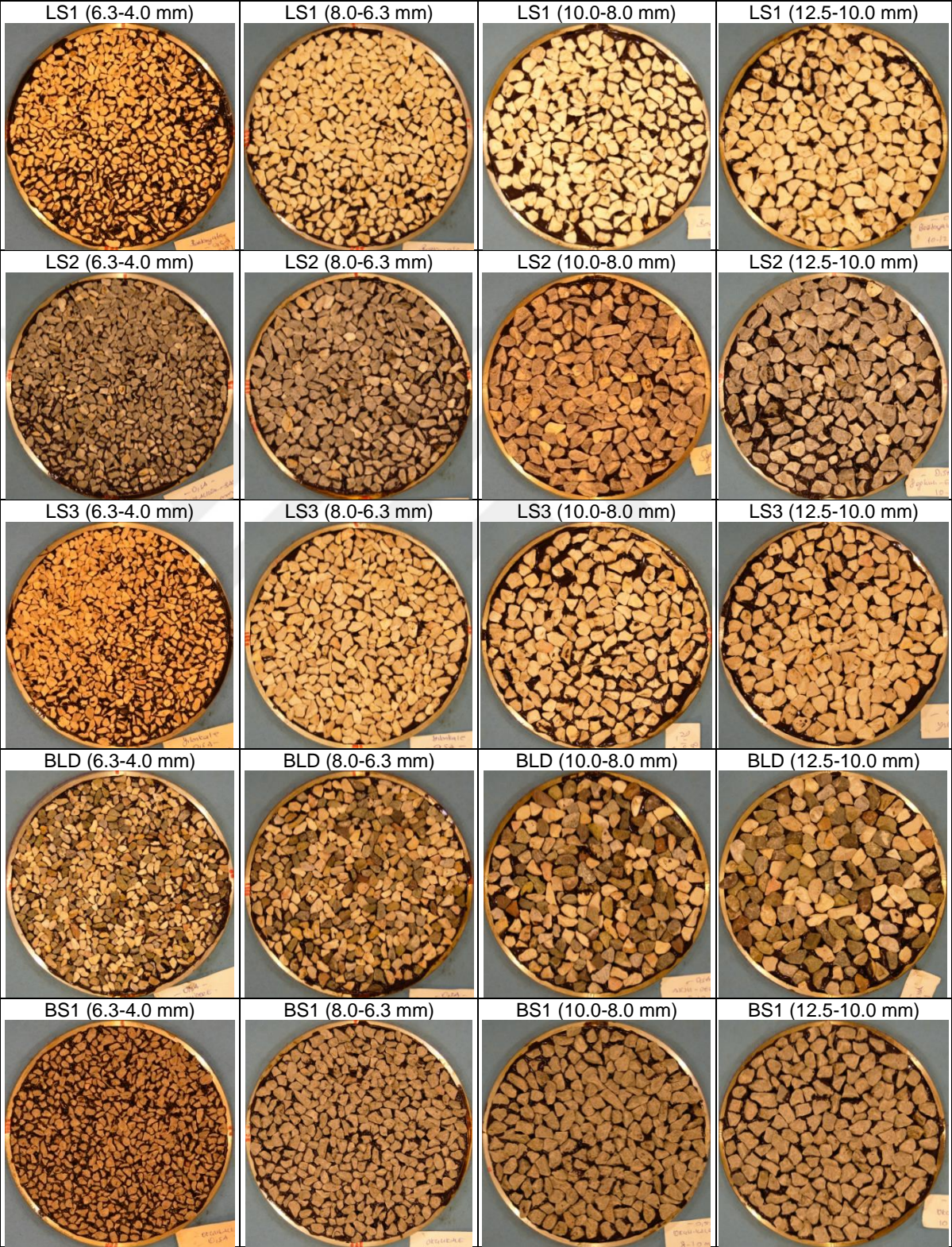
Figure 14. Images for chip seal samples with polished aggregates at 3rd polishing level

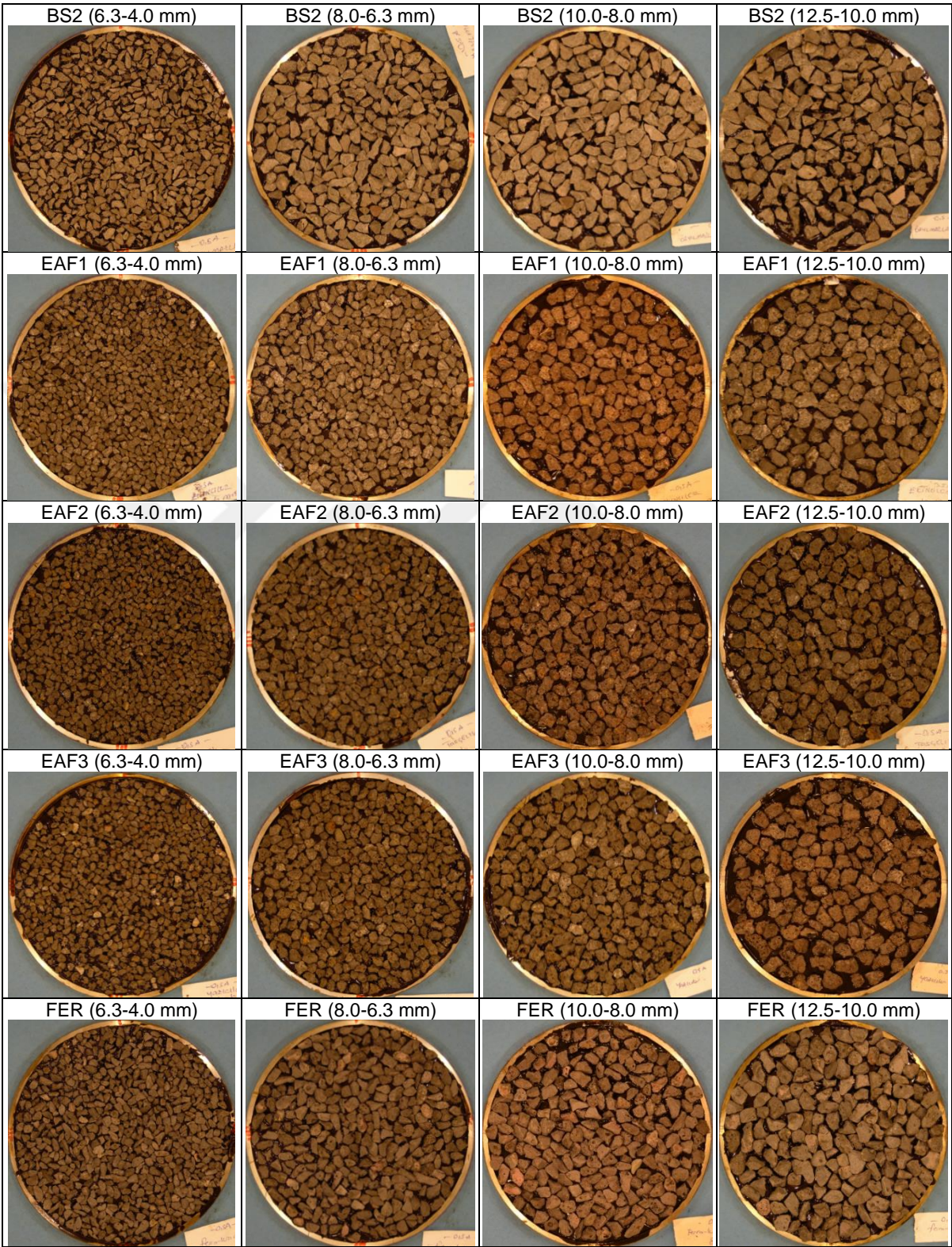| LS1 (6.3-4.0 mm)	LS1 (8.0-6.3 mm)	LS1 (10.0-8.0 mm)	LS1 (12.5-10.0 mm)
LS2 (6.3-4.0 mm)	LS2 (8.0-6.3 mm)	LS2 (10.0-8.0 mm)	LS2 (12.5-10.0 mm)
LS3 (6.3-4.0 mm)	LS3 (8.0-6.3 mm)	LS3 (10.0-8.0 mm)	LS3 (12.5-10.0 mm)
BLD (6.3-4.0 mm)	BLD (8.0-6.3 mm)	BLD (10.0-8.0 mm)	BLD (12.5-10.0 mm)
BS1 (6.3-4.0 mm)	BS1 (8.0-6.3 mm)	BS1 (10.0-8.0 mm)	BS1 (12.5-10.0 mm)

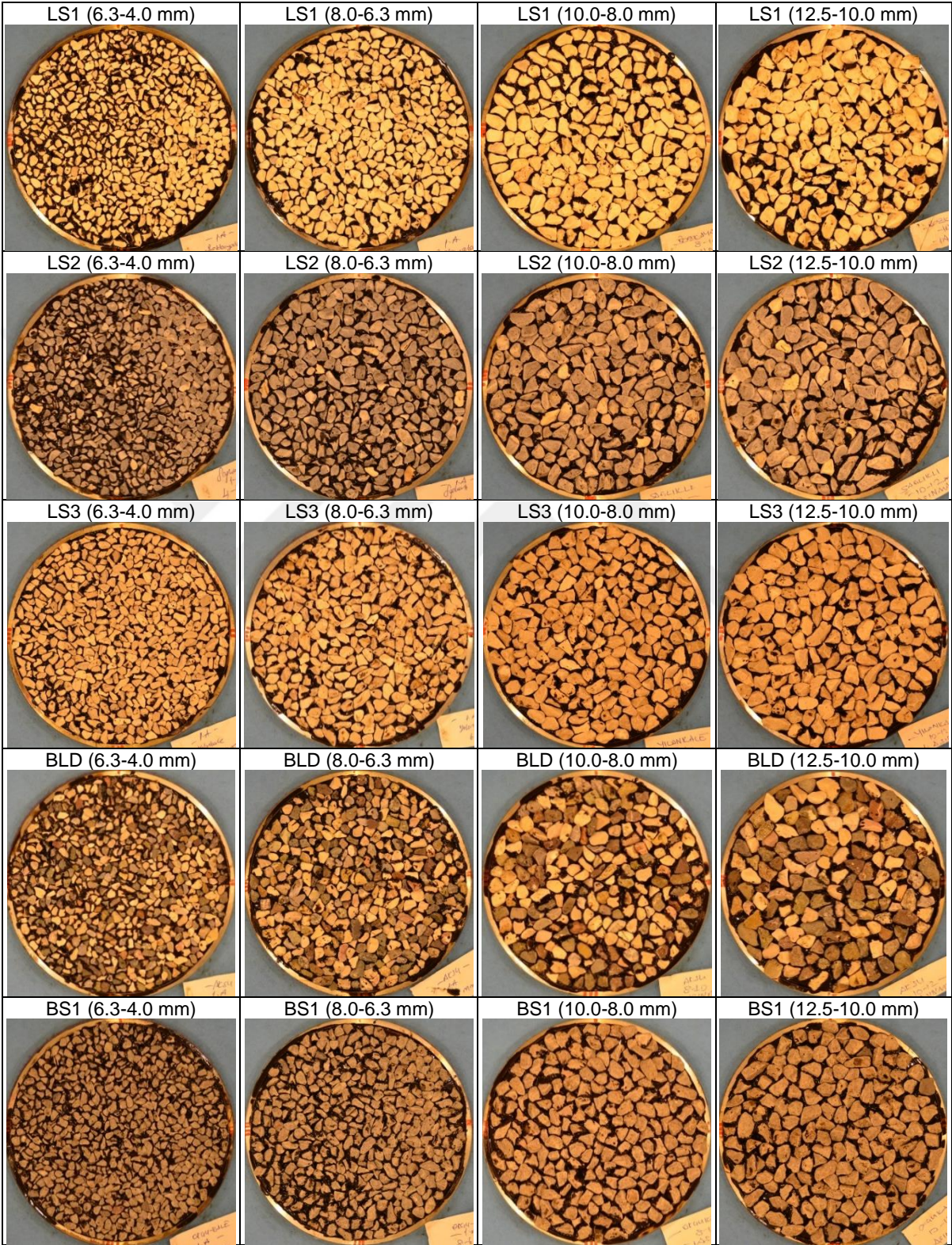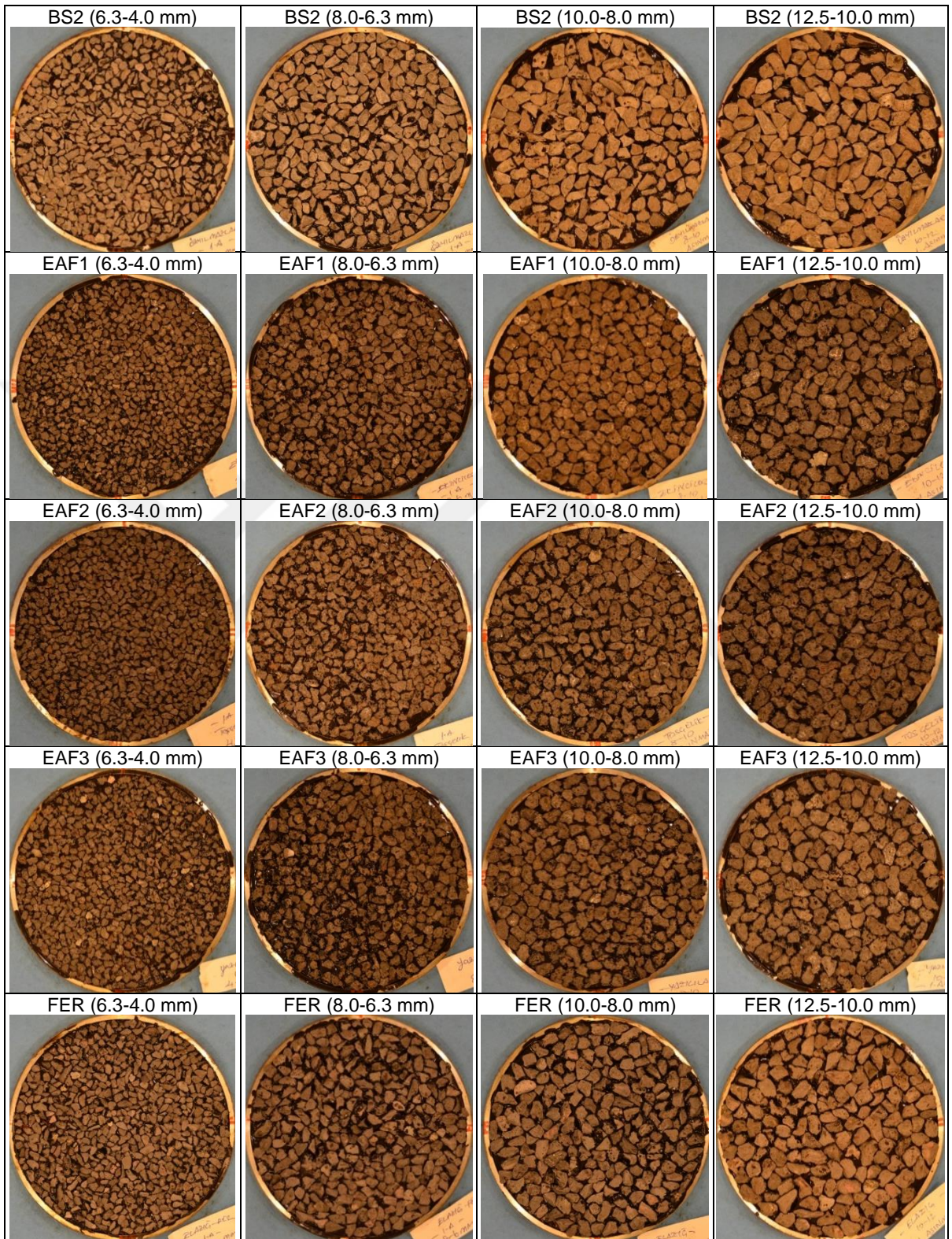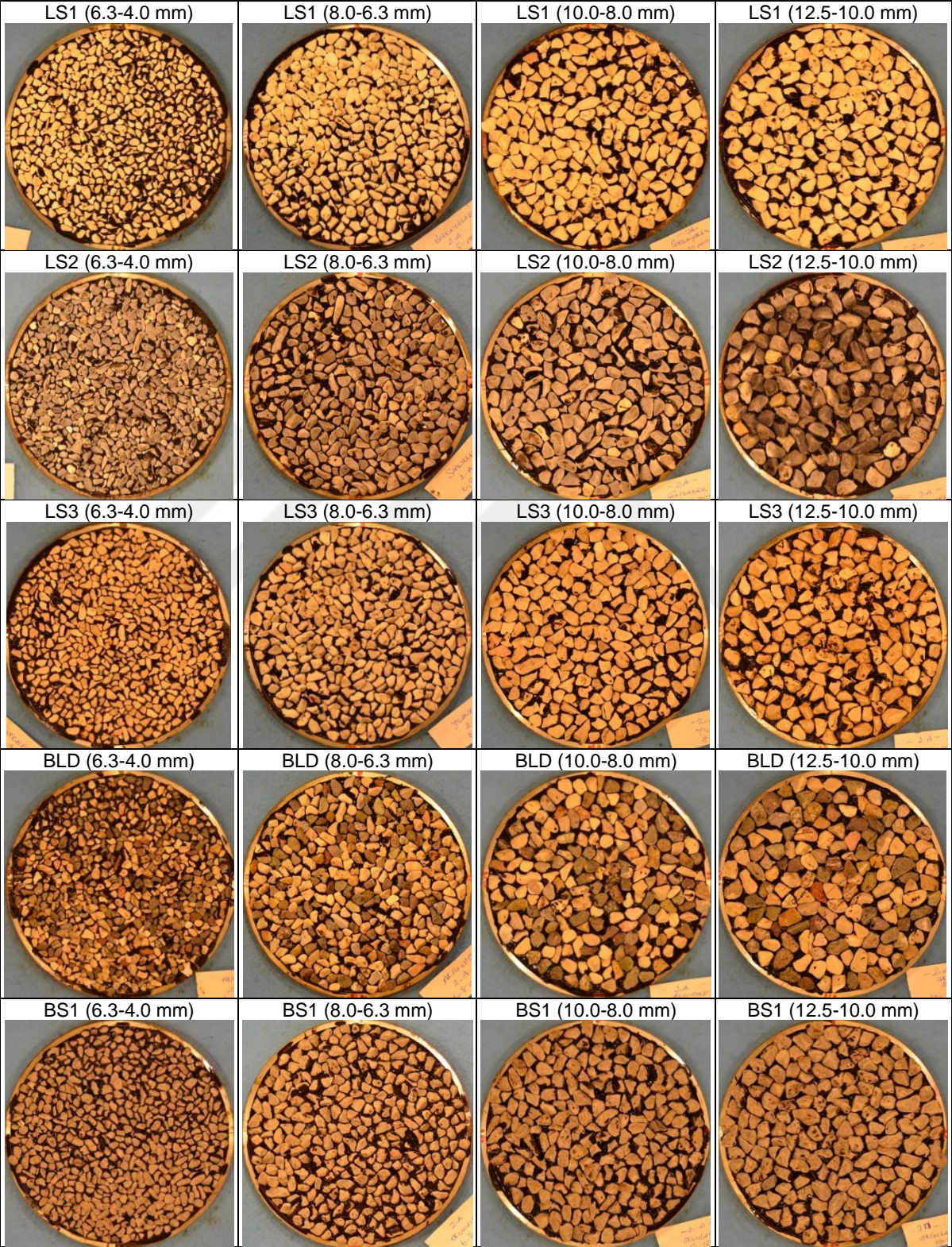Figure 15. Images for chip seal samples with polished aggregates at 4th polishing level

LS1 (6.3-4.0 mm)	LS1 (8.0-6.3 mm)	LS1 (10.0-8.0 mm)	LS1 (12.5-10.0 mm)
LS2 (6.3-4.0 mm)	LS2 (8.0-6.3 mm)	LS2 (10.0-8.0 mm)	LS2 (12.5-10.0 mm)
LS3 (6.3-4.0 mm)	LS3 (8.0-6.3 mm)	LS3 (10.0-8.0 mm)	LS3 (12.5-10.0 mm)
BLD (6.3-4.0 mm)	BLD (8.0-6.3 mm)	BLD (10.0-8.0 mm)	BLD (12.5-10.0 mm)
(6.3-4.0 mm)	BS1 (8.0-6.3 mm)	BS1 (10.0-8.0 mm)	BS1 (12.5-10.0 mm)

BS2 (6.3-4.0 mm)   BS2 (8.0-6.3 mm)   BS2 (10.0-8.0 mm)   BS2 (12.5-10.0 mm)

EAF1 (6.3-4.0 mm)   EAF1 (8.0-6.3 mm)   EAF1 (10.0-8.0 mm)   EAF1 (12.5-10.0 mm)

EAF2 (6.3-4.0 mm)   EAF2 (8.0-6.3 mm)   EAF2 (10.0-8.0 mm)   EAF2 (12.5-10.0 mm)

EAF3 (6.3-4.0 mm)   EAF3 (8.0-6.3 mm)   EAF3 (10.0-8.0 mm)   EAF3 (12.5-10.0 mm)

FER (6.3-4.0 mm)   FER (8.0-6.3 mm)   FER (10.0-8.0 mm)   FER (12.5-10.0 mm)
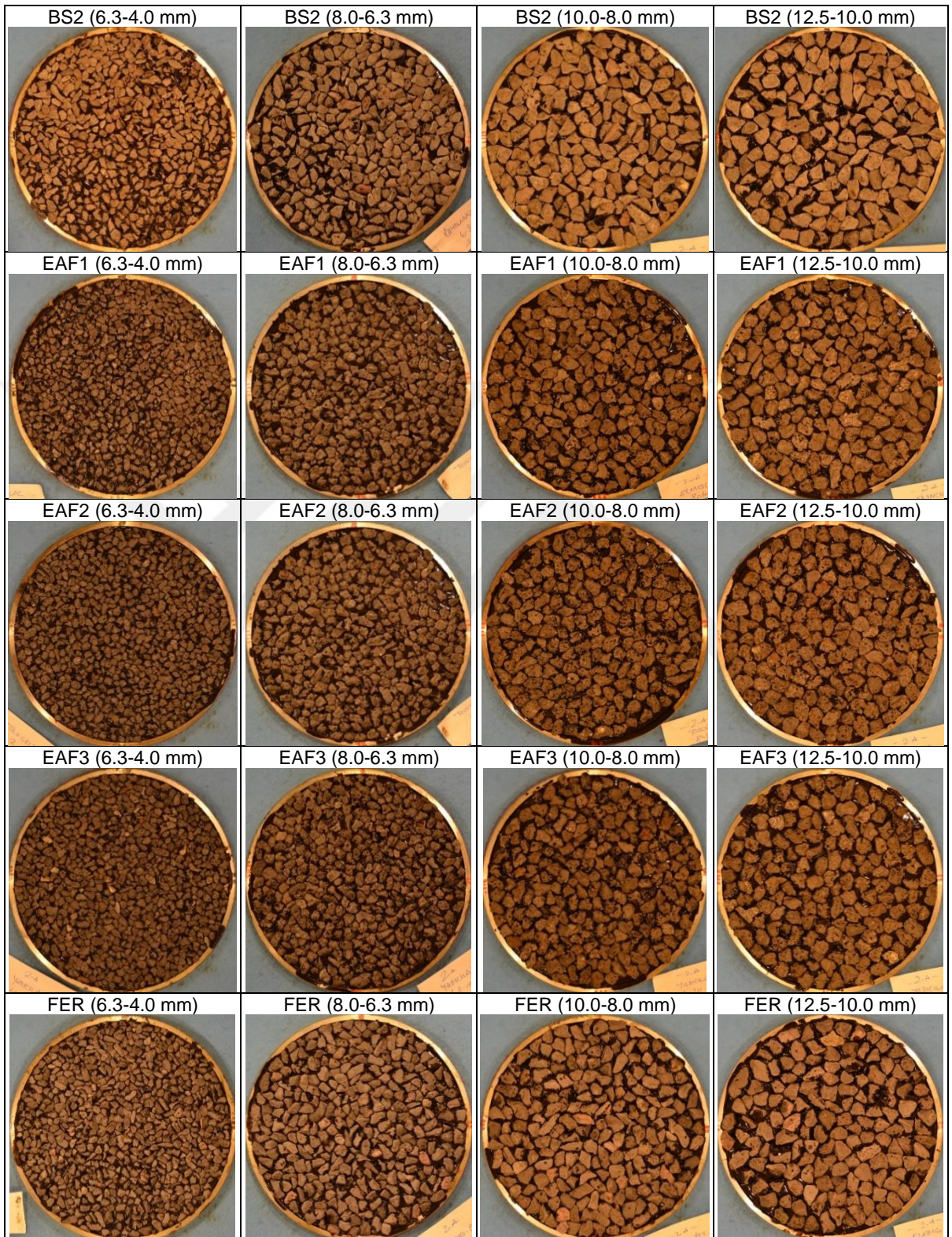
Figure 16. Images for chip seal samples with polished aggregates at 5th polishing level
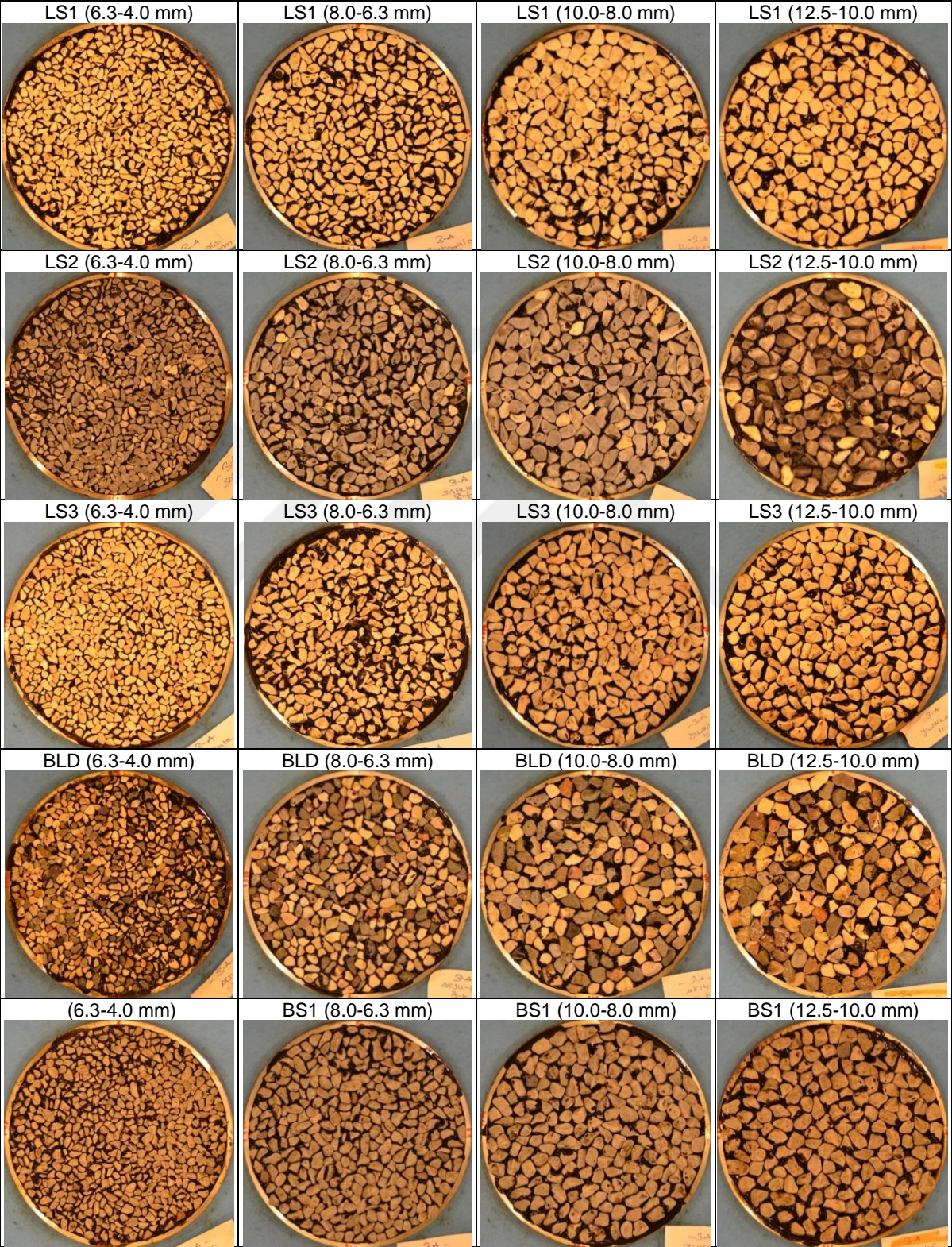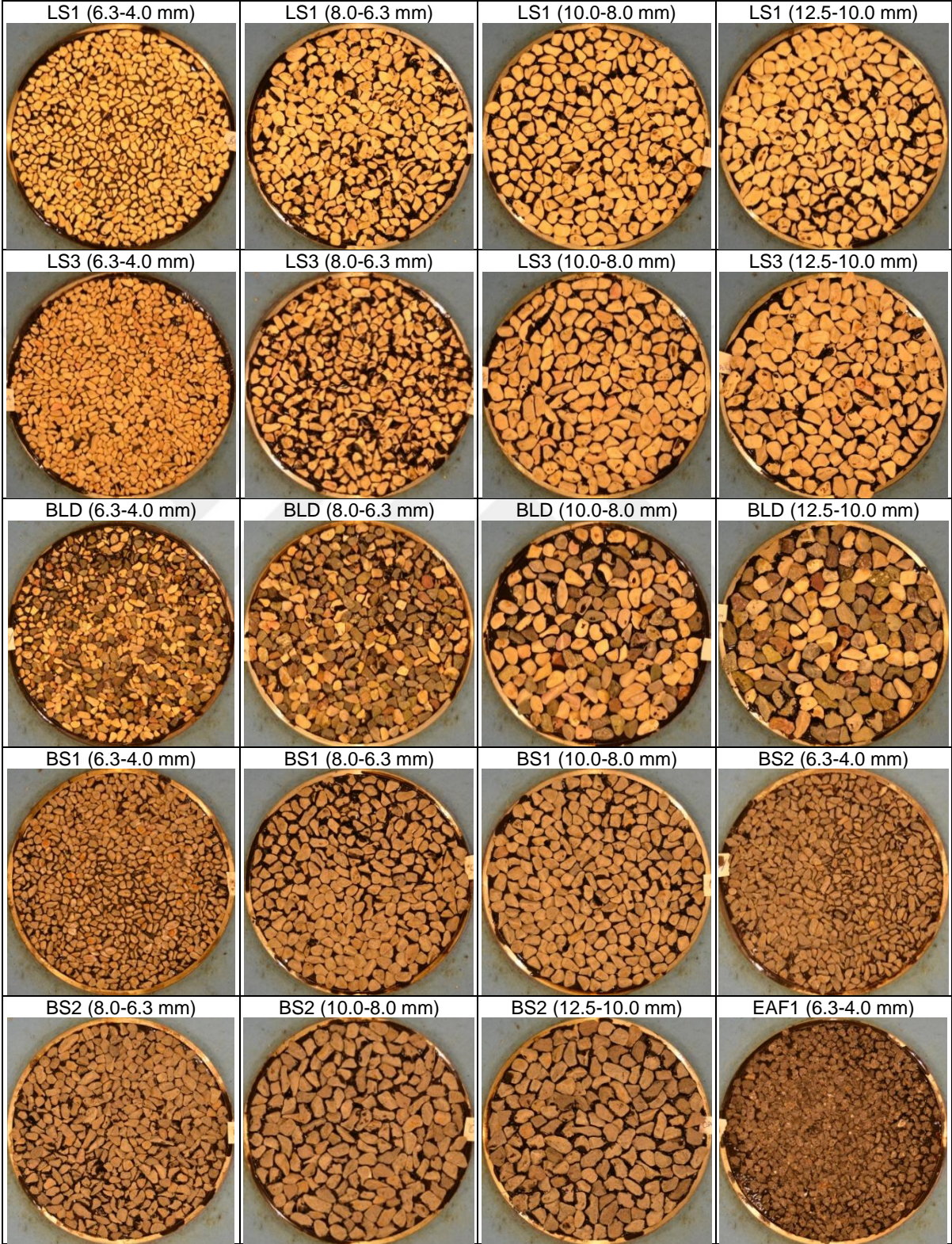
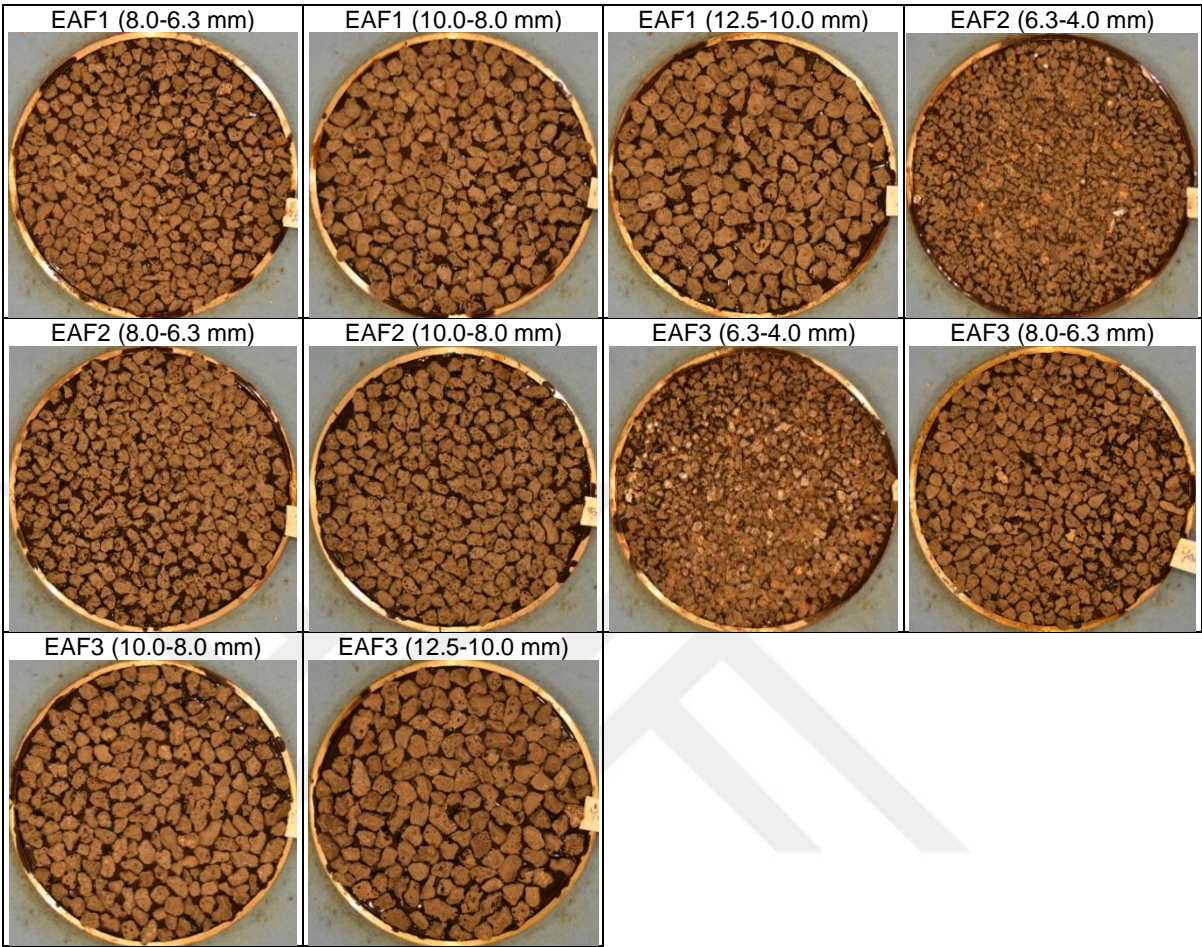| EAF1 (8.0-6.3 mm) | EAF1 (10.0-8.0 mm) | EAF1 (12.5-10.0 mm) | EAF2 (6.3-4.0 mm) |
| EAF2 (8.0-6.3 mm) | EAF2 (10.0-8.0 mm) | EAF3 (6.3-4.0 mm) | EAF3 (8.0-6.3 mm) |
| EAF3 (10.0-8.0 mm) | EAF3 (12.5-10.0 mm) | | |

Figure 17. Images for slurry seal samples within Type I II and III

LS-1 TYPE-I	LS-1 TYPE-II	LS-1 TYPE-III	LS-2 TYPE-I
LS-2 TYPE-II	LS-2 TYPE-III	LS-3 TYPE-I	LS-3 TYPE-II
LS-3 TYPE-III	BLD TYPE-I	BLD TYPE-II	BLD TYPE-III
BS-2 TYPE-I	BS-2 TYPE-II	BS-2 TYPE-III	EAF-1 TYPE I

EAF-1 TYPE II	EAF-1 TYPE III	EAF-2 TYPE I	EAF-2 TYPE II
EAF-1 TYPE III	EAF-3 TYPE I	EAF-3 TYPE II	EAF-3 TYPE III
FER- TYPE I	FER- TYPE II	FER- TYPE III	